Czech Technical University in Prague

Faculty of Electrical Engineering

Department of Circuit Theory

Artificial Neural Networks Application in Ophthalmology

Intraocular Lens Power Calculation Improvement for Patients Undergoing Cataract Surgery

Doctoral Thesis

Martin Šramka

Prague, July 2019

Ph.D. Programme: P2612 Electrical Engineering and Information Technology

Branch of study: 2602V013 Electrical Engineering Theory

Supervisor: Prof. Ing. Jana Tučková, CSc.

Supervisor-Specialist: prim. MUDr. Pavel Stodůlka, Ph.D.

The doctoral thesis was written during the combined form of doctoral study at the Department of Circuit Theory, Faculty of Electrical Engineering of the Czech Technical University in Prague.

Ph.D. Candidate: Ing. Martin Šramka
Head of Biomedical Research and Development Department
Gemini Eye Clinic
U Gemini 360, 760 01 Zlín, Czech Republic
sramka@gemini.cz

Department of Circuit Theory
Faculty of Electrical Engineering
Czech Technical University in Prague
Technická 2, 166 27 Prague 6, Czech Republic
sramkma2@fel.cvut.cz

Supervisor: Prof. Ing. Jana Tučková, CSc.
Department of Circuit Theory
Faculty of Electrical Engineering
Czech Technical University in Prague
Technická 2, 166 27 Prague 6, Czech Republic
tuckova@fel.cvut.cz

Supervisor-Specialist: prim. MUDr. Pavel Stodůlka, Ph.D.
Chief Eye Surgeon
Gemini Eye Clinic
U Gemini 360, 760 01 Zlín, Czech Republic
stodulka@lasik.cz

ABSTRACT

The aim of this Ph.D. thesis is to evaluate the potential of machine learning algorithms as an intraocular lens power calculation improvement for clinical workflow. Current intraocular lens power calculation methods offer limited accuracy, and in eyes with an unusual ocular dimension, the accuracy may decrease. In the case where the power of the intraocular lens used in cataract or refractive lens exchange surgery is improperly calculated, there is a risk of re-operation or further refractive correction. This may potentially induce complications and discomfort to the patient. A dataset containing information about 2194 eyes was obtained using a data mining process from the Electronic Health Record system database of the Gemini Eye Clinic. The dataset was optimized and split into a Selection set (used in the design of models and training), and a Verification set (used in the evaluation). A set of prediction errors and a distribution of predicted refractive errors were evaluated for all models and clinical results. In retrospective comparison to the method currently used in a clinical setting, most of the machine learning models have achieved significantly better results in intraocular lens calculations, and therefore, there is a strong potential for improved clinical cataract refractive outcomes. This statement is supported by the prospective results achieved using the CS2_radbas model which was selected for prospective evaluation. Rapid improvement occurred in all monitored error categories when compared to the clinical results and to the accuracy presented in the state-of-the-art literature.

Keywords: machine learning; artificial neural networks; calculation; cataract; intraocular lens power; refraction

ABSTRAKT

Cílem této disertační práce je zhodnotit potenciál algoritmů strojového učení pro zpřesnění výpočtů optické mohutnosti nitrooční čočky v klinickém provozu. Aktuální metody výpočtu optické mohutnosti nitrooční čočky nabízejí omezenou přesnost a zejména u očí s neobvyklými biometrickými parametry může přesnost ještě klesnout. V případě nesprávně vypočtené nitrooční čočky při kataraktovém nebo refrakčním chirurgickém zákroku existuje riziko nutnosti opětovné operace nebo další refrakční korekce. To může potenciálně vyvolat komplikace a nepohodlí pro pacienta. Pomocí procesu vytěžování dat (data mining) z database informačního systému Oční kliniky Gemini byl získán soubor dat obsahující informace o 2194 očích. Tento soubor dat byl optimalizován a rozdělen do "Selection setu" (používaného při návrhu modelů a tréninku) a "Verification setu" (použitého při hodnocení). Byla vyhodnocena sada středních chyb předpovědi a distribuce předpovězené refrakční chyby u všech modelů a pro skutečné klinické výsledky. V porovnání s metodou, která se v současné době používá v klinickém prostředí, většina modelů strojového učení dosáhla výrazně lepších výsledků ve výpočtech nitrooční čočky, a proto existuje silný potenciál ke zlepšení klinických refrakčních výsledků katarakty. Toto tvrzení je podpořeno prospektivními výsledky dosaženými pomocí modelu CS2_radbas, který byl vybrán pro prospektivní testování. Ve srovnání s klinickými výsledky a přesností kalkulací prezentovanou v nejmodernější literatuře došlo k rapidnímu zlepšení ve všech sledovaných kategoriích chyb.

Klíčová slova: strojové učení; umělé neuronové sítě; kalkulace; šedý zákal; optická mohutnost nitrooční čočky; refrakce;

AUTHOR STATEMENT

I declare that this research is the result of my own work. I certify that all sources are fully acknowledged in accordance with standard referencing practices. All procedures performed in studies involving human participants were in accordance with the ethical standards of the institutional and national research committee and with the Declaration of Helsinki. This research was approved by the ethics committee of the Gemini Eye Clinic (IRB number 2019-04).

Author in Zlín, 12. 7. 2019

ACKNOWLEDGMENT

I would like to thank my supervisor, professor Jana Tučková, for her patience, valuable suggestions, and persistent support during my studies at the Czech Technical University. I am also grateful to my supervisor-specialist, employer and colleague, doctor Pavel Stodůlka for the opportunity to work with him, for the extraordinary experience I gained and for the chance to learn.

I would like to thank my fellow colleagues for their cooperation, feedback, and friendship.

I would also like to thank my friends for always being there for me.

Last but certainly not least, I would like to thank my family and especially my parents for supporting me spiritually and throughout my entire life.

Dedicated to my parents

In loving memory of Anna Šramková

CONTENTS

1. INTRODUCTION AND MOTIVATION

1.1. Introduction

Cataract surgery is the major refractive surgical procedure performed in adult patients and one of the most commonly performed surgical procedures today [1]. Every year, over 11 million people undergo cataract surgery with intraocular lens (IOL) implantation worldwide. In 1990, an estimated 37 million people were blind worldwide, 40% of them because of cataracts [2]. 20 years later, in 2010, there were 10.8 million blind people across the globe due to cataracts, accounting for a third of all blind people worldwide [3–5]. The World Health Organization has estimated that this number will increase to 40 million in 2025 as the earth's population grows [5]. In many countries, cataract surgery remains one of the most commonly performed surgical procedures [6–10].

Phacoemulsification and IOL implantation is currently the most common method of treating cataracts and many refractive vision errors for which other conventional methods are not suitable [11] and offers significant improvements to the quality of life for patients of all ages [12–14]. Modern cataract surgery is an efficacious and safe procedure [4, 15]. Numerous developments have led to improved results after IOL implantation [16–23]. The primary aim of cataract surgery is to improve the throughput of the optical medium caused by the cataractous lens and achieve complete postoperative independence of ocular correction. With the significant developments of cataract and refractive surgeries over the past 20 years, we are now even closer in meeting this target, although there are still areas we can improve.

The quality of the patient's post-operative vision depends on the correct choice of IOL optical power, which influences the residual post-operative refraction. Improvement of the refractive result of the cataract surgery is a challenge for the IOL manufacturers but also for the methods used in the calculation of suitable IOL power.

1.2. Problem definition

The refractive power of the human eye depends on the power of the cornea, lens, axial length (AL) of the eye and the axial position of the lens. All of these factors play a major role in determining postoperative visual outcomes [24]. Good refractive predictability is mandatory for any cataract or refractive procedure.

Despite advances in modern IOL power calculations, the inability to accurately predict pseudophakic anterior chamber depth (ACD) and hence, postoperative effective lens position (ELP), is a significant roadblock in calculation accuracy. The formulas used today implement a more refined ACD algorithm that increases accuracy when predicting pseudophakic ACD. It has been previously shown that prediction error of postoperative ACD likely account for between 20% and 40% of the refractive prediction error at spectacle plane [25, 26]. An incorrect IOL power calculation resulting from incorrect measurements of the eye is the most likely cause of refractive errors after cataract surgery with IOL implantation [27, 28]. Furthermore, current standards regarding IOL power

labeling allow a certain tolerance, and therefore, the power on the IOL label might not be the precise power of the IOL itself [27, 29].

Even though refractive outcomes after IOL implantation have improved considerably over time, patient demands and expectations for precise healthcare as well as favorable postoperative refractive outcomes are continuously increasing. During the last several years, a great deal of energy has been put forth in realizing spectacle independence through improvements in the operative techniques, acquisition of biometric data, and refinement of IOL power formulae [30–33]. The prediction of refractive outcomes following cataract surgery has steadily improved, with more recent IOL power formulas generally outperforming those of prior generations [32, 34, 35]. However, there are many schools of thought regarding the formula that is the most accurate in predicting refraction. Unfortunately, research supports the claim that there isn't one formula that demonstrates high levels of accuracy on eyes of varying characteristics. As such, some researchers recommend that different formulas be used to support cataract surgery depending on the ocular dimension of the eye in question [34, 36, 37]. Numerous studies have sought and failed to find a perfect IOL power calculation formula for such eyes, so the search for a more accurate IOL calculation method must continue.

Several recent publications also state that the refractive outcome of each surgery is not influenced only by artificial lens optical properties in relation to eye anatomy [38, 39] but by many other factors [25], such as the examination methodology [40], measurement accuracy [41], the surgeon's habits and the clinical workflow [42–45]. That means that in order to achieve an accurate IOL power calculation, a series of scientific and therapeutic approaches need to be made; accurate determination of the reason for the vision loss [46], preoperative ocular surface preparation, patient visual preferences, eye biometric measurements [41, 47], precise eye surgery and IOL positioning [48], and last but certainly not least, an accurate IOL power calculation method [25, 44].

So, no matter how difficult the clinical assumptions are or the eye models the specific calculation formula is based on, it is complicated to take all these factors into account. In the case of an improperly calculated power of the IOL, there is a risk of re-operation or further refractive correction, which may potentially induce complications for the patient. There are, therefore, sufficient motivating factors to find the most accurate IOL calculation method [49].

1.3. State-of-the-art

In order to determine the optimal IOL power, calculation formulas are used. These formulas use data from preoperative measurements, examinations and IOL parameters, which may all influence the overall outcome.

The calculation formulas can be divided into Refraction, Regression, Vergence, Artificial Intelligence and Ray Tracing categories based on their calculation method [50]. Currently, the most commonly used formulas are from the Vergence formula category and are based on different clinical assumptions or eye models, but all of the formulas

work as universal calculators for different types of artificial IOLs. Particular lens type optical behavior is specified by one numeric constant as it is in Holladay [51], SRK/T [52], Hoffer Q [53], Olsen [54], Hill-RBF [55], and Barrett [56] formulas or by several numeric constants as it is in the Haigis formula [57].

The accuracy of individual calculation formulas is presented in many contemporary works. In relation to the accuracy of calculations, the influence of various factors, such as the biometrics of a particular eye, the design and type of IOL, the method of surgery, and the occurrence of any previous ophthalmic surgeries is examined.

In [58], a comparison of the current new generation of formulas used for 400 patients undergoing cataract and lens replacement surgery is presented. All presented formulas achieved better than 78.3% of the intended eye refraction prediction error within ±0.5 diopters (D). The Hill-RBF and Barrett formulas are better in short and long eyes, respectively, and the Barrett Universal II formula had the lowest number of refractive surprises higher than 1 D.

Accuracy comparison of Holladay 1, SRK/T, Hoffer Q, Haigis, Barrett Universal II, Holladay 2, and Olsen formulas for eyes with an axial length longer than 26.0 mm is provided by [59]. SRK/T, Hoffer Q, Haigis, Barrett Universal II, Holladay 2, and Olsen formulas have a prediction error of ±0.5 D in at least 71.0% of the eyes and ±1.0 D in 93.0% of the eyes.

A calculation for 53 eyes across 36 patients with axial length more than 27.0 mm by the IOL Master is evaluated in [60] for the Holladay 1, Holladay 2, SRK/T, Hoffer Q, and Haigis formulas. For eyes longer than 27.0 mm, the Haigis formula is found to be most accurate followed by SRK/T, Holladay 2, Holladay 1 and then Hoffer Q. All formulas predicted a more myopic outcome than the actual results achieved by the surgery.

Refractive outcomes for small eyes and calculations associated with Hoffer Q, Holladay 1, Holladay 2, Haigis, SRK-T, and SRK-II are observed in [61]. The Hoffer Q formula provided the best refractive outcomes, where 39%, 61%, and 89% of the eyes had final refraction within ±0.5 D, ±1.0 D, and ±2.0 D of the target, respectively.

The Artificial Neural Network (ANN) based IOL calculating method, which dates back to nineties, is provided by [62]. The accuracy of ANN and the Holladay 1 formula is compared. In 72.5% of cases that used ANN and in 50% of cases that used the Holladay 1 formula, an error of less than ±0.75 D was achieved. ANN performed significantly better.

The concept for the Ray Tracing IOL power estimation is presented in [54]. Haigis, Hoffer Q, Holladay 1 and SRK/T formulas are compared to the Olsen formula using the C constant. There was no significant difference found when using the Haigis, Hoffer Q, Holladay 1, and SRK/T formulas. Compared to the SRK/T formula, the Olsen formula showed an improvement of 14% in the mean absolute error and an 85% reduction in the number of errors higher than 1.0 D.

The accuracy of Hoffer Q and Haigis formulas according to the anterior chamber depth in small eyes is evaluated in [63]. 75 eyes of 75 patients with an axial length of less

than 22.0 mm were included in the study. In eyes with short axial lengths, the predicted refractive error difference between the Haigis and Hoffer Q formulas increased as ACD decreased. No significant difference was found when the anterior chamber depth was longer than 2.40 mm.

The IOL power calculation of 50 eyes of an axial length shorter than 22 mm were analyzed by Shrivastava [64] with the result that there were no significant differences in accuracy between Barrett Universal II, Haigis, Hoffer Q, Holladay 2, Hill-RBF and SRK/T formulas.

Accuracy of Barrett Universal II, Haigis, Hill-RBF, Hoffer Q, Holladay 1, Holladay 2, Olsen, SRK/T, and T2 formulas were evaluated by Shajari [65] with results that suggested that using the Barrett Universal II, Hill-RBF, Olsen, or T2 formulas will ensure 80% of the cases fall within ±0.50 D range.

The effect of anterior chamber depth length on the accuracy of eight IOL calculation formulas in patients with normal axial lengths is investigated by Gökce [26].

IOL power calculations of 171 eyes with high and low keratometry readings were evaluated by Reitblat [66].

A study by Melles [34] showed that the Barrett Universal II formula had the lowest prediction error for two specific IOLs.

The only currently used IOL calculation approach using Artificial Intelligence is the Hill-RBF formula, which has a reported accuracy of 91% of the eyes within ±0.5 D range from the intended target refraction [67]. However, there are a number of papers indicating that Hill-RBF accuracy is not significantly different from the Vergence formula category [31, 58, 65]. Unfortunately, there is no research that addresses the Hill-RBF principle in any peer-reviewed scientific journal, so the only information about the principle itself must be obtained from widely available resources on the Internet. Based on this accessible information, it is possible to determine that the Hill-RBF core is a Radial Basis Function and that the algorithm was trained on the data of more than 12,000 eyes. There is no evidence whatsoever that identifies the specific machine learning method that was used [67–70].

2. GOALS OF THE THESIS

This research is aimed at exploring the use of artificial neural networks (ANN) and machine learning methods in relation to IOL power calculations. The following goals of this doctoral thesis were established:

1) Investigate the state-of-the-art IOL power calculations and determine the accuracy of the current calculation methods and the factors that can affect them.

2) Describe the methodology of selecting and optimizing a dataset suitable for training and evaluation of ANN and machine learning models.

3) Select the appropriate ANN topologies and compare ANN performance for Radial Basis, Hyperbolic Tangent Sigmoid, Log-sigmoid, and Linear transfer functions. Compare ANN accuracy with other appropriate machine learning algorithms.

4) Evaluate all ANN and machine learning models in relation to clinical results. Mutually evaluate all models and select the best model for prospective testing.

5) With regard to safety, perform a prospective evaluation of the best model and assess the potential shortcomings of this approach.

3. MATERIALS AND METHODS

This chapter is structured into three main parts: Dataset Preparation, Model Design & Training, and Evaluation (Figure 1).

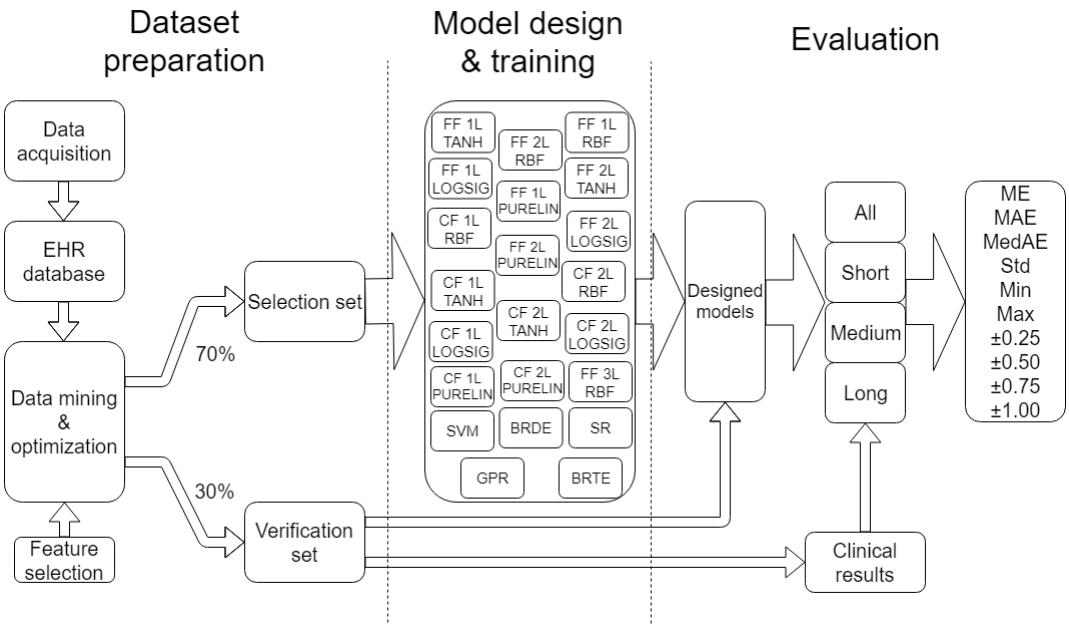

Figure 1. Research diagram

The data preparation part focuses on the methods used in data collection, storing data in the Electronic Health Record (EHR) database, as well as data mining, cleaning, and optimizing in order to obtain a suitable dataset for training and evaluation. Incorrect integration of these processes could lead to a degradation of data sources and the distortion of the result's quality.

The model design and training part focuses on the set-up of suitable ANN and machine learning models and their training using the dataset.

The evaluation part describes the outcome measures and how the data was analyzed.

This study used the data of patients who underwent cataract or refractive lens exchange surgery from December 2014 to November 2018 at the Gemini Eye Clinic in the Czech Republic. This study was approved by the Institutional Ethics Committee of the Gemini Eye Clinic (IRB approval number 2019-04) and adhered to the tenets of the Declaration of Helsinki.

3.1. Data acquisition

Data was acquired, recorded and entered by skilled staff into the central EHR system at the Gemini Eye Clinic usually before surgery and during follow up visits and post-operative examinations.

The preoperative patient evaluation included distance objective refraction (Rx_{pre}), distance subjective refraction, mean keratometry (K), ACD, axial length of the eye (AL), uncorrected distance visual acuity (UDVA), corrected distance visual acuity (CDVA), slit lamp examination, retinal examination and intraocular pressure examination. Anterior and posterior segment evaluations and biometry measurements were conducted on all patients in the dataset. All biometry examinations (K, ACD, AL) were conducted using a Carl Zeiss IOL Master 500 (Carl Zeiss, Jena, Germany) [71]. All measurements of objective refraction and intraocular pressure were conducted using a Nidek Tonoref II Auto Refractometer (Nidek, Gamagori, Japan).

All patients in the dataset underwent surgeries using a clear corneal incision made by a Stellaris PC (Bausch and Lomb, Bridgewater, New York, USA) surgical device. Continuous curvilinear capsulorhexis, phacoaspiration and IOL implantation in the capsular bag were performed such that the eye was stabilized using an irrigating handpiece introduced into the eye through a side port incision. In some cases, a 4.8 mm diameter laser-capsulotomy and laser fragmentation in combination with two circular and six radial cuts were performed using a Victus laser platform (Bausch and Lomb, Bridgewater, New York, USA). A FineVision Micro F Trifocal IOL (Physiol, Lüttich, Belgium) was then implanted. All IOLs in the dataset were calculated using the SRK/T formula [52] with an A constant equal to 119.1. In some rare cases, the optical power of the IOL was adjusted at the discretion of the surgeon, especially for eyes with non-standard biometric specificities. All patients' targeted refraction was on emmetropia.

At each follow-up visit, a complete slit-lamp evaluation, non-contact tonometry, distance objective refraction (Rx_{post}), distance subjective refraction, near subjective refraction, keratometry, UDVA, CDVA, uncorrected near visual acuity (UNVA), and corrected near visual acuity (CNVA) measurements were performed.

All refraction values are expressed using a spherical equivalent. The post-operative examinations were collected after at least 25 days following surgery, which is the shortest time considered suitable for sufficient vision recovery based on conclusions from the work of Conrad-Hengerer [72].

3.2. Feature selection

Based on the database data integrity, we selected K, ACD, AL, Age, and Rx_{pre} as our model input parameters (input features). Rx_{post} and the optical power of the implanted IOL ($IOL_{Implanted}$) were used in training target definition. A potential limitation of this selection is discussed further in the Discussion and Conclusions chapter.

3.3. Data mining and optimization

The EHR system data is stored using SQL Server (Microsoft, Redmond, USA) relational database technology. A single purpose SQL script was designed to obtain an initial data view, which was then further data mined to obtain a master dataset (MD). The following inclusion and exclusion criteria were used in order to filter the data from physiologically implausible entries and non-standard surgical cases.

The following inclusion criteria were used to obtain an MD:

- ACD between 1 and 5 mm
- Preoperative and postoperative UDVA > CDVA in [logMAR]
- AL between 15 and 40 mm
- Mean K between 30 and 60 D
- Patient age between 18 and 99
- Optical power of the implanted IOL between 6 and 35 D

Examinations and values were excluded from the MD for each eye in case of:

- Non-standard surgical procedure used or intraoperative complications or any other complications affecting postoperative vision recovery
    - Surgery record contains any of the following strings: “ruptura“, “fenestrum“, “vitrektom“, “praskl“, “sklivec“, “prolaps“, “explant“, “sulc“, “sulk“, “rzp“, “key hole“
- Ocular disease or any corneal pathology
    - Patient record contains any of the following strings: “otok”, “striat”, “edem”, “odchlípen”, “PEX”, “jizv”, “amoc”, “aparát”, “defekt”, “degener”, “endotelpati”, “fibrin”, “guttat”, “haze”, “hemoftalm”, “hemophtalm”, “luxov”, “membrán”, “precip”, “zonul”
- Previous intraocular surgery or corneal refractive surgery
    - Patient diagnosis record contains any of the following strings: “LASIK”, “LASEK”, “PRK”, “LASER”, “RELEX”, “DMEK”, “DALK”, “PKP”
- Post-operative CDVA higher than 0.3 logMAR, which is widely considered the driving standard limit (Visual Standards for Driving in Europe, Consensus paper, European Council of Optometry and Optics)
- Incomplete biometry and refraction measurements
- Preoperative corneal astigmatism of more than 3.0 diopters
- Incomplete EHR documentation
- The difference in AL to the second eye > 1 mm

All of the excluded cases, which were identified using strings, comes from Czech medical terminology and indicate an undesirable contraindication for our application.

All samples containing outliers for K, ACD, AL, Age, Rx_{pre}, Rx_{post} were excluded from the MD based on a ±3 sigma rule as these samples can be considered errors in measurement and inappropriate for model training [73, 74].

The principle of preparing data suitable for machine learning model training is to find the ideal value for the already implanted IOL (IOL_{Ideal}). IOL_{Ideal} is considered to be an IOL that will not induce any residual postoperative refraction for the patient's eye or will not deviate from the intended target refraction (for distance vision this was considered as 0 D). To find such an IOL_{Ideal}, the following information is needed:

- Optical power of the $IOL_{Implanted}$
- Measured residual refraction Rx_{post}
- Interrelationship of Rx_{post} and $IOL_{Implanted}$

It is generally known that 1.0 D of IOL prediction error produces approximately 0.7 D of refractive prediction error at the spectacle plane [34]. However, this is a general assumption, and since the eye is a complex optical system, it may not reach sufficient accuracy in all eyes. The interrelationship between Rx_{post} and $IOL_{Implanted}$ thus should also consider eye biometrical parameters representative of the optical system of the eye, such as the eye AL and the power of the cornea K. The interrelationship of these two variables was determined using the reversed Eye Vergence Formula Eq. (1) [75, 76].

$$Rx_{theorPost} = \frac{1}{\frac{V}{1000} - \frac{1}{1000 * \left(\frac{K}{1000} - \frac{1}{1000 * \left(\frac{ELP}{1336} - \frac{1}{1336 * \left(\frac{IOL}{1336} - \frac{1}{AL - ELP} \right)} \right)} \right)}}$$

Equation 1. Reversed eye vergence formula

$Rx_{theorPost}$ is the calculated refraction for the eye with specific K in [D], AL in [mm], V (vertex distance) in [mm], IOL power in [D] and Effective Lens Position (ELP) in [mm] calculated using recommendations by [52].

The change in refraction at the spectacle plane as a result of changing the IOL power value was computed using Eq. (2), and then the IOL_{Ideal} calculation is expressed by Eq. (3)

$$Rx_{05IOL} = Rx_{theorPost}(IOL) - Rx_{theorPost}(IOL + 0.5)$$

Equation 2. Dioptric change of refraction at the spectacle plane in case of an IOL value change of 0.5 [D]

$$IOL_{Ideal} = IOL_{Implanted} + \left(\frac{Rx_{post}}{Rx_{05IOL}} \right) * 0.5$$

Equation 3. Calculation of the ideal power value of an IOL for the specific eye

MD was then randomly divided into the Selection set or the Verification set in a 70% to 30% proportion, respectively. The Selection set variables were normalized using the **mapminmax** Matlab 2017a (MathWorks, Natick, MA, USA) routine, which maps row minimal and maximal values between -1 and 1. Every Verification set variable was cleared of samples outside of the minimum and maximum range of the Selection set to avoid a prediction error on non-trained data. The Verification set variables were then normalized using **mapminmax** with the same normalization parameters.

3.4. Dataset population characteristics

After a retrospective analysis, we identified 2194 eyes (1111 right eyes, 1083 left eyes) of 1759 patients (812 male, 947 female) who underwent IOL replacement surgery and met all discussed dataset criteria. The mean patient age was 56.85 ± 7.42 (35 – 78) years (mean ± standard deviation (minimum - maximum)). The MD population characteristics are summarized in Table 1.

Parameter	Value
Patients [count]	1759
Male	812
Female	947
Eyes [count]	2194
Right	1111
Left	1083
Mean Age [years]	56.85
Std	7.42
Min	35
Max	78

Table 1. Master dataset population characteristics

3.4.1. Selection set population characteristics

The Selection set contained 70% randomly chosen eyes from the whole dataset. That means 1539 eyes (771 right eyes, 768 left eyes) of 1080 patients (540 male, 628 female) were selected. The mean patient age was 56.89 ± 7.25 (36 – 78) years.

To statistically describe the Selection set, the Mean, Median, Standard Deviation (Std), Minimum (Min) and Maximum (Max) indicators were calculated. Shapiro-Wilk (P_{SW}) and D'Agostino-Pearson's K2 (P_{DP}) test p values were calculated to assess whether the data came from a normal distribution. The significance level alfa for the test was 0.001. The Selection set population characteristics are summarized in Table 2, and histograms of the individual variables are presented in Figure 2.

Age failed in normality by Shapiro-Wilk, but normality was confirmed by the D'Agostino-Pearson's K2 test and the mean to median difference and histogram analysis. Rx_{pre} and IOL_{Ideal} failed the normality assessment by both normality tests. However, the mean to median and histogram analysis tended to confirm normality.

	Mean	Median	Std	Min	Max	P_{SW}	P_{DP}
Age [years]	56.89	57.00	7.25	36.00	78.00	0.000	0.091
K [D]	43.27	43.25	1.40	39.39	47.51	0.252	0.547
ACD [mm]	3.10	3.10	0.32	2.21	4.10	0.189	0.350
AL [mm]	23.03	23.07	0.92	19.94	26.26	0.010	0.111
Rx_{pre} [D]	1.85	1.88	1.52	-3.88	6.63	0.000	0.000
IOL_{Ideal} [D]	22.80	22.50	2.74	12.62	34.17	0.000	0.000

Table 2. Selection set population characteristics

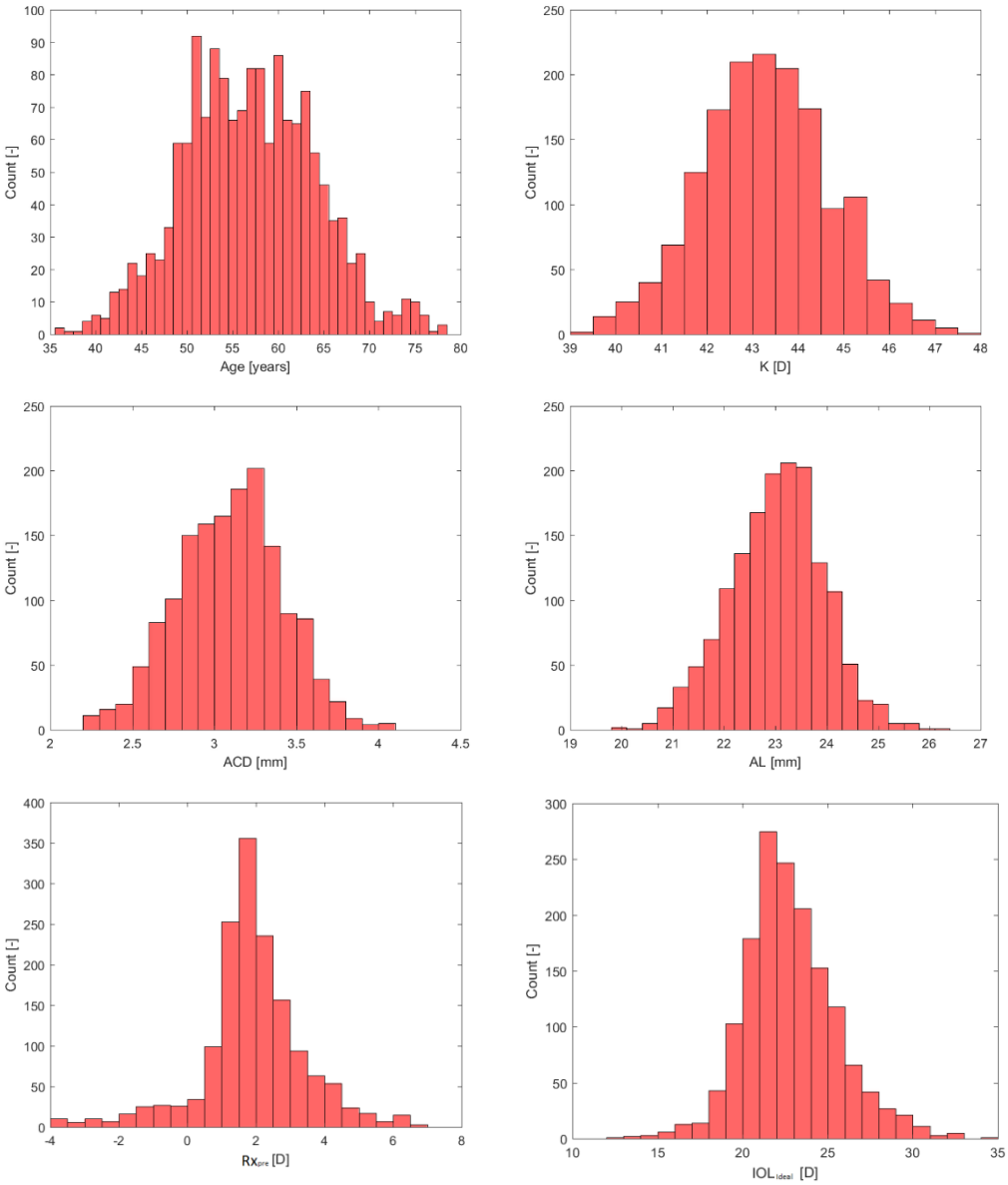

Figure 2. Selection set variables histograms. (1,1) Age, (1,2) Mean Keratometry (K), (2,1) Anterior Chamber Depth (ACD), (2,2) Axial Length (AL), (3,1) Objective Distance Spherical Equivalent Rx_{pre}, (3,2) Ideal Intraocular Lens Power (IOL_{Ideal})

3.4.2. *Verification set population characteristics*

The Verification set contained the remaining 30% of the eyes from the entire dataset. That means 655 eyes (340 right eyes, 315 left eyes) of 591 patients (272 male, 319 female) were selected. The mean patient age was 56.83 ± 7.29 (37 – 76) years.

In order to statistically describe the Verification set, the same analyses were performed like that for the Selection set case. The population characteristics are summarized in Table 3, and histograms of the individual variables are presented in Figure 3.

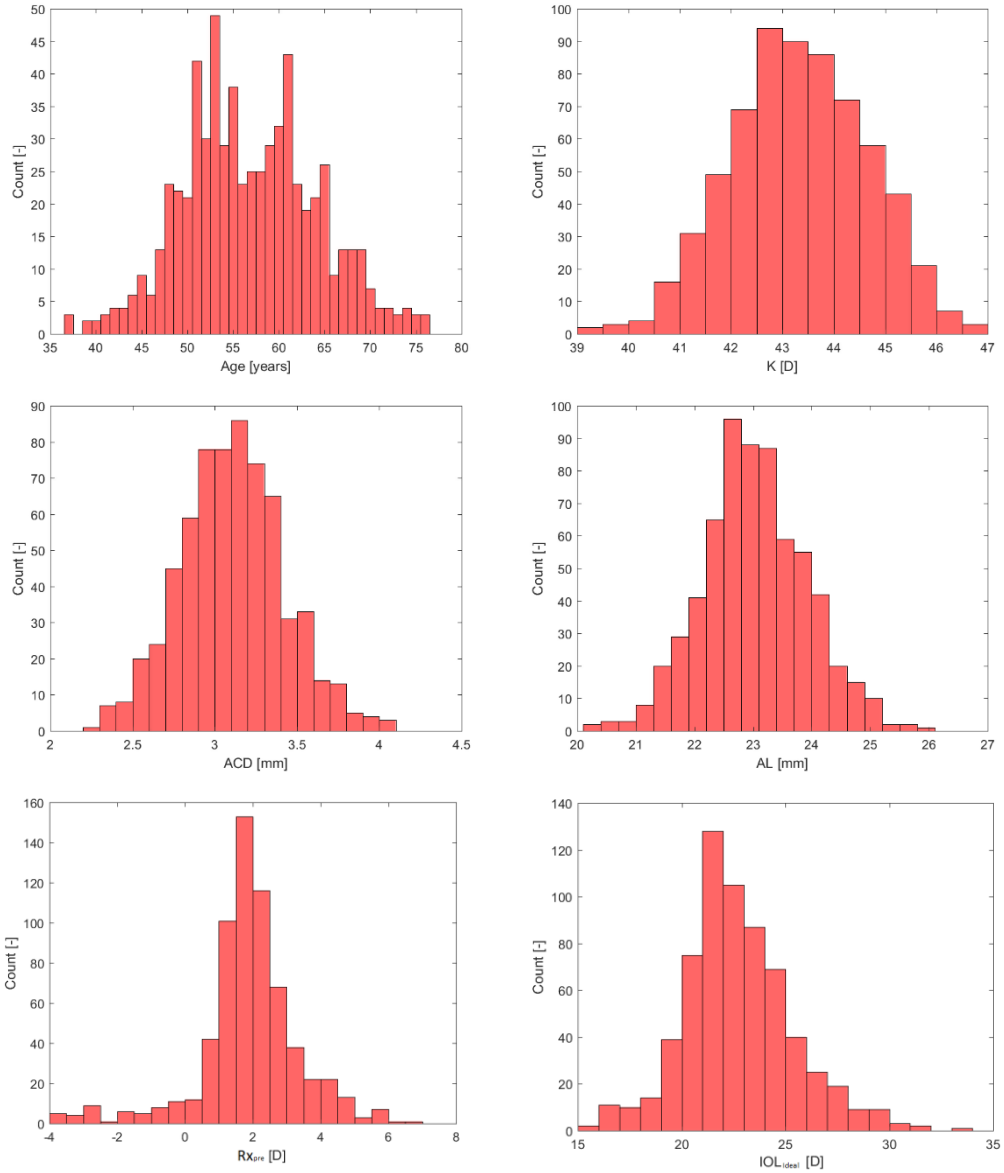

Figure 3. Verification set variables histograms. (1,1) Age, (1,2) Mean Keratometry (K), (2,1) Anterior Chamber Depth (ACD), (2,2) Axial Length (AL), (3,1) Objective Distance Spherical Equivalent Rx_{pre}, (3,2) Ideal Intraocular Lens Power (IOL_{Ideal})

Only Rx_{pre} and IOL_{Ideal} failed the normality assessment using both normality tests. However, the mean to median and histogram analysis tended to confirm normality.

	Mean	Median	Std	Min	Max	P_{SW}	P_{DP}
Age [years]	56.83	56.00	7.29	37.00	76.00	0.003	0.161
K [D]	43.33	43.30	1.33	39.41	46.92	0.263	0.199
ACD [mm]	3.11	3.10	0.32	2.29	4.06	0.183	0.206
AL [mm]	23.03	22.99	0.90	20.17	25.88	0.530	0.417
Rx_{pre} [D]	1.83	1.75	1.49	-3.88	6.63	0.000	0.000
IOL_{Ideal}[D]	22.71	22.42	2.64	15.32	33.51	0.000	0.000

Table 3. Verification set population characteristics

3.5. Main principal and used algorithms

For the design and training of each model, the Selection set was used. The Verification set was used for results evaluation. No samples from the Verification set were introduced to the model during the design and training phase, and vice versa no samples from the Selection set were used for model evaluation. Our model predictors are variables mentioned in the Feature selection section as K, ACD, AL, Age, and Rx_{pre}. The training target was IOL_{Ideal} , and the prediction outcome was $IOL_{Predicted}$.

This work focuses on the application of artificial neural networks (ANN) in the field of artificial intraocular lens power calculations. Within this research, a total of 17 ANN models of two ANN architectures with four transfer functions (also called activation functions) were evaluated. However, since ANN isn't the only machine learning algorithm used for regression, function fitting, and interpolation and approximation, several other machine learning algorithms were also evaluated:

- Feed-Forward Multilayer Neural Networks (MLNN)
    - One hidden layer
        - Radial Basis transfer function (FF1_radbas)
        - Hyperbolic Tangent Sigmoid transfer function (FF1_tansig)
        - Log-sigmoid transfer function (FF1_logsig)
        - Linear transfer function (FF1_purelin)
    - Two hidden layers
        - Radial Basis transfer function (FF2_radbas)
        - Hyperbolic Tangent Sigmoid transfer function (FF2_tansig)
        - Log-sigmoid transfer function (FF2_logsig)
        - Linear transfer function (FF2_purelin)
    - Three hidden layers
        - Radial Basis transfer function (FF3_radbas)
- Cascade-Forward Multilayer Neural Networks
    - One hidden layer
        - Radial Basis transfer function (CS1_radbas)
        - Hyperbolic Tangent Sigmoid transfer function (CS1_tansig)
        - Log-sigmoid transfer function (CS1_logsig)
        - Linear transfer function (CS1_purelin)
    - Two hidden layers
        - Radial Basis transfer function (CS2_radbas)
        - Hyperbolic Tangent Sigmoid transfer function (CS2_tansig)
        - Log-sigmoid transfer function (CS2_logsig)
        - Linear transfer function (CS2_purelin)
- Support Vector Machine (SVM)
- Binary Regression Decision Tree (BRDT)
- Gaussian Process Regression (GPR)
- Boosted Regression Tree Ensembles (BRTE)
- Stepwise Regression (SR)

Abbreviations used in the mutual evaluation section are listed in parentheses after the name of each algorithm in the previous list.

All presented models were designed, trained and tested using Matlab 2017a (MathWorks, Natick, MA, USA). A description of all the functions and features used (in the text highlighted by **bold**) can be found in the software documentation [77].

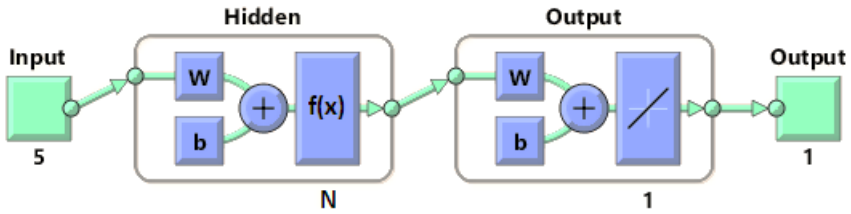

Figure 4. Feed-forward MLNN model with one hidden layer, an f(x) transfer function and N hidden layer neurons

Feed-forward and Cascade-forward ANN are known for their exceptional ability to approximate continuous functions [78, 79]. This pattern recognition method is able to effectively approximate the environment that affects the refractive result for a particular artificial IOL type. The refraction result of the surgery is a function of all known and unknown variables which are implemented into the ANN during the learning process. ANN has been widely used in function approximation, prediction, recognition and classification [62, 80–82]. ANN consists of a collection of inputs and processing units known as neurons which are organized in the ANN layers. Neuron parameters are set up by the training process. The learning process consists of minimizing the error function between the desired and actual output [83, 84].

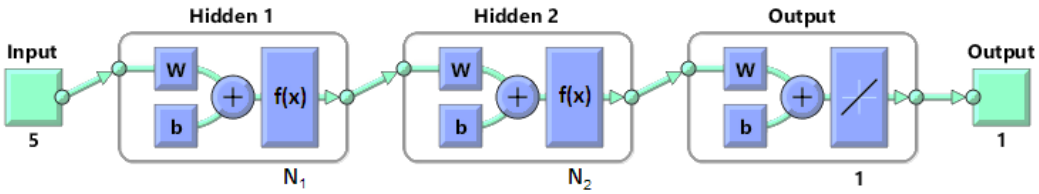

Figure 5. Feed-forward MLNN model with two hidden layers, an f(x) transfer function and N_x hidden layer neurons

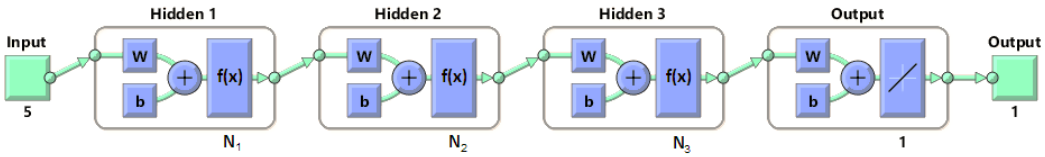

Figure 6. Feed-forward MLNN model with three hidden layers, an f(x) transfer function and N_x hidden layer neurons

Feed-forward and Cascade-forward Multilayer Neural Network (MLNN) models were designed and trained by using **fitnet** and **cascadeforwardnet** functions and had one,

two or three hidden layers and one output layer with one neuron with a linear transfer function (Figure 4 – 8). The internal structure and links of MLNN are described, for example, by Tuckova [85], Haykin [86], Novák [87] or in Matlab 2017a documentation [77]. The Levenberg-Marquardt backpropagation algorithm was used for model training using the **trainlm** method [88].

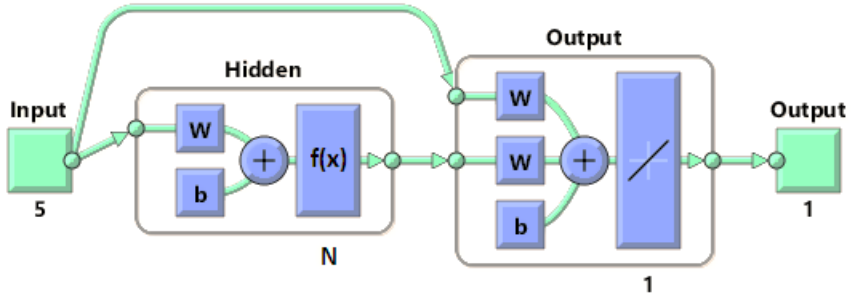

Figure 7. Cascade-forward MLNN model with one hidden layer, an f(x) transfer function and N hidden layer neurons

MLNN performance was improved using the ensemble median. This seems a better alternative to ensemble averaging [89]. The ensemble median factor was set to 10, which means that 10 MLNN models were trained using the Selection set in order to produce the desired output taken as a median of all outputs. Weights and biases were initialized by the Nguyen-Widrow initialization function for each ensemble training cycle [90].

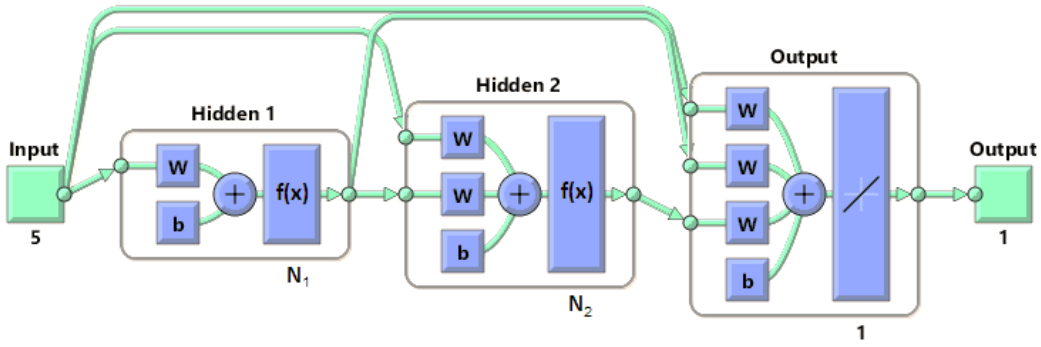

Figure 8. Cascade-forward MLNN model with two hidden layers, an f(x) transfer function and N_x hidden layer neurons

The Selection set was randomly divided into three groups (training, validation and testing subset) in a 70:15:15 ratio, respectively [91]. An early stopping algorithm was used to prevent the model from overfitting each ensemble training cycle. The mean squared normalized error (MSE) was used as a measure of model performance. Model training was stopped when the performance assessed using the validation subset group failed to improve or remained the same for 20 epochs. The weights and biases at the minimum of the validation error were returned for each ensemble model.

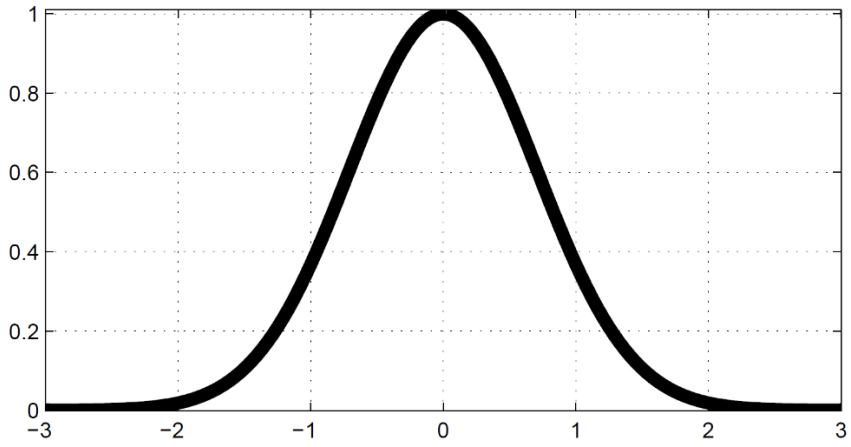

Figure 9. Radial Basis transfer function (radbas)

$$f(x) = e^{-x^2}$$

Equation 4. Radial Basis transfer function

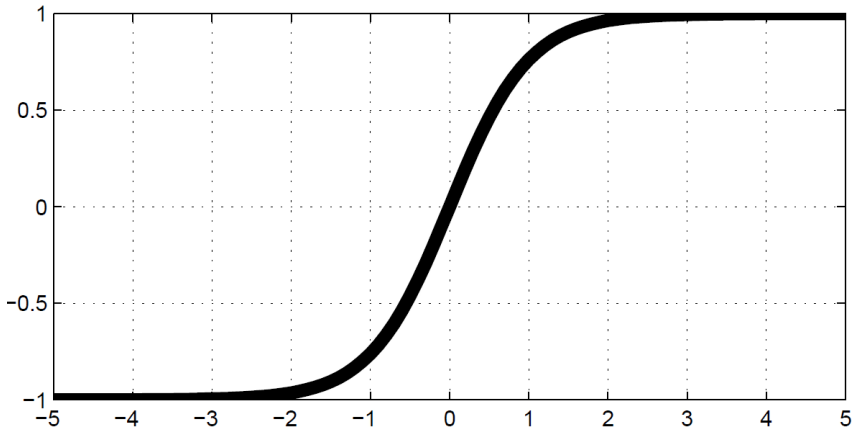

Figure 10. Hyperbolic Tangent Sigmoid transfer function (tansig)

$$f(x) = \frac{2}{(1 + e^{(-2x)})} - 1$$

Equation 5. Hyperbolic Tangent Sigmoid transfer function

The optimal number of neurons in hidden layers (or optimal ANN topology, in other words) for all evaluated MLNN models were found iteratively. All possible combinations of neurons in hidden layers were combined to the maximum count of 100 neurons in each hidden layer for every evaluated MLNN model. For each MLNN ensemble (hidden neurons combination), the median and standard deviation from MSE of the testing subset was calculated. The optimal topology was the one that had the smallest S_{err} (Eq.6) value. This process is described in Figure 11.

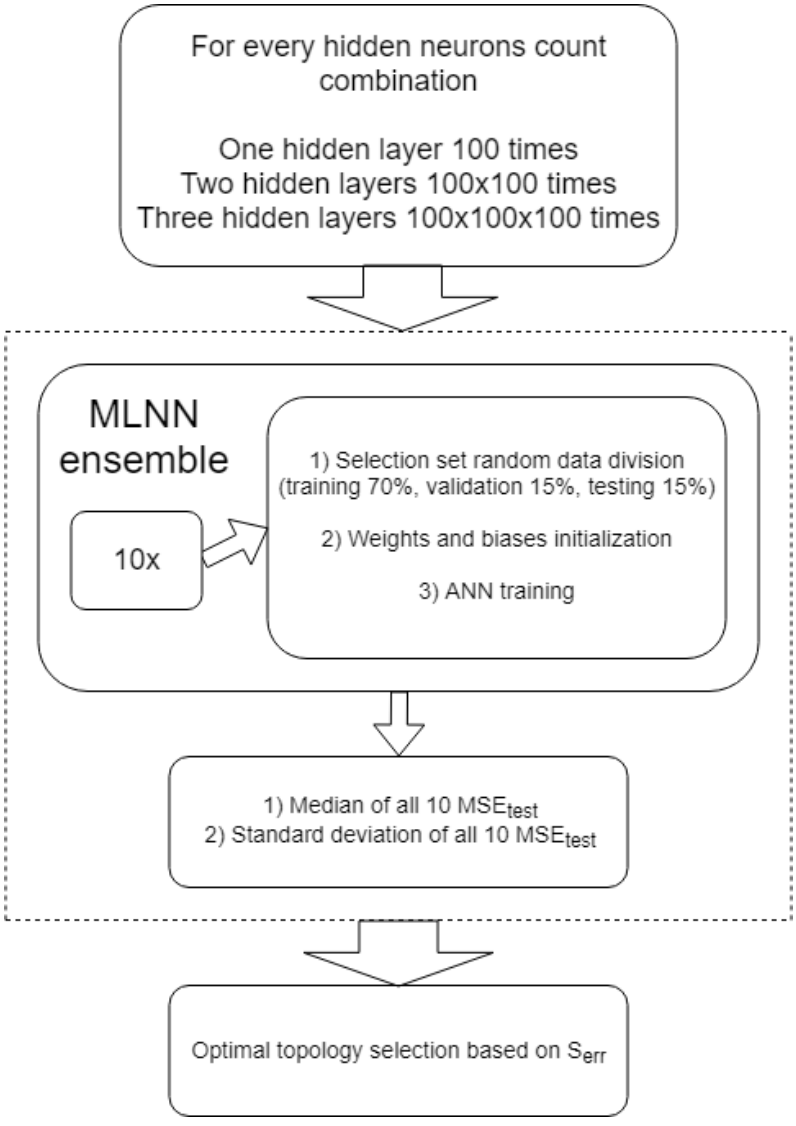

Figure 11. Optimal hidden layer neuron number selection process

$$\boldsymbol{S_{\mathrm{Err}} = Median(MSE_{Test}) + SD(MSE_{Test})} \quad [-]$$

Equation 6. S_{err} for optimal topology selection

The Radial Basis transfer Function (radbas) (Figure 9, Eq.(4)), Hyperbolic Tangent Sigmoid transfer Function (tansig) (Figure 10, Eq.(5)), Log-sigmoid transfer Function (logsig) (Figure 12, Eq.(7)) and Linear transfer Function (purelin) (Figure 13, Eq.(8)) were evaluated in the hidden layers. Radbas, tansig and logsig functions are presented for their good ability to approximate multivariate functions [79, 81, 92–95] and purelin to evaluate regression power in the nonlinear space.

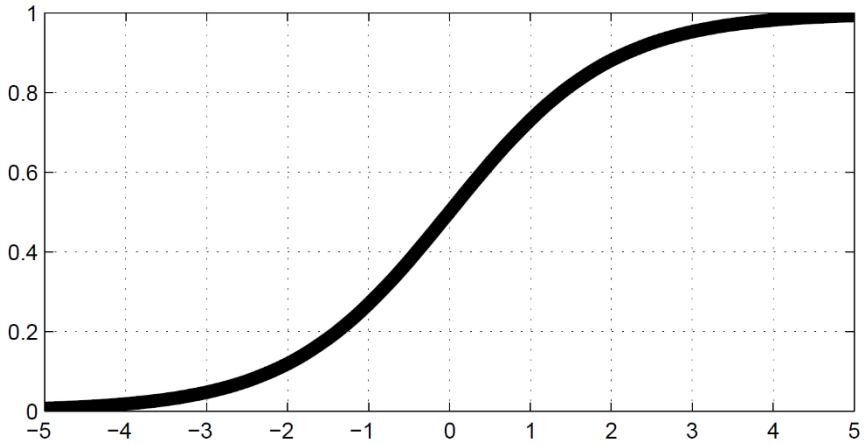

Figure 12. Log-sigmoid transfer function (logsig)

$$f(x) = \frac{1}{1 + e^{-x}}$$

Equation 7. Log-sigmoid transfer function

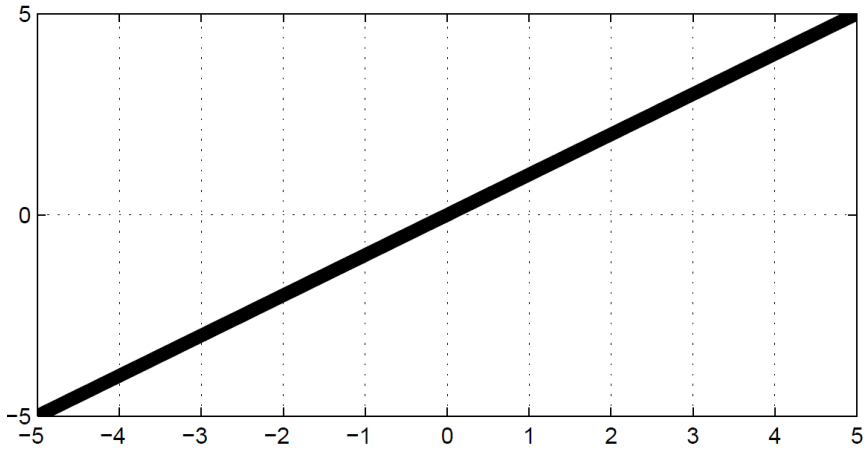

Figure 13. Linear transfer function (purelin)

$$f(x) = x$$

Equation 8. Linear transfer function

SVM is a supervised machine learning method that serves mainly for classification and, in our case, for regression analysis. The aim of this algorithm is to find a super-plane that optimally splits the feature space so that training data belonging to different classes lie in separable spaces. To find such a super-plane for non-linear data, a kernel trick is used which takes the existing feature space data and maps it into space with a greater number of dimensions where it is already linearly separable [96, 97]. SVM methods find their application, for example, in the field of financial forecasting [98], travel time prediction [99] and flood forecasting [100].

This particular SVM model was designed and trained using the **fitrsvm** method. Determining the appropriate hyperparameters for a given task is one of the most important steps in designing the model, and for which the duration of training and testing, but above all, the accuracy of the model depends [101]. A sequential minimal optimization algorithm [102] with 30% randomly selected data for holdout validation was used. The optimal hyperparameters of the model were identified using **OptimizeHyperparameters.** The Bayesian Optimizer (BO) [103] with an Expected Improvement Plus (EIP) Acquisition Function, which is considered a better alternative to a grid or random search [104], searched for the optimal kernel function, kernel scale, epsilon, box constraint and polynomial order.

BRTE is a machine learning algorithm that consists of a sequence of decisions that results in the inclusion of an object into one of the end nodes based on the properties of the object under investigation. In each leaf node, the variable is determined by two conditions; how the data file is divided and the boundary that determines where the split is to be performed. The root of the tree contains the entire data file. Each tree node grows into two more branches. Each end node is assigned a value that is calculated as the arithmetic mean of all object values in the relevant sheet [105]. Decision tree regression is used for diabetes prediction [106], soft classification [107] or feature selection [108].

Our BRTE model was designed and trained using the **fitrtree** method. **OptimizeHyperparameters** using BO with the EIP Acquisition Function searched for the minimal number of leaf node observations and the maximal number of branch nodes.

Individual ensemble learning models, and in our case regression trees, are composed of a weighted combination of several regression trees to yield a final model with increased predictive performance. Boosting is the technique where the models are built sequentially in series, and the parameters of each new model are adjusted based on the learning success of the previously trained model [109, 110]. Ensembling was also used for all ANN models presented in this work. The ensemble median is calculated for several randomly trained ANN models as proposed since it has shown to be a better technique for error elimination than average [111].

The ensemble model was designed and trained using the **fitrensemble** method. **OptimizeHyperparameters** using BO with the EIP Acquisition Function searched for the ensemble aggregation method, optimal number of predictors to select at random for each split, number of ensemble learning cycles, learn rate, minimal number of leaf node

observations, maximal number of branch nodes and number of predictors to select at random for each split.

GPR regression is a probabilistic nonparametric algorithm and a simple extension to the linear regression model. It shows that any finite collection of observations has a multivariate normal distribution, and its characteristics can be completely specified by their mean function or kernel (covariance) function. The response of the model is modeled using a probability distribution over a space of functions. Whereas the Gaussian process is probabilistic, it is possible to compute the prediction intervals using the trained model. The largest variance occurs in regions with several training sessions, while the highest degree of certainty is in regions with a significant number of training sessions [112]. Gaussian process regression is ubiquitous in spatial statistics, surrogate modeling of computer simulation experiments, and ordinal or large dataset regression [113, 114].

Our GPR model was designed and trained using the **fitrgp** method. **OptimizeHyperparameters** using BO with the EIP Acquisition Function searched for the explicit basis function in the GPR model, optimal covariance function, value of the kernel scale parameter and initial value for the standard deviation of noise of the Gaussian process model.

SR is a method of finding a model with the highest quality of prediction and the lowest number of independent inputs. The principle of SR is that the regression model is built step-by-step so that at each step, we examine all the predictors and find out which one describes the best variability of the dependent variable. An algorithm that controls the order of the variables entering the model can work either in a forward or backward mode. In forward mode, predictors are added to the final model and, conversely, are excluded in the backward mode. The insertion of the predictor into the model or its exclusion is done by sequential F-tests. After selecting the model variables, the linear regression function parameters are estimated, and the regression quality is evaluated by the determination index [115]. Application of stepwise regression can be found in the field of electric energy consumption prediction [116] or plant health detection [117].

The SR model was designed and trained using the **stepwiselm** method. The starting model for stepwise regression contained and intercept, linear terms for each predictor, and all products of pairs of distinct predictors. The P-value criterion for an F-test of the change in the sum of the squared error that determines whether to add or remove the terms was set to 0.05. Any linearly dependent term was removed. The specific model is described by Wilkinson notation [118].

Unless otherwise mentioned, the default values of the Matlab functions were used and can be found in the Matlab documentation [77]. As a conclusion drawn from the above, all these machine learning algorithms should be able to effectively approximate the environment that affects the refractive result for a particular artificial IOL type.

3.6. Results evaluation and statistical analysis

The results predicted by each model were compared to the achieved clinical results (CR), and all models were compared mutually at the end of the results chapter. In the results evaluation and statistical analysis, the recommendations described in the work of Wang [119] were followed. The mean numerical prediction error (ME), mean absolute prediction error (MAE), median absolute prediction error (MedAE), standard deviation (STD), minimum prediction error (Min), and maximum prediction error (Max) as well as the percentage of eyes within prediction error (PE) targets of ±0.25 D, ±0.50 D, ±0.75 D, ±1.00 D were determined for Rx_{post} in the case of the CR and for the refraction calculated from $IOL_{Predicted}$ ($Rx_{predicted}$) in the case of the result predicted by the model (MPR). The $Rx_{predicted}$ calculation is described by Eq.(9).

$$Rx_{predicted} = \left(\frac{IOL_{Implanted} - IOL_{Predicted}}{0.5}\right) * Rx_{05IOL} + Rx_{post}$$

Equation 9. Calculation of $Rx_{predicted}$ from $IOL_{Predicted}$

Since axial length (AL) of the eye is considered the most important characteristic in predicting IOL power [120], the evaluation process is usually divided into subgroups based on AL [119]. The Verification set was thus divided into the following AL subgroups:

- SHORT eyes group – eyes with AL <= 22 mm (81 samples)
- MEDIUM eyes group – eyes with 22 mm < AL < 24 mm (480 samples)
- LONG eyes group – eyes with AL => 24 mm (94 samples)
- ALL eyes group – entire Verification set of all eyes (655 samples)

The statistical analysis was performed using Matlab 2017a (MathWorks, Natick, MA, USA).

The Wilcoxon test [121] was used to asses MAE and MedAE differences between the CR and MPR. The McNemar test with Yates' correction [122] was used to evaluate the difference in the percentage of eyes of certain PE diopter groups between CR and MPR. Statistical significance of ME is reported only for MPR in case of its significant difference from zero evaluated using one sample T-Test. The Cochran Q test [123] was used to test the difference across models. Since some statisticians recommend not ever correcting for multiple comparisons, all individual P values and significance levels (P<.05, P<.01, P<.001, P<.0001) were reported [124, 125].

In the mutual evaluation section, the best models were selected based on the following criterion:

- Best result in the ±0.25 D PE group
- Best or insignificantly worse results in the ±0.50 D, ±0.75 D and ±1.00 D PE groups as compared to all models with higher accuracy tested using the McNemar test with Yates' correction

4. RESULTS

The results of the evaluated algorithms are separated into tables for clarity. First, the model parameter tables obtained in the design and training phase using the Selection set are presented. The MPR – model prediction results for ALL, SHORT, MEDIUM, and LONG eyes that were obtained using the Verification set are presented in context to the CR – clinical results. At the end of this chapter, the results of all methods are summarized and mutually compared and then disc insignificantlyussed in the Discussion and Conclusions chapter.

4.1. Feed-Forward MLNN - One hidden layer

4.1.1. Radial Basis transfer function

The model had one hidden layer with six hidden layer neurons (Table 4).

Layer	Neurons	Transfer function
Input	5	-
Hidden	6	radbas
Output	1	purelin

Table 4. ANN topology description - One hidden layer (radbas)

The model's train, validation, and test performances are presented in Table 5.

Parameter	Mean	Median	Std	Min	Max
Train	0.00302	0.00298	0.00008	0.00288	0.00313
Validation	0.00322	0.00321	0.00015	0.00300	0.00349
Test	0.00332	0.00323	0.00024	0.00293	0.00380
Epoch	26.4	19	18.1	9	70

Table 5. ANN model performance - One hidden layer (radbas)

MPR for the ALL eyes group are presented in Table 6. Compared to the CR, the ANN model with one hidden layer using RBF as a transfer function produces better results for all evaluated parameters. Compared to CR, all statistically tested parameters are significantly better at the level of significance 0.0001. The maximum prediction error is slightly worse for the ANN model.

PE [D]	CR	MPR	P value
ME	-0.46	-0.01	CR: < .0001, MPR: 0.68
MAE	0.52	0.31	< .0001
MedAE	0.50	0.26	
Std	0.43	0.39	-
Min	-1.87	-1.51	-
Max	1.12	1.31	-
Eyes within PE [%]			
±0.25	33.4	48.8	< .0001
±0.50	57.7	82.3	< .0001
±0.75	79.3	93.9	< .0001
±1.00	91.7	97.6	< .0001

Table 6. Prediction errors in the ALL axial length group - One hidden layer (radbas)

MPR for the SHORT eyes group are presented in Table 7. Compared to the CR, the ANN model performs better for most cases. Only the ±0.25 and ±1.00 prediction error groups fail to prove significance at a level of 0.05.

PE [D]	CR	MPR	P value
ME	-0.37	0.05	CR: < .0001, MPR: 0.28
MAE	0.46	0.32	< .0001
MedAE	0.50	0.25	
Std	0.46	0.40	-
Min	-1.50	-0.92	-
Max	1.13	1.01	-
Eyes within PE [%]			
±0.25	40.7	51.9	0.21
±0.50	62.9	77.8	< .05
±0.75	85.1	95.1	< .05
±1.00	92.5	98.8	0.13

Table 7. Prediction errors in the SHORT axial length group - One hidden layer (radbas)

MPR for the MEDIUM eyes group are presented in Table 8. Compared to the CR, the ANN model performs significantly better for all statistically tested cases at the level 0.0001 except the ±1.00 PE group where the result was significantly better at the level 0.001. The maximum prediction error is slightly worse for the ANN model.

PE [D]	CR	MPR	P value
ME	-0.47	-0.01	CR: < .0001, MPR: 0.82
MAE	0.52	0.31	< .0001
MedAE	0.50	0.26	
Std	0.42	0.40	-
Min	-1.88	-1.52	-
Max	0.88	1.31	-
Eyes within PE [%]			
±0.25	33.1	48.5	< .0001
±0.50	56.8	82.7	< .0001
±0.75	79.7	93.8	< .0001
±1.00	92.9	97.7	< .001

Table 8. Prediction errors in the MEDIUM axial length group - One hidden layer (radbas)

MPR for the LONG eyes group are presented in Table 9. Compared to the CR, the ANN model performs significantly better for all statistically tested cases; for the MAE, MedAE, ±0.50 PE group and ±0.75 PE group at the level 0.0001, for the ±1.00 PE group at the level 0.001 and for the ±0.25 PE group at the level 0.05. The maximum prediction error is slightly worse for the ANN model.

PE [D]	CR	MPR	P value
ME	-0.53	-0.08	CR: < .0001, MPR: 0.08
MAE	0.57	0.31	< .0001
MedAE	0.50	0.26	
Std	0.44	0.40	-
Min	-1.63	-1.03	-
Max	0.88	1.32	-
Eyes within PE [%]			
±0.25	28.7	47.9	< .05
±0.50	57.4	84.0	< .0001
±0.75	72.3	93.6	< .0001
±1.00	85.1	95.7	< .001

Table 9. Prediction errors in the LONG axial length group - One hidden layer (radbas)

4.1.2. Hyperbolic Tangent Sigmoid transfer function

The model had one hidden layer with 13 hidden layer neurons (Table 10).

Layer	Neurons	Transfer function
Input	5	-
Hidden	13	tansig
Output	1	purelin

Table 10. ANN topology description - One hidden layer (tansig)

The model's train, validation, and test performances are presented in Table 11.

Parameter	Mean	Median	Std	Min	Max
Train	0.00285	0.00289	0.00007	0.00267	0.00297
Validation	0.00330	0.00327	0.00025	0.00292	0.00385
Test	0.00338	0.00336	0.00038	0.00295	0.00399
Epoch	9.6	8	5.2	5	20

Table 11. ANN model performance - One hidden layer (tansig)

MPR for the ALL eyes group are presented in Table 12. Compared to CR the ANN model with one hidden layer using Hyperbolic Tangent Sigmoid as a transfer function produces better results for all evaluated parameters. All statistically tested parameters prove that results are significantly better at the level of significance 0.0001. The maximum prediction error is slightly worse for the ANN model.

PE [D]	CR	MPR	P value
ME	-0.46	0.00	CR: < .0001, MPR: 0.58
MAE	0.52	0.31	< .0001
MedAE	0.50	0.26	
Std	0.43	0.39	-
Min	-1.87	-1.54	-
Max	1.12	1.29	-
Eyes within PE [%]			
±0.25	33.4	47.6	< .0001
±0.50	57.7	82.6	< .0001
±0.75	79.3	93.7	< .0001
±1.00	91.7	97.6	< .0001

Table 12. Prediction errors in the ALL axial length group - One hidden layer (tansig)

MPR for the SHORT eyes group are presented in Table 13. Compared to the CR, the ANN model performs significantly better for most cases; for MAE and MedAE at the level 0.0001, for the ±0.50, ±0.75 and ±1.00 PE groups at the level 0.05. Only ±0.25 prediction error group fails to prove significance at the level of 0.05.

PE [D]	CR	MPR	P value
ME	-0.37	0.00	CR: < .0001, MPR: 0.76
MAE	0.46	0.33	< .0001
MedAE	0.50	0.29	
Std	0.46	0.40	-
Min	-1.50	-0.95	-
Max	1.13	0.89	-
Eyes within PE [%]			
±0.25	40.7	48.1	0.40
±0.50	63.0	77.8	< .05
±0.75	85.2	95.1	< .05
±1.00	92.6	100.0	< .05

Table 13. Prediction errors in the SHORT axial length group - One hidden layer (tansig)

MPR for the MEDIUM eyes group are presented in Table 14. Compared to the CR, the ANN model performs significantly better for all statistically tested cases at level 0.0001. The maximum prediction error is worse for the ANN model.

PE [D]	CR	MPR	P value
ME	-0.47	0.01	CR: < .0001, MPR: 0.42
MAE	0.52	0.31	< .0001
MedAE	0.50	0.26	
Std	0.42	0.40	-
Min	-1.88	-1.55	-
Max	0.88	1.30	-
Eyes within PE [%]			
±0.25	33.1	48.3	< .0001
±0.50	56.9	83.1	< .0001
±0.75	79.8	93.5	< .0001
±1.00	92.9	97.1	< .0001

Table 14. Prediction errors in the MEDIUM axial length group - One hidden layer (tansig)

MPR for the LONG eyes group are presented in Table 15. Compared to the CR, the ANN model performs significantly better for most cases at level 0.0001. Only the ±0.25 prediction error group fails to prove significance at the level of 0.05.

PE [D]	CR	MPR	P value
ME	-0.53	-0.04	CR: < .0001. MPR: 0.42
MAE	0.57	0.31	< .0001
MedAE	0.50	0.28	-
Std	0.44	0.39	-
Min	-1.63	-1.01	-
Max	0.88	1.25	-
Eyes within PE [%]			
±0.25	28.7	43.6	0.06
±0.50	57.4	84.0	< .0001
±0.75	72.3	93.6	< .0001
±1.00	85.1	97.9	< .0001

Table 15. Prediction errors in the LONG axial length group - One hidden layer (tansig)

4.1.3. Log-Sigmoid transfer function

The model had one hidden layer with five hidden layer neurons (Table 16).

Layer	Neurons	Transfer function
Input	5	-
Hidden	5	logsig
Output	1	purelin

Table 16. ANN topology description - One hidden layer (logsig)

The model's train, validation, and test performances are presented in Table 17.

Parameter	Mean	Median	Std	Min	Max
Train	0.00302	0.00304	0.00011	0.00286	0.00320
Validation	0.00320	0.00313	0.00032	0.00287	0.00378
Test	0.00333	0.00330	0.00025	0.00293	0.00381
Epoch	21.9	20	11.1	9	46

Table 17. ANN model performance - One hidden layer (logsig)

MPR for the ALL eyes group are presented in Table 18. Compared to the CR, the ANN model with one hidden layer using Log-Sigmoid as a transfer function produces better results for all evaluated parameters. All statistically tested parameters prove that results are significantly better at the level of significance 0.0001. The maximum prediction error is slightly worse for the ANN model.

PE [D]	CR	MPR	P value
ME	-0.46	0.01	CR: < .0001, MPR: 0.48
MAE	0.52	0.31	< .0001
MedAE	0.50	0.26	
Std	0.43	0.40	-
Min	-1.88	-1.52	-
Max	1.13	1.35	-
Eyes within PE [%]			
±0.25	33.4	48.4	< .0001
±0.50	57.7	82.6	< .0001
±0.75	79.4	93.4	< .0001
±1.00	91.8	97.9	< .0001

Table 18. Prediction errors in the ALL axial length group - One hidden layer (logsig)

MPR for the SHORT eyes group are presented in Table 19. Compared to the CR, the ANN model performs significantly better for MAE and MedAE at level 0.0001, and for ±0.50 and ±0.75 PE groups at level 0.05. Only the ±0.25 and ±1.00 prediction error groups fail to prove significance at level 0.05.

PE [D]	CR	MPR	P value
ME	-0.37	0.02	CR: < .0001, MPR: 0.42
MAE	0.46	0.33	< .0001
MedAE	0.50	0.27	
Std	0.46	0.41	-
Min	-1.50	-1.03	-
Max	1.13	0.95	-
Eyes within PE [%]			
±0.25	40.7	46.9	0.52
±0.50	63.0	76.5	< .05
±0.75	85.2	93.8	< .05
±1.00	92.6	98.8	0.07

Table 19. Prediction errors in the SHORT axial length group - One hidden layer (logsig)

MPR for the MEDIUM eyes group are presented in Table 20. Compared to the CR, the ANN model performs significantly better for all statistically tested cases at level 0.0001. The maximum prediction error is worse for the ANN model.

PE [D]	CR	MPR	P value
ME	-0.47	0.01	CR: < .0001, MPR: 0.50
MAE	0.52	0.31	< .0001
MedAE	0.50	0.25	
Std	0.42	0.40	-
Min	-1.88	-1.52	-
Max	0.88	1.34	-
Eyes within PE [%]			
±0.25	33.1	49.2	< .0001
±0.50	56.9	83.3	< .0001
±0.75	79.8	93.3	< .0001
±1.00	92.9	97.5	< .0001

Table 20. Prediction errors in the MEDIUM axial length group - One hidden layer (logsig)

MPR for the LONG eyes group are presented in Table 21. Compared to the CR, the ANN model performs significantly better for most cases at level 0.0001 except for the ±0.25 PE group, which is significantly better at level 0.05. The maximum prediction error is worse for the ANN model.

PE [D]	CR	MPR	P value
ME	-0.53	-0.03	CR: < .0001, MPR: 0.56
MAE	0.57	0.32	< .0001
MedAE	0.50	0.28	
Std	0.44	0.40	-
Min	-1.63	-0.99	-
Max	0.88	1.35	-
Eyes within PE [%]			
±0.25	28.7	45.7	< .05
±0.50	57.4	84.0	< .0001
±0.75	72.3	93.6	< .0001
±1.00	85.1	98.9	< .0001

Table 21. Prediction errors in the LONG axial length group - One hidden layer (logsig)

4.1.4. Linear transfer function

The model had one hidden layer with five hidden layer neurons (Table 22).

Layer	Neurons	Transfer function
Input	5	-
Hidden	5	purelin
Output	1	purelin

Table 22. ANN model topology - One hidden layer (purelin)

The model's train, validation, and test performances are presented in Table 23.

Parameter	Mean	Median	Std	Min	Max
Train	0.00345	0.00341	0.00010	0.00335	0.00370
Validation	0.00331	0.00327	0.00034	0.00286	0.00393
Test	0.00347	0.00352	0.00028	0.00303	0.00395
Epoch	3.5	3.5	0.5	3	4

Table 23. ANN model performance - One hidden layer (purelin)

MPR for the ALL eyes group are presented in Table 24. Compared to the CR, the ANN model with one hidden layer using the Linear transfer function produces better results for all evaluated parameters. All statistically tested parameters are significantly better at the level of significance of 0.0001. The maximum prediction error is worse for the ANN model.

PE [D]	CR	MPR	P value
ME	-0.46	0.01	CR: < .0001, MPR: 0.67
MAE	0.52	0.33	< .0001
MedAE	0.50	0.28	
Std	0.43	0.42	-
Min	-1.88	-1.57	-
Max	1.13	2.05	-
Eyes within PE [%]			
±0.25	33.4	45.3	< .0001
±0.50	57.7	79.8	< .0001
±0.75	79.4	93.4	< .0001
±1.00	91.8	97.9	< .0001

Table 24. Prediction errors in the ALL axial length group - One hidden layer (purelin)

MPR for the SHORT eyes group are presented in Table 25. Compared to the CR, the ANN model performs insignificantly worse for the ±0.25 PE group. MAE and MedAE are significantly better at level 0.0001. All other prediction error groups are insignificantly better. The standard deviation appears to be the same. ME is significantly different from zero for the model.

PE [D]	CR	MPR	P value
ME	-0.37	0.19	CR: < .0001, MPR: < .001
MAE	0.46	0.39	< .0001
MedAE	0.50	0.36	
Std	0.46	0.46	-
Min	-1.50	-0.65	-
Max	1.13	1.85	-
Eyes within PE [%]			
±0.25	40.7	38.3	0.88
±0.50	63.0	71.6	0.32
±0.75	85.2	93.8	0.12
±1.00	92.6	96.3	0.45

Table 25. Prediction errors in the SHORT axial length group - One hidden layer (purelin)

MPR for the MEDIUM eyes group are presented in Table 26. Compared to the CR, the ANN model performs significantly better for all prediction error groups. ME is significantly different from zero for the model. MAE is significantly better for the ANN model. MedAE is better for the ANN model. The maximum prediction error is worse for the ANN model.

PE [D]	CR	MPR	P value
ME	-0.47	-0.05	CR: < .0001, MPR: < .05
MAE	0.52	0.31	< .0001
MedAE	0.50	0.27	
Std	0.42	0.39	-
Min	-1.88	-1.57	-
Max	0.88	1.27	-
Eyes within PE [%]			
±0.25	33.1	46.3	< .0001
±0.50	56.9	82.5	< .0001
±0.75	79.8	93.5	< .0001
±1.00	92.9	98.1	< .0001

Table 26. Prediction errors in the MEDIUM axial length group - One hidden layer (purelin)

MPR for the LONG eyes group are presented in Table 27. Compared to the CR, the ANN model performs significantly better for MAE and MedAE at level 0.0001 and for the ±0.25, ±0.50, ±0.75 and ±1.00 PE groups at level 0.05. The maximum prediction error and standard deviation are worse for the ANN model. ME is significantly different from zero for the model.

PE [D]	**CR**	**MPR**	**P value**
ME	-0.53	0.14	CR: < .0001, MPR: < .05
MAE	0.57	0.36	< .0001
MedAE	0.50	0.29	
Std	0.44	0.46	-
Min	-1.63	-0.80	-
Max	0.88	2.05	-
Eyes within PE [%]			
±0.25	28.7	46.8	< .05
±0.50	57.4	73.4	< .05
±0.75	72.3	92.6	< .05
±1.00	85.1	97.9	< .05

Table 27. Prediction errors in the LONG axial length group - One hidden layer (purelin)

4.2. Feed-Forward MLNN - Two hidden layers

4.2.1. Radial Basis transfer function

The model had two hidden layers with 10 hidden layer neurons in the first hidden layer and three hidden layer neurons in the second hidden layer (Table 28).

Layer	Neurons	Transfer function
Input	5	-
Hidden - First	10	radbas
Hidden - Second	3	radbas
Output	1	purelin

Table 28. ANN topology description - Two hidden layers (radbas)

The model's train, validation, and test performances are presented in Table 29.

Parameter	Mean	Median	Std	Min	Max
Train	0.00300	0.00297	0.00020	0.00273	0.00332
Validation	0.00357	0.00360	0.00040	0.00304	0.00413
Test	0.00354	0.00368	0.00038	0.00284	0.00398
Epoch	18.5	15	10.1	11	45

Table 29. ANN model performance - Two hidden layers, Radial Basis transfer Function

MPR for the ALL eyes group are presented in Table 30. All tested parameters are significantly better than CR. The maximum prediction error is worse for the ANN model.

PE [D]	CR	MPR	P value
ME	-0.46	0.00	CR: < .0001, MPR: 0.62
MAE	0.52	0.31	< .0001
MedAE	0.50	0.26	
Std	0.43	0.40	-
Min	-1.88	-1.49	-
Max	1.13	1.31	-
Eyes within PE [%]			
±0.25	33.4	47.8	< .0001
±0.50	57.7	82.1	< .0001
±0.75	79.4	93.6	< .0001
±1.00	91.8	97.7	< .0001

Table 30. Prediction errors in the ALL axial length group - Two hidden layers (radbas)

MPR for the SHORT eyes group are presented in Table 31. MAE and MedAE are significantly better for the ANN model. MPR for PE groups ±0.25, ±0.50, ±0.75 and ±1.00 are insignificantly better. The maximum prediction error is worse for the ANN model.

PE [D]	CR	MPR	P value
ME	-0.37	0.07	CR: < .0001, MPR: 0.12
MAE	0.46	0.34	< .0001
MedAE	0.50	0.28	
Std	0.46	0.42	-
Min	-1.50	-0.99	-
Max	1.13	1.31	-
Eyes within PE [%]			
±0.25	40.7	46.9	0.54
±0.50	62.9	74.1	0.15
±0.75	85.1	93.8	0.10
±1.00	92.5	98.8	0.13

Table 31. Prediction errors in the SHORT axial length group - Two hidden layers (radbas)

MPR for the MEDIUM eyes group are presented in Table 32. Most of the tested variables are significantly better for the ANN model at level 0.0001. PE group ±1.00 is significantly better at level 0.001. The maximum prediction error is worse for the ANN model.

PE [D]	CR	MPR	P value
ME	-0.47	0.00	CR: < .0001, MPR: 0.66
MAE	0.52	0.31	< .0001
MedAE	0.50	0.25	
Std	0.42	0.39	-
Min	-1.88	-1.49	-
Max	0.88	1.28	-
Eyes within PE [%]			
±0.25	33.1	48.5	< .0001
±0.50	56.9	83.1	< .0001
±0.75	79.8	93.5	< .0001
±1.00	92.9	97.5	< .001

Table 32. Prediction errors in the MEDIUM axial length group - Two hidden layers (radbas)

MPR for the LONG eyes group are presented in Table 33. All tested variables are significantly better for the ANN model; MAE, MedAE, ±0.50 PE group and ±0.75 PE group at level 0.0001 and ±0.25 and ±0.75 PE group at level 0.05. The maximum prediction error is worse for the ANN model.

PE [D]	CR	MPR	P value
ME	-0.53	-0.06	CR: < .0001, MPR: 0.22
MAE	0.57	0.32	< .0001
MedAE	0.50	0.27	
Std	0.44	0.39	-
Min	-1.63	-1.05	-
Max	0.88	1.09	-
Eyes within PE [%]			
±0.25	28.7	44.7	< .05
±0.50	57.4	84.0	< .0001
±0.75	72.3	93.6	< .0001
±1.00	85.1	97.9	< .05

Table 33. Prediction errors in the LONG axial length group - Two hidden layers (radbas)

4.2.2. Hyperbolic Tangent Sigmoid transfer function

The model had two hidden layers with five hidden layer neurons in the first hidden layer and four hidden layer neurons in the second hidden layer (Table 34).

Layer	Neurons	Transfer function
Input	5	-
Hidden - First	5	tansig
Hidden - Second	4	tansig
Output	1	purelin

Table 34. ANN topology description - Two hidden layers (tansig)

The model's train, validation, and test performances are presented in Table 35.

Parameter	Mean	Median	Std	Min	Max
Train	0.00297	0.00297	0.00013	0.00278	0.00327
Validation	0.00339	0.00335	0.00030	0.00293	0.00397
Test	0.00353	0.00361	0.00032	0.00298	0.00394
Epoch	16.7	15	6.2	9	27

Table 35. ANN model performance - Two hidden layers (tansig)

MPR for the ALL eyes group are presented in Table 36. All tested parameters are significantly better than CR at level 0.0001. The maximum prediction error is worse for the ANN model.

PE [D]	CR	MPR	P value
ME	-0.46	0.01	CR: < .0001, MPR: 0.44
MAE	0.52	0.31	< .0001
MedAE	0.50	0.25	
Std	0.43	0.39	-
Min	-1.88	-1.52	-
Max	1.13	1.34	-
Eyes within PE [%]			
±0.25	33.4	47.8	< .0001
±0.50	57.7	82.6	< .0001
±0.75	79.4	94.0	< .0001
±1.00	91.8	97.9	< .0001

Table 36. Prediction errors in the ALL axial length group - Two hidden layers (tansig)

MPR for the SHORT eyes group are presented in Table 37. MAE and MedAE are significantly better than CR at level 0.0001. The ±0.50 and ±0.75 PE groups at level 0.05 and the ±0.25 and ±1.00 PE groups fail to prove significance at level 0.05.

PE [D]	CR	MPR	P value
ME	-0.37	0.01	CR: < .0001, MPR: 0.57
MAE	0.46	0.32	< .0001
MedAE	0.50	0.28	
Std	0.46	0.40	-
Min	-1.50	-0.97	-
Max	1.13	1.07	-
Eyes within PE [%]			
±0.25	40.7	46.9	0.635
±0.50	63.0	74.1	< .05
±0.75	85.2	93.8	< .05
±1.00	92.6	98.8	0.131

Table 37. Prediction errors in the SHORT axial length group - Two hidden layers (tansig)

MPR for the MEDIUM eyes group are presented in Table 38. All tested parameters are significantly better than CR at level 0.0001 and 0.001 for ±1.00 PE group. The maximum prediction error is worse for the ANN model.

PE [D]	CR	MPR	P value
ME	-0.47	0.01	CR: < .0001, MPR: 0.42
MAE	0.52	0.30	< .0001
MedAE	0.50	0.25	
Std	0.42	0.39	-
Min	-1.88	-1.52	-
Max	0.88	1.34	-
Eyes within PE [%]			
±0.25	33.1	48.5	< .0001
±0.50	56.9	83.1	< .0001
±0.75	79.8	93.5	< .0001
±1.00	92.9	97.5	< .001

Table 38. Prediction errors in the MEDIUM axial length group - Two hidden layers (tansig)

MPR for the LONG eyes group are presented in Table 39. Most of the parameters tested are significantly better than CR; MAE, MedAE, ±0.50 PE group and ±0.75 PE group at level 0.0001; PE group ±1.00 at level 0.001. PE group ±0.25 is insignificantly better. The maximum prediction error is worse for the ANN model.

PE [D]	CR	MPR	P value
ME	-0.53	-0.02	CR: < .0001, MPR: 0.68
MAE	0.57	0.31	< .0001
MedAE	0.50	0.28	
Std	0.44	0.39	-
Min	-1.63	-0.99	-
Max	0.88	1.29	-
Eyes within PE [%]			
±0.25	28.7	44.7	0.05
±0.50	57.4	84.0	< .0001
±0.75	72.3	93.6	< .0001
±1.00	85.1	97.9	< .001

Table 39. Prediction errors in the LONG axial length group - Two hidden layers (tansig)

4.2.3. Log-Sigmoid transfer function

The model had two hidden layers with five hidden layer neurons in the first hidden layer and four hidden layer neurons in the second hidden layer (Table 40).

Layer	Neurons	Transfer function
Input	5	-
Hidden - First	5	logsig
Hidden - Second	4	logsig
Output	1	purelin

Table 40. ANN topology description - Two hidden layers (logsig)

The model's train, validation, and test performances are presented in Table 41.

Parameter	Mean	Median	Std	Min	Max
Train	0.00294	0.00294	0.00010	0.00273	0.00306
Validation	0.00329	0.00325	0.00022	0.00303	0.00369
Test	0.00335	0.00337	0.00036	0.00286	0.00400
Epoch	19	16.5	10.5	8	41

Table 41. ANN model performance - Two hidden layers (logsig)

MPR for the ALL eyes group are presented in Table 42. All tested parameters are significantly better than CR. The maximum prediction error is worse for the ANN model.

PE [D]	CR	MPR	P value
ME	-0.46	0.00	CR: < .0001, MPR: 0.62
MAE	0.52	0.31	< .0001
MedAE	0.50	0.26	
Std	0.43	0.39	-
Min	-1.88	-1.53	-
Max	1.13	1.36	-
Eyes within PE [%]			
±0.25	33.4	48.1	< .0001
±0.50	57.7	82.3	< .0001
±0.75	79.4	93.6	< .0001
±1.00	91.8	97.6	< .0001

Table 42. Prediction errors in the ALL axial length group - Two hidden layers (logsig)

MPR for the SHORT eyes group are presented in Table 43. MAE and MedAE are significantly better at level 0.0001 and PE group ±0.50 and ±0.75 at level 0.05. Only the ±0.25 and ±1.00 PE groups are insignificantly better.

PE [D]	CR	MPR	P value
ME	-0.37	0.00	CR: < .0001, MPR: 0.76
MAE	0.46	0.32	< .0001
MedAE	0.50	0.28	
Std	0.46	0.40	-
Min	-1.50	-1.07	-
Max	1.13	1.03	-
Eyes within PE [%]			
±0.25	40.7	45.7	0.63
±0.50	63.0	72.8	< .05
±0.75	85.2	93.8	< .05
±1.00	92.6	97.5	0.22

Table 43. Prediction errors in the SHORT axial length group - Two hidden layers (logsig)

MPR for the MEDIUM eyes group are presented in Table 44. The ANN model performed significantly better for all variables at level 0.0001 except for the ±1.00 PE group, which was significant at level 0.001. The maximum prediction error is worse for the ANN model.

PE [D]	CR	MPR	P value
ME	-0.47	0.01	CR: < .0001, MPR: 0.47
MAE	0.52	0.31	< .0001
MedAE	0.50	0.25	
Std	0.42	0.39	-
Min	-1.88	-1.53	-
Max	0.88	1.30	-
Eyes within PE [%]			
±0.25	33.1	49.0	< .0001
±0.50	56.9	83.5	< .0001
±0.75	79.8	93.5	< .0001
±1.00	92.9	97.5	< .001

Table 44. Prediction errors in the MEDIUM axial length group - Two hidden layers (logsig)

MPR for the LONG eyes group are presented in Table 45. The ANN model performed significantly better for all variables; for MAE, MedAE, ±0.50 PE group and ±0.75 PE group at level 0.0001, for ±0.25 PE group and ±0.75 PE group at level 0.05 and 0.001, respectively. The maximum prediction error is worse for the ANN model.

PE [D]	CR	MPR	P value
ME	-0.53	-0.04	CR: < .0001, MPR: 0.47
MAE	0.57	0.31	< .0001
MedAE	0.50	0.28	
Std	0.44	0.40	-
Min	-1.63	-1.00	-
Max	0.88	1.36	-
Eyes within PE [%]			
±0.25	28.7	45.7	< .05
±0.50	57.4	84.0	< .0001
±0.75	72.3	93.6	< .0001
±1.00	85.1	97.9	< .001

Table 45. Prediction errors in the LONG axial length group - Two hidden layers (logsig)

4.2.4. Linear transfer function

The model had two hidden layers with 17 hidden layer neurons in the first hidden layer and seven hidden layer neurons in the second hidden layer (Table 46).

Layers	Neurons	Transfer function
Input	5	-
Hidden - First	17	purelin
Hidden - Second	7	purelin
Output	1	purelin

Table 46. ANN model topology - Two hidden layers (purelin)

The model's train, validation, and test performances are presented in Table 47.

Parameter	Mean	Median	Std	Min	Max
Train	0.00344	0.00344	0.00003	0.00339	0.00349
Validation	0.00339	0.00341	0.00022	0.00314	0.00383
Test	0.00337	0.00332	0.00025	0.00310	0.00386
Epoch	3.8	4	1.0	2	5

Table 47. ANN model performance - Two hidden layers (purelin)

MPR for the ALL eyes group are presented in Table 48. All tested parameters are significantly better than CR at level 0.0001. The maximum prediction error is worse for the ANN model.

PE [D]	CR	MPR	P value
ME	-0.46	0.01	CR: < .0001, MPR: 0.54
MAE	0.52	0.33	< .0001
MedAE	0.50	0.28	
Std	0.43	0.42	-
Min	-1.88	-1.57	-
Max	1.13	2.04	-
Eyes within PE [%]			
±0.25	33.4	45.5	< .0001
±0.50	57.7	80.3	< .0001
±0.75	79.4	92.8	< .0001
±1.00	91.8	97.9	< .0001

Table 48. Prediction errors in the ALL axial length group - Two hidden layers (purelin)

MPR for the SHORT eyes group are presented in Table 49. PE groups ±0.50, ±0.75, and ±1.00 are insignificantly better than CR. The maximum prediction error is worse for the ANN model. The standard deviation is the same for CR and MPR. ME is better but significantly different from zero for the ANN model. MAE and MedAE are significantly better for the ANN model. PE group ±0.25 is worse for the ANN model.

PE [D]	CR	MPR	P value
ME	-0.37	0.20	CR: < .0001, MPR: < .001
MAE	0.46	0.39	< .0001
MedAE	0.50	0.37	
Std	0.46	0.46	-
Min	-1.50	-0.64	-
Max	1.13	1.87	-
Eyes within PE [%]			
±0.25	40.7	38.3	0.89
±0.50	63.0	70.4	0.42
±0.75	85.2	90.1	0.48
±1.00	92.6	96.3	0.45

Table 49. Prediction errors in the SHORT axial length group - Two hidden layers (purelin)

MPR for the MEDIUM eyes group are presented in Table 50. All tested parameters are significantly better than CR at level 0.0001. ME is better but significantly different from zero for the ANN model. The maximum prediction error is worse for the ANN model.

PE [D]	CR	MPR	P value
ME	-0.47	-0.04	CR: < .0001, MPR: < .05
MAE	0.52	0.31	< .0001
MedAE	0.50	0.27	
Std	0.42	0.40	-
Min	-1.88	-1.57	-
Max	0.88	1.28	-
Eyes within PE [%]			
±0.25	33.1	46.5	< .0001
±0.50	56.9	83.1	< .0001
±0.75	79.8	93.3	< .0001
±1.00	92.9	98.1	< .0001

Table 50. Prediction errors in the MEDIUM axial length group - Two hidden layers (purelin)

MPR for the LONG eyes group are presented in Table 51. All tested parameters are significantly better than CR. For MAE and MedAE at level 0.0001, for ±0.75 PE group at level 0.001, for ±0.25, ±0.50, ±1.00 PE groups at level 0.05. ME is better but significantly different from zero for the ANN model. The maximum prediction error is worse for the ANN model.

PE [D]	CR	MPR	P value
ME	-0.53	0.13	CR: < .0001, MPR: < .05
MAE	0.57	0.36	< .0001
MedAE	0.50	0.29	
Std	0.44	0.45	-
Min	-1.63	-0.81	-
Max	0.88	2.04	-
Eyes within PE [%]			
±0.25	28.7	46.8	< .05
±0.50	57.4	74.5	< .05
±0.75	72.3	92.6	< .001
±1.00	85.1	97.9	< .05

Table 51. Prediction errors in the LONG axial length group - Two hidden layers (purelin)

4.3. Feed-Forward MLNN - Three hidden layers

4.3.1. Radial Basis transfer function

The model had three hidden layers with two hidden layer neurons in the first hidden layer, four hidden layer neurons in the second hidden layer and 14 hidden layer neurons in the third layer (Table 52).

Layer	Neurons	Transfer function
Input	5	-
Hidden - First	2	radbas
Hidden - Second	4	radbas
Hidden - Third	14	radbas
Output	1	purelin

Table 52. ANN topology description - Three hidden layers (radbas)

The model's train, validation, and test performances are presented in Table 53.

Parameter	Mean	Median	Std	Min	Max
Train	0.00503	0.00372	0.00394	0.00302	0.01592
Validation	0.00667	0.00458	0.00665	0.00318	0.02529
Test	0.00628	0.00415	0.00547	0.00337	0.02126
Epoch	50	39	28.8	25	117

Table 53. ANN model performance - Three hidden layers (radbas)

MPR for the ALL eyes group are presented in Table 54. All tested parameters are significantly better than CR at level 0.0001. The maximum prediction error is worse for the ANN model.

PE [D]	CR	MPR	P value
ME	-0.46	-0.01	CR: < .0001, MPR: 0.54
MAE	0.52	0.32	< .0001
MedAE	0.50	0.27	
Std	0.43	0.41	-
Min	-1.88	-1.53	-
Max	1.13	1.48	-
Eyes within PE [%]			
±0.25	33.4	47.0	< .0001
±0.50	57.7	80.3	< .0001
±0.75	79.4	93.9	< .0001
±1.00	91.8	98.0	< .0001

Table 54. Prediction errors in the ALL axial length group - Three hidden layers (radbas)

MPR for the SHORT eyes group are presented in Table 55. The ANN model PE groups ±0.25, ±0.50, ±0.75 and ±1.00 are insignificantly better than CR. The maximum prediction error is worse for the ANN model. Standard deviation is the same for CR and MPR. MAE and MedAE are significantly better for the ANN model at level 0.0001.

PE [D]	CR	MPR	P value
ME	-0.37	0.08	CR: < .0001, MPR: 0.14
MAE	0.46	0.36	< .0001
MedAE	0.50	0.31	
Std	0.46	0.45	-
Min	-1.50	-0.75	-
Max	1.13	1.48	-
Eyes within PE [%]			
±0.25	40.7	43.2	0.87
±0.50	63.0	70.4	0.39
±0.75	85.2	93.8	0.12
±1.00	92.6	97.5	0.29

Table 55. Prediction errors in the SHORT axial length group - Three hidden layers (radbas)

MPR for the MEDIUM eyes group are presented in Table 56. All tested parameters are significantly better than CR at level 0.0001. The maximum prediction error is worse for the ANN model.

PE [D]	CR	MPR	P value
ME	-0.47	-0.02	CR: < .0001, MPR: 0.34
MAE	0.52	0.31	< .0001
MedAE	0.50	0.26	
Std	0.42	0.39	-
Min	-1.88	-1.53	-
Max	0.88	1.41	-
Eyes within PE [%]			
±0.25	33.1	48.3	< .0001
±0.50	56.9	82.9	< .0001
±0.75	79.8	94.4	< .0001
±1.00	92.9	97.9	< .0001

Table 56. Prediction errors in the MEDIUM axial length group - Three hidden layers (radbas)

MPR for the LONG eyes group are presented in Table 57. All tested parameters are significantly better than CR except PE group ±0.25; MAE and MedAE at level 0.0001; PE group ±0.75 at level 0.001; ±0.50 and ±0.75 at level 0.05. The maximum prediction error is worse for the ANN model.

PE [D]	CR	MPR	P value
ME	-0.53	-0.04	CR: < .0001, MPR: 0.38
MAE	0.57	0.35	< .0001
MedAE	0.50	0.29	
Std	0.44	0.43	-
Min	-1.63	-0.96	-
Max	0.88	1.22	-
Eyes within PE [%]			
±0.25	28.7	43.6	0.05
±0.50	57.4	75.5	< .05
±0.75	72.3	91.5	< .001
±1.00	85.1	98.9	< .05

Table 57. Prediction errors in the LONG axial length group - Three hidden layers (radbas)

4.4. Cascade-Forward MLNN - One hidden layer

4.4.1. Radial Basis transfer function

The model had one hidden layer with 12 hidden layer neurons (Table 58).

Layer	Neurons	Transfer function
Input	5	-
Hidden	12	radbas
Output	1	purelin

Table 58. ANN topology description - One hidden layer (radbas)

The model's train, validation, and test performances are presented in Table 59.

Parameter	Mean	Median	Std	Min	Max
Train	0.00292	0.00290	0.00012	0.00270	0.00312
Validation	0.00325	0.00328	0.00029	0.00293	0.00393
Test	0.00324	0.00325	0.00030	0.00277	0.00371
Epoch	5.6	5.5	1.4	4	8

Table 59. ANN model performance - One hidden layer (radbas)

MPR for the ALL eyes group are presented in Table 60. All tested parameters are significantly better than CR at level 0.0001. The maximum prediction error is worse for the ANN model.

PE [D]	CR	MPR	P value
ME	-0.46	0.00	CR: < .0001, MPR: 0.83
MAE	0.52	0.31	< .0001
MedAE	0.50	0.26	
Std	0.43	0.40	-
Min	-1.88	-1.50	-
Max	1.13	1.47	-
Eyes within PE [%]			
±0.25	33.44	48.9	< .0001
±0.50	57.71	82.7	< .0001
±0.75	79.39	93.6	< .0001
±1.00	91.76	97.6	< .0001

Table 60. Prediction errors in the ALL axial length group - One hidden layer (radbas)

MPR for the SHORT eyes group are presented in Table 61. The ANN model performs better for all prediction error groups, but the ±0.25, ±0.50 and ±1.00 prediction error groups fail to prove significance at the level of 0.05. MAE and MedAE are significantly better for the ANN model at level 0.0001. The ±0.75 PE group is significantly better at level 0.05. The maximum prediction error is worse for the ANN model.

PE [D]	CR	MPR	P value
ME	-0.37	0.03	CR: < .0001, MPR: 0.37
MAE	0.46	0.33	< .0001
MedAE	0.50	0.28	
Std	0.46	0.40	-
Min	-1.50	-0.91	-
Max	1.13	1.15	-
Eyes within PE [%]			
±0.25	40.74	48.1	0.42
±0.50	62.96	75.3	0.07
±0.75	85.19	95.1	< .05
±1.00	92.59	98.8	0.13

Table 61. Prediction errors in the SHORT axial length group - One hidden layer (radbas)

MPR for the MEDIUM eyes group are presented in Table 62. All tested parameters are significantly better for the ANN model at level 0.0001 except for the ±1.00 PE group, which is at level 0.001. The maximum prediction error is worse for the ANN model.

PE [D]	CR	MPR	P value
ME	-0.47	0.00	CR: < .0001, MPR: 0.94
MAE	0.52	0.31	< .0001
MedAE	0.50	0.26	
Std	0.42	0.40	
Min	-1.88	-1.50	
Max	0.88	1.25	
Eyes within PE [%]			
±0.25	33.13	49.0	< .0001
±0.50	56.88	84.0	< .0001
±0.75	79.79	93.3	< .0001
±1.00	92.92	97.5	< .001

Table 62. Prediction errors in the MEDIUM axial length group - One hidden layer (radbas)

MPR for the LONG eyes group are presented in Table 63. All tested parameters are significantly better for the ANN model; MAE, MedAE and ±0.75 PE group at level 0.0001, ±0.50 PE group at level 0.001 and ±0.25 with ±1.00 PE group at level 0.05. The maximum prediction error is worse for the ANN model.

PE [D]	CR	MPR	P value
ME	-0.53	-0.03	CR: < .0001, MPR: 0.59
MAE	0.57	0.31	< .0001
MedAE	0.50	0.26	
Std	0.44	0.40	-
Min	-1.63	-1.05	-
Max	0.88	1.47	-
Eyes within PE [%]			
±0.25	28.72	48.9	< .05
±0.50	57.45	83.0	< .001
±0.75	72.34	93.6	< .0001
±1.00	85.11	96.8	< .05

Table 63. Prediction errors in the LONG axial length group - One hidden layer (radbas)

4.4.2. Hyperbolic Tangent Sigmoid transfer function

The model had one hidden layer with 12 hidden layer neurons (Table 64).

Layer	Neurons	Transfer function
Input	5	-
Hidden	12	tansig
Output	1	purelin

Table 64. ANN topology description - One hidden layer (tansig)

The model's train, validation, and test performances are presented in Table 65.

Parameter	Mean	Median	Std	Min	Max
Train	0.00300	0.00300	0.00008	0.00284	0.00316
Validation	0.00323	0.00324	0.00023	0.00294	0.00369
Test	0.00317	0.00321	0.00023	0.00272	0.00344
Epoch	5.2	4	3.7	3	14

Table 65. ANN model performance - One hidden layer (tansig)

MPR for the ALL eyes group are presented in Table 66. All statistically tested parameters are significantly better for MPR at level 0.0001. The maximum prediction error is worse for the ANN model.

PE [D]	CR	MPR	P value
ME	-0.46	0.01	CR: < .0001, MPR: 0.52
MAE	0.52	0.31	< .0001
MedAE	0.50	0.26	
Std	0.43	0.40	-
Min	-1.88	-1.53	-
Max	1.13	1.47	-
Eyes within PE [%]			
±0.25	33.44	47.9	< .0001
±0.50	57.71	82.6	< .0001
±0.75	79.4	93.9	< .0001
±1.00	91.8	97.7	< .0001

Table 66. Prediction errors in the ALL axial length group - One hidden layer (tansig)

MPR for the SHORT eyes group are presented in Table 67. The ANN model performs better for all prediction error groups, but the ±0.25, ±0.50 and ±1.00 prediction error groups fail to prove significance at level 0.05. MAE and MedAE are significantly better for the ANN model at level 0.0001. PE group ±0.75 is significantly better at level 0.05.

PE [D]	CR	MPR	P value
ME	-0.37	0.06	CR: < .0001, MPR: 0.13
MAE	0.46	0.33	< .0001
MedAE	0.50	0.28	
Std	0.46	0.40	-
Min	-1.50	-0.93	-
Max	1.13	1.08	-
Eyes within PE [%]			
±0.25	40.7	45.7	0.64
±0.50	63.0	76.5	0.06
±0.75	85.2	95.1	< .05
±1.00	92.6	98.8	0.13

Table 67. Prediction errors in the SHORT axial length group - One hidden layer (tansig)

MPR for the MEDIUM eyes group are presented in Table 68. Compared to the CR, the ANN model performs significantly better for all statistically tested cases at level 0.0001 except the ±1.00 PE group, which was statistically significant at level 0.001. The maximum prediction error is worse for the ANN model.

PE [D]	CR	MPR	P value
ME	-0.47	0.00	CR: < .0001, MPR: 0.82
MAE	0.52	0.31	< .0001
MedAE	0.50	0.26	
Std	0.42	0.39	-
Min	-1.88	-1.53	-
Max	0.88	1.30	-
Eyes within PE [%]			
±0.25	33.1	48.3	< .0001
±0.50	56.9	83.3	< .0001
±0.75	79.8	93.5	< .0001
±1.00	92.9	97.5	< .001

Table 68. Prediction errors in the MEDIUM axial length group - One hidden layer (tansig)

MPR for the LONG eyes group are presented in Table 69. Compared to the CR, the ANN model performs significantly better for all cases; for MAE, MedAE, ±0.50 PE group and ±0.75 PE group at level 0.0001, for ±0.25 and ±1.00 PE groups at level 0.05. The maximum prediction error is worse for the ANN model.

PE [D]	CR	MPR	P value
ME	-0.53	-0.02	CR: < .0001, MPR: 0.76
MAE	0.57	0.31	< .0001
MedAE	0.50	0.27	
Std	0.44	0.41	-
Min	-1.63	-1.06	-
Max	0.88	1.47	-
Eyes within PE [%]			
±0.25	28.7	46.8	< .05
±0.50	57.4	84.0	< .0001
±0.75	72.3	94.7	< .0001
±1.00	85.1	97.9	< .05

Table 69. Prediction errors in the LONG axial length group - One hidden layer (tansig)

4.4.3. Log-Sigmoid transfer function

The model had one hidden layer with 13 hidden layer neurons (Table 70).

Layer	Neurons	Transfer function
Input	5	-
Hidden	13	logsig
Output	1	purelin

Table 70. ANN topology description - One hidden layer (logsig)

The model's train, validation, and test performances are presented in Table 71.

Parameter	Mean	Median	Std	Min	Max
Train	0.00302	0.00302	0.00013	0.00281	0.00328
Validation	0.00304	0.00313	0.00018	0.00276	0.00325
Test	0.00318	0.00315	0.00021	0.00287	0.00360
Epoch	4.9	5	2.1	2	8

Table 71. ANN model performance - One hidden layer (logsig)

MPR for the ALL eyes group are presented in Table 72. Compared to the CR, the ANN model with one hidden layer using Log-Sigmoid as a transfer function produces better results for all evaluated parameters. All statistically tested parameters are significantly better at level 0.0001. The maximum prediction error is slightly worse for the ANN model.

PE [D]	CR	MPR	P value
ME	-0.46	0.01	CR: < .0001, MPR: 0.48
MAE	0.52	0.31	< .0001
MedAE	0.50	0.26	
Std	0.43	0.40	-
Min	-1.88	-1.49	-
Max	1.13	1.54	-
Eyes within PE [%]			
±0.25	33.44	48.9	< .0001
±0.50	57.71	82.0	< .0001
±0.75	79.39	94.0	< .0001
±1.00	91.76	97.6	< .0001

Table 72. Prediction errors in the ALL axial length group - One hidden layer (logsig)

MPR for the SHORT eyes group are presented in Table 73. Compared to the CR, the ANN model performs significantly better for MAE and MedAE at level 0.0001 and the ±0.75 PE group at level 0.05. PE group ±0.25, ±0.05 and ±1.00 are insignificantly better. The maximum prediction error is slightly worse for the ANN model.

PE [D]	CR	MPR	P value
ME	-0.37	0.04	CR: < .0001, MPR: 0.27
MAE	0.46	0.32	< .0001
MedAE	0.50	0.26	
Std	0.46	0.40	-
Min	-1.50	-0.85	-
Max	1.13	1.14	-
Eyes within PE [%]			
±0.25	40.74	49.4	0.34
±0.50	62.96	75.3	0.09
±0.75	85.19	95.1	< .05
±1.00	92.59	98.8	0.13

Table 73. Prediction errors in the SHORT axial length group - One hidden layer (logsig)

MPR for the MEDIUM eyes group are presented in Table 74. Compared to the CR, the ANN model performs significantly better for all statistically tested cases at level 0.0001 except ±1.00 PE group, which is significantly better at level 0.001. The maximum prediction error is worse for the ANN model.

PE [D]	CR	MPR	P value
ME	-0.47	0.01	CR: < .0001, MPR: 0.52
MAE	0.52	0.31	< .0001
MedAE	0.50	0.25	
Std	0.42	0.40	-
Min	-1.88	-1.49	-
Max	0.88	1.33	-
Eyes within PE [%]			
±0.25	33.13	49.4	< .0001
±0.50	56.88	82.9	< .0001
±0.75	79.79	94.0	< .0001
±1.00	92.92	97.5	< .001

Table 74. Prediction errors in the MEDIUM axial length group - One hidden layer (logsig)

MPR for the LONG eyes group are presented in Table 75. Compared to the CR, the ANN model performs significantly better for all cases; for MAE, MedAE and the ±0.75 PE group at level 0.0001, for ±0.50 and ±1.00 PE groups at level 0.001 and for ±0.25 PE group at level 0.05. The maximum prediction error is worse for the ANN model.

PE [D]	CR	MPR	P value
ME	-0.53	-0.03	CR: < .0001, MPR: 0.53
MAE	0.57	0.32	< .0001
MedAE	0.50	0.26	
Std	0.44	0.41	-
Min	-1.63	-1.03	-
Max	0.88	1.54	-
Eyes within PE [%]			
±0.25	28.72	45.7	< .05
±0.50	57.45	83.0	< .001
±0.75	72.34	93.6	< .0001
±1.00	85.11	96.8	< .001

Table 75. Prediction errors in the LONG axial length group - One hidden layer (logsig)

4.4.4. Linear transfer function

The model had one hidden layer with 13 hidden layer neurons (Table 76).

Layer	Neurons	Transfer function
Input	5	-
Hidden	13	purelin
Output	1	purelin

Table 76. ANN model topology - One hidden layer (purelin)

The model's train, validation, and test performances are presented in Table 77.

Parameter	Mean	Median	Std	Min	Max
Train	0.00341	0.00341	0.00006	0.00331	0.00351
Validation	0.00333	0.00334	0.00021	0.00299	0.00379
Test	0.00359	0.00355	0.00035	0.00307	0.00429
Epoch	2.7	2.5	0.8	2	4

Table 77. ANN model performance - One hidden layer (purelin)

MPR for the ALL eyes group are presented in Table 78. Compared to the CR, the ANN model with one hidden layer using the Linear transfer function produces better results for all evaluated parameters. All statistically tested parameters are significantly better at the level of significance of 0.0001. The maximum prediction error is worse for the ANN model.

PE [D]	CR	MPR	P value
ME	-0.46	0.01	CR: < .0001, MPR: 0.63
MAE	0.52	0.33	< .0001
MedAE	0.50	0.28	
Std	0.43	0.42	-
Min	-1.88	-1.57	-
Max	1.13	2.06	-
Eyes within PE [%]			
±0.25	33.4	45.8	< .0001
±0.50	57.7	79.7	< .0001
±0.75	79.4	93.1	< .0001
±1.00	91.8	97.9	< .0001

Table 78. Prediction errors in the ALL axial length group - One hidden layer (purelin)

MPR for the SHORT eyes group are presented in Table 79. Compared to the CR, the ANN model performs worse for the ±0.25 prediction error group. All other prediction error groups are insignificantly better. The standard deviation appears to be the same, ME is better but significantly different from zero, and MAE and MedAE are significantly better at level 0.0001. The maximum prediction error is worse for the ANN model.

PE [D]	CR	MPR	P value
ME	-0.37	0.19	CR: < .0001, MPR: < .001
MAE	0.46	0.39	< .0001
MedAE	0.50	0.36	
Std	0.46	0.46	-
Min	-1.50	-0.65	-
Max	1.13	1.85	-
Eyes within PE [%]			
±0.25	40.7	39.5	1.00
±0.50	63.0	71.6	0.32
±0.75	85.2	93.8	0.12
±1.00	92.6	96.3	0.45

Table 79. Prediction errors in the SHORT axial length group - One hidden layer (purelin)

MPR for the MEDIUM eyes group are presented in Table 80. Compared to the CR, the ANN model performs significantly better for all prediction error groups at level 0.0001. MAE and MedAE are significantly better for the ANN model. ME is better for the ANN model but significantly different from zero at level 0.05. The maximum prediction error is worse for the ANN model.

PE [D]	CR	MPR	P value
ME	-0.47	-0.04	CR: < .0001, MPR: < .05
MAE	0.52	0.31	< .0001
MedAE	0.50	0.27	
Std	0.42	0.39	-
Min	-1.88	-1.57	-
Max	0.88	1.29	-
Eyes within PE [%]			
±0.25	33.1	46.5	< .0001
±0.50	56.9	82.5	< .0001
±0.75	79.8	93.1	< .0001
±1.00	92.9	98.1	< .0001

Table 80. Prediction errors in the MEDIUM axial length group - One hidden layer (purelin)

MPR for the LONG eyes group are presented in Table 81. Compared to the CR, the ANN model performs significantly better for all tested variables except the ±0.50 PE group; for MAE and MedAE at level 0.0001 and for ±0.25, ±0.75 and ±1.00 PE groups at level 0.05. The maximum prediction error is considerably worse for the ANN model. The standard deviation is higher for the ANN model. ME is significantly different from zero for MPR at level 0.05.

PE [D]	CR	MPR	P value
ME	-0.53	0.14	CR: < .0001, MPR: < .05
MAE	0.57	0.36	< .0001
MedAE	0.50	0.29	
Std	0.44	0.46	-
Min	-1.63	-0.79	-
Max	0.88	2.06	-
Eyes within PE [%]			
±0.25	28.7	47.9	< .05
±0.50	57.4	72.3	0.05
±0.75	72.3	92.6	< .05
±1.00	85.1	97.9	< .05

Table 81. Prediction errors in the LONG axial length group - One hidden layer (purelin)

4.5. Cascade-Forward MLNN - Two hidden layers

4.5.1. Radial Basis transfer function

The model had two hidden layers with one hidden layer neuron in the first hidden layer and 13 hidden layer neurons in the second hidden layer (Table 82).

Layer	Neurons	Transfer function
Input	5	-
Hidden - First	1	radbas
Hidden - Second	13	radbas
Output	1	purelin

Table 82. ANN topology description - Two hidden layers (radbas)

The model's train, validation, and test performances are presented in Table 83.

Parameter	Mean	Median	Std	Min	Max
Train	0.00305	0.00307	0.00020	0.00277	0.00347
Validation	0.00310	0.00306	0.00023	0.00273	0.00360
Test	0.00337	0.00343	0.00033	0.00282	0.00381
Epoch	3.9	3.5	1.5	2	7

Table 83. ANN model performance - Two hidden layers (radbas)

MPR for the ALL eyes group are presented in Table 84. All tested parameters are significantly better than CR at level 0.0001. The maximum prediction error is worse for the ANN model.

PE [D]	CR	MPR	P value
ME	-0.46	0.01	CR: < .0001, MPR: 0.40
MAE	0.52	0.31	< .0001
MedAE	0.50	0.25	
Std	0.43	0.40	-
Min	-1.88	-1.51	-
Max	1.13	1.58	-
Eyes within PE [%]			
±0.25	33.4	49.9	< .0001
±0.50	57.7	82.0	< .0001
±0.75	79.4	94.0	< .0001
±1.00	91.8	97.7	< .0001

Table 84. Prediction errors in the ALL axial length group - Two hidden layers (radbas)

MPR for the SHORT eyes group are presented in Table 85. The ANN model performs better for all prediction error groups, but the results are not significant in the ±0.25 and ±1.00 PE groups. The maximum prediction error is worse for the ANN model. MAE and MedAE are significantly better for the ANN model at level 0.0001.

PE [D]	CR	MPR	P value
ME	-0.37	0.02	CR: < .0001, MPR: 0.52
MAE	0.46	0.33	< .0001
MedAE	0.50	0.26	
Std	0.46	0.41	-
Min	-1.50	-0.94	-
Max	1.13	1.20	-
Eyes within PE [%]			
±0.25	40.74	48.1	0.42
±0.50	62.96	77.8	< .05
±0.75	85.19	95.1	< .05
±1.00	92.59	98.8	0.13

Table 85. Prediction errors in the SHORT axial length group - Two hidden layers (radbas)

MPR for the MEDIUM eyes group are presented in Table 86. All tested parameters are significantly better than CR at level 0.0001 except for the ±1.00 PE group, which is significantly better at level 0.001. The maximum prediction error is worse for the ANN model.

PE [D]	CR	MPR	P value
ME	-0.47	0.01	CR: < .0001, MPR: 0.41
MAE	0.52	0.31	< .0001
MedAE	0.50	0.25	
Std	0.42	0.39	-
Min	-1.88	-1.51	-
Max	0.88	1.31	-
Eyes within PE [%]			
±0.25	33.1	50.4	< .0001
±0.50	56.9	82.9	< .0001
±0.75	79.8	93.8	< .0001
±1.00	92.9	97.5	< .001

Table 86. Prediction errors in the MEDIUM axial length group - Two hidden layers (radbas)

MPR for the LONG eyes group are presented in Table 87. All tested parameters are significantly better than CR; MAE, MedAE and the ±0.75 PE group at level 0.0001, ±0.50 PE group at level 0.001 and ±0.25 and ±1.00 PE groups at level 0.05. The maximum prediction error is worse for the ANN model.

PE [D]	CR	MPR	P value
ME	-0.53	-0.01	CR: < .0001, MPR: 0.79
MAE	0.57	0.32	< .0001
MedAE	0.50	0.27	
Std	0.44	0.41	
Min	-1.63	-1.02	
Max	0.88	1.58	
Eyes within PE [%]			
±0.25	28.7	48.9	< .05
±0.50	57.4	80.9	< .001
±0.75	72.3	94.7	< .0001
±1.00	85.1	97.9	< .05

Table 87. Prediction errors in the LONG axial length group - One hidden layer (radbas)

4.5.2. Hyperbolic Tangent Sigmoid transfer function

The model had two hidden layers with three hidden layer neurons in the first hidden layer and four hidden layer neurons in the second hidden layer (Table 88).

Layer	Neurons	Transfer function
Input	5	-
Hidden - First	3	tansig
Hidden - Second	4	tansig
Output	1	purelin

Table 88. ANN topology description - Two hidden layers (tansig)

The model's train, validation, and test performances are presented in Table 89.

Parameter	Mean	Median	Std	Min	Max
Train	0.00299	0.00298	0.00015	0.00283	0.00334
Validation	0.00322	0.00331	0.00024	0.00261	0.00341
Test	0.00337	0.00341	0.00031	0.00287	0.00392
Epoch	7	6	3.3	3	14

Table 89. ANN model performance - Two hidden layers (tansig)

MPR for the ALL eyes group are presented in Table 90. All tested parameters are significantly better than CR at level 0.0001. The maximum prediction error is worse for the ANN model.

PE [D]	CR	MPR	P value
ME	-0.46	0.00	CR: < .0001, MPR: 0.62
MAE	0.52	0.31	< .0001
MedAE	0.50	0.26	
Std	0.43	0.40	-
Min	-1.88	-1.56	-
Max	1.13	1.43	-
Eyes within PE [%]			
±0.25	33.4	48.7	< .0001
±0.50	57.7	82.9	< .0001
±0.75	79.4	93.6	< .0001
±1.00	91.8	97.6	< .0001

Table 90. Prediction errors in the ALL axial length group - Two hidden layers (tansig)

MPR for the SHORT eyes group are presented in Table 91. MAE and MedAE are significantly better at level 0.0001. The ±0.50 and ±0.75 PE groups are significantly better at level 0.05. The ±0.25 and ±1.00 PE groups are insignificantly better.

PE [D]	CR	MPR	P value
ME	-0.37	0.05	CR: < .0001, MPR: 0.21
MAE	0.46	0.33	< .0001
MedAE	0.50	0.27	
Std	0.46	0.40	-
Min	-1.50	-0.94	-
Max	1.13	1.09	-
Eyes within PE [%]			
±0.25	40.7	46.9	0.53
±0.50	63.0	77.8	< .05
±0.75	85.2	96.3	< .05
±1.00	92.6	98.8	0.13

Table 91. Prediction errors in the SHORT axial length group - Two hidden layers (tansig)

MPR for the MEDIUM eyes group are presented in Table 92. All tested parameters are significantly better than CR at level 0.0001 except for the ±1.00 PE group, which is significantly better at level 0.001. The maximum prediction error is worse for the ANN model.

PE [D]	CR	MPR	P value
ME	-0.47	0.00	CR: < .0001, MPR: 0.73
MAE	0.52	0.31	< .0001
MedAE	0.50	0.25	
Std	0.42	0.40	-
Min	-1.88	-1.56	-
Max	0.88	1.35	-
Eyes within PE [%]			
±0.25	33.1	50.0	< .0001
±0.50	56.9	83.5	< .0001
±0.75	79.8	93.1	< .0001
±1.00	92.9	97.5	< .001

Table 92. Prediction errors in the MEDIUM axial length group - Two hidden layers (tansig)

MPR for the LONG eyes group are presented in Table 93. MAE, MedAE, the ±0.50 PE group and the ±0.75 PE group are significantly better at level 0.0001. The ±1.00 PE group is better at level 0.05. The maximum prediction error is worse the for ANN model. The ±0.25 PE group is insignificantly better.

PE [D]	CR	MPR	P value
ME	-0.53	-0.04	CR: < .0001, MPR: 0.44
MAE	0.57	0.31	< .0001
MedAE	0.50	0.27	
Std	0.44	0.40	
Min	-1.63	-1.04	
Max	0.88	1.43	
Eyes within PE [%]			
±0.25	28.7	43.6	0.07
±0.50	57.4	84.0	< .0001
±0.75	72.3	93.6	< .0001
±1.00	85.1	96.8	< .05

Table 93. Prediction errors in the LONG axial length group - Two hidden layers (tansig)

4.5.3. Log-Sigmoid transfer function

The model had two hidden layers with two hidden layer neurons in the first hidden layer and 11 hidden layer neurons in the second hidden layer (Table 94).

Layer	Neurons	Transfer function
Input	5	-
Hidden - First	2	logsig
Hidden - Second	11	logsig
Output	1	purelin

Table 94. ANN topology description - Two hidden layers (logsig)

The model's train, validation, and test performances are presented in Table 95.

Parameter	Mean	Median	Std	Min	Max
Train	0.00305	0.00305	0.00013	0.00288	0.00335
Validation	0.00307	0.00317	0.00023	0.00250	0.00327
Test	0.00307	0.00310	0.00021	0.00268	0.00340
Epoch	5.4	5	2.7	2	9

Table 95. ANN model performance - Two hidden layers (logsig)

MPR for the ALL eyes group are presented in Table 96. All tested parameters are significantly better than CR at level 0.0001. The maximum prediction error is worse for the ANN model.

PE [D]	CR	MPR	P value
ME	-0.46	0.01	CR: < .0001, MPR: 0.47
MAE	0.52	0.31	< .0001
MedAE	0.50	0.26	
Std	0.43	0.40	-
Min	-1.88	-1.53	-
Max	1.13	1.47	-
Eyes within PE [%]			
±0.25	33.4	47.2	< .0001
±0.50	57.7	81.8	< .0001
±0.75	79.4	93.6	< .0001
±1.00	91.8	97.4	< .0001

Table 96. Prediction errors in the ALL axial length group - Two hidden layers (logsig)

MPR for the SHORT eyes group are presented in Table 97. MAE and MedAE are significantly better at level 0.0001, and the ±0.50 PE group is significantly better at level 0.05. The ±0.25, ±0.75 and ±1.00 PE groups are insignificantly better.

PE [D]	CR	MPR	P value
ME	-0.37	0.04	CR: < .0001, MPR: 0.31
MAE	0.46	0.33	< .0001
MedAE	0.50	0.27	
Std	0.46	0.41	-
Min	-1.50	-1.03	-
Max	1.13	1.12	-
Eyes within PE [%]			
±0.25	40.7	45.7	0.63
±0.50	63.0	77.8	< .05
±0.75	85.2	93.8	0.05
±1.00	92.6	97.5	0.22

Table 97. Prediction errors in the SHORT axial length group - Two hidden layers (logsig)

MPR for the MEDIUM eyes group are presented in Table 98. The ANN model performed significantly better for all variables at level 0.0001 except for the ±1.00 PE group, which was significantly better at level 0.001. The maximum prediction error is worse for the ANN model.

PE [D]	CR	MPR	P value
ME	-0.47	0.01	CR: < .0001, MPR: 0.53
MAE	0.52	0.31	< .0001
MedAE	0.50	0.26	
Std	0.42	0.40	-
Min	-1.88	-1.53	-
Max	0.88	1.34	-
Eyes within PE [%]			
±0.25	33.1	48.1	< .0001
±0.50	56.9	82.5	< .0001
±0.75	79.8	93.5	< .0001
±1.00	92.9	97.5	< .001

Table 98. Prediction errors in the MEDIUM axial length group - Two hidden layers (logsig)

MPR for the LONG eyes group are presented in Table 99. MAE, MedAE and the ±0.75 PE group are significantly better at level 0.0001, ±0.50 PE group is significantly better at level 0.001 and ±1.00 PE group is significantly better at level 0.05. The ±0.25 PE group is insignificantly better for the ANN model. The maximum prediction error is worse for the ANN model.

PE [D]	CR	MPR	P value
ME	-0.53	-0.03	CR: < .0001, MPR: 0.57
MAE	0.57	0.32	< .0001
MedAE	0.50	0.28	
Std	0.44	0.41	-
Min	-1.63	-1.04	-
Max	0.88	1.47	-
Eyes within PE [%]			
±0.25	28.7	43.6	0.06
±0.50	57.4	81.9	< .001
±0.75	72.3	93.6	< .0001
±1.00	85.1	96.8	< .05

Table 99. Prediction errors in the LONG axial length group - Two hidden layers (logsig)

4.5.4. Linear transfer Function

The model had two hidden layers with 23 hidden layer neurons in the first hidden layer and two hidden layer neurons in the second hidden layer (Table 100).

Layer	Neurons	Transfer function
Input	5	-
Hidden - First	23	purelin
Hidden - Second	2	purelin
Output	1	purelin

Table 100. ANN model topology - Two hidden layers (purelin)

The model's train, validation, and test performances are presented in Table 101.

Parameter	Mean	Median	Std	Min	Max
Train	0.00338	0.00341	0.00008	0.00322	0.00346
Validation	0.00347	0.00342	0.00026	0.00309	0.00389
Test	0.00356	0.00351	0.00032	0.00318	0.00419
Epoch	2.5	2	0.7	2	4

Table 101. ANN model performance - Two hidden layers (purelin)

MPR for the ALL eyes group are presented in Table 102. All tested parameters are significantly better than CR at level 0.0001 except for the ±0.25 PE group, which is significantly better at level 0.001. The maximum prediction error is worse for the ANN model.

PE [D]	CR	MPR	P value
ME	-0.46	0.01	CR: < .0001, MPR: 0.69
MAE	0.52	0.33	< .0001
MedAE	0.50	0.28	
Std	0.43	0.42	-
Min	-1.88	-1.57	-
Max	1.13	2.02	-
Eyes within PE [%]			
±0.25	33.4	45.8	< .001
±0.50	57.7	79.8	< .0001
±0.75	79.4	92.8	< .0001
±1.00	91.8	97.9	< .0001

Table 102. Prediction errors in the ALL axial length group - Two hidden layers (purelin)

MPR for the SHORT eyes group are presented in Table 103. ME is significantly different from zero at level 0.001. MAE and MedAE are significantly better at level 0.0001. The ±0.50, ±0.75, and ±1.00 PE groups are insignificantly better than CR. The maximum prediction error is worse for the ANN model. The standard deviation is the same for CR and MPR. The ±0.25 PE group is worse for the ANN model. ME is significantly different from zero for the model.

PE [D]	CR	MPR	P value
ME	-0.37	0.21	CR: < .0001, MPR: < .001
MAE	0.46	0.40	< .0001
MedAE	0.50	0.37	
Std	0.46	0.46	-
Min	-1.50	-0.64	-
Max	1.13	1.88	-
Eyes within PE [%]			
±0.25	40.7	37.0	0.77
±0.50	63.0	70.4	0.42
±0.75	85.2	90.1	0.48
±1.00	92.6	96.3	0.45

Table 103. Prediction errors in the SHORT axial length group - Two hidden layers (purelin)

MPR for the MEDIUM eyes group are presented in Table 104. All tested parameters are significantly better than CR at level 0.0001. The maximum prediction error is worse for the ANN model. ME is significantly different from zero for the model.

PE [D]	CR	MPR	P value
ME	-0.47	-0.04	CR: < .0001, MPR: < .01
MAE	0.52	0.31	< .0001
MedAE	0.50	0.27	
Std	0.42	0.39	-
Min	-1.88	-1.57	-
Max	0.88	1.27	-
Eyes within PE [%]			
±0.25	33.1	46.9	< .0001
±0.50	56.9	82.5	< .0001
±0.75	79.8	93.3	< .0001
±1.00	92.9	98.1	< .0001

Table 104. Prediction errors in the MEDIUM axial length group - Two hidden layers (purelin)

MPR for the LONG eyes group are presented in Table 105. All tested parameters are significantly better than CR; MAE and MedAE at level 0.0001, ±0.75 PE group at level 0.001 and ±0.25, ±0.50, ±1.00 PE groups at level 0.05. ME is significantly different from zero for MPR at level 0.05. The maximum prediction error is worse for the ANN model.

PE [D]	CR	MPR	P value
ME	-0.53	0.12	CR: < .0001, MPR: < .05
MAE	0.57	0.36	< .0001
MedAE	0.50	0.28	
Std	0.44	0.45	-
Min	-1.63	-0.82	-
Max	0.88	2.02	-
Eyes within PE [%]			
±0.25	28.7	47.9	< .05
±0.50	57.4	74.5	< .05
±0.75	72.3	92.6	< .001
±1.00	85.1	97.9	< .05

Table 105. Prediction errors in the LONG axial length group - Two hidden layers (purelin)

4.6. Support Vector Machines

Support Vector Machine (SVM) model parameters are presented in Table 106.

Kernel function	Polynomial
Kernel Scale	1
Epsilon	0.0261
Box constraint	0.1528
Polynomial order	3
Number of iterations	4255
Verification set MSE	0.0028
Verification set RMSE	0.0527

Table 106. SVM model parameters

MPR for the ALL eyes group are presented in Table 107. Compared to the CR, the SVM model performs better for all evaluated parameters at level 0.0001. The maximum prediction error is slightly worse for the SVM model.

PE [D]	CR	MPR	P value
ME	-0.46	0.01	CR: < .0001, MPR: 0.43
MAE	0.52	0.31	< .0001
MedAE	0.50	0.26	
Std	0.43	0.40	-
Min	-1.88	-1.52	-
Max	1.13	1.31	-
Eyes within PE [%]			
±0.25	33.44	48.9	< .0001
±0.50	57.71	83.5	< .0001
±0.75	79.39	93.6	< .0001
±1.00	91.76	97.4	< .0001

Table 107. Prediction errors in the ALL axial length group - SVM

MPR for the SHORT eyes group are presented in Table 108. MAE and MedAE are significantly better at level 0.0001. The ±0.50 and ±1.00 PE groups are significantly better at level 0.05. The ±0.25 and ±0.75 PE groups are insignificantly better.

PE [D]	CR	MPR	P value
ME	-0.37	-0.01	CR: < .0001, MPR: 0.95
MAE	0.46	0.33	< .0001
MedAE	0.50	0.27	
Std	0.46	0.40	-
Min	-1.50	-1.14	-
Max	1.13	0.81	-
Eyes within PE [%]			
±0.25	40.74	48.1	0.40
±0.50	62.96	77.8	< .05
±0.75	85.19	95.1	< .05
±1.00	92.59	98.8	0.07

Table 108. Prediction errors in the SHORT axial length group - SVM

MPR for the MEDIUM eyes group are presented in Table 109. Compared to the CR, the SVM model performs significantly better for all statistically tested cases at level 0.0001 except for the ±1.00 PE group, which is significantly better at level 0.001. The maximum prediction error is higher for the SVM model.

PE [D]	CR	MPR	P value
ME	-0.47	0.02	CR: < .0001, MPR: 0.59
MAE	0.52	0.30	< .0001
MedAE	0.50	0.25	
Std	0.42	0.39	-
Min	-1.88	-1.52	-
Max	0.88	1.31	-
Eyes within PE [%]			
±0.25	33.13	49.6	< .0001
±0.50	56.88	84.2	< .0001
±0.75	79.79	93.3	< .0001
±1.00	92.92	97.5	< .001

Table 109. Prediction errors in the MEDIUM axial length group - SVM

MPR for the LONG eyes group are presented in Table 110. Compared to the CR, the SVM model performs significantly better for most cases; for MAE, MedAE, ±0.50 PE group and ±0.75 PE group at level 0.0001 and for ±1.00 PE group at level 0.001. The ±0.25 PE group is significantly better at level 0.05.

PE [D]	CR	MPR	P value
ME	-0.53	-0.06	CR: < .0001, MPR: 0.20
MAE	0.57	0.31	< .0001
MedAE	0.50	0.26	
Std	0.44	0.40	-
Min	-1.63	-1.30	-
Max	0.88	1.19	-
Eyes within PE [%]			
±0.25	28.72	45.7	< .05
±0.50	57.45	85.1	< .0001
±0.75	72.34	93.6	< .0001
±1.00	85.11	95.7	< .001

Table 110. Prediction errors in the LONG axial length group - SVM

4.7. Binary Regression Decision Tree

Binary Regression Decision Tree (BRDT) model parameters are presented in Table 111.

Nodes	401
Minimal observations per leaf	6
Minimal observations per parent	12
Split criterion	MSE
Verification set MSE	0.0055
Verification set RMSE	0.0741

Table 111. BRDT model parameters

MPR for the ALL eyes group are presented in Table 112. The maximum prediction error and standard deviation are higher for the BRDT model. Performance in ±1.00 PE group is insignificantly better for the BRDT model. The ±0.25 PE group is insignificantly better for the BRDT model. The ±0.50 and ±0.75 PE groups are significantly better for the BRDT model at levels 0.0001 and 0.05, respectively.

PE [D]	**CR**	**MPR**	**P value**
ME	-0.46	0.04	CR: < .0001, MPR: 0.13
MAE	0.52	0.43	< .0001
MedAE	0.50	0.35	
Std	0.43	0.56	-
Min	-1.88	-2.12	-
Max	1.13	1.98	-
Eyes within PE [%]			
±0.25	33.44	37.3	0.16
±0.50	57.71	66.6	< .0001
±0.75	79.39	84.0	< 0.05
±1.00	91.76	92.1	0.75

Table 112. Prediction errors in the ALL axial length group - BRDT

MPR for the SHORT eyes group are presented in Table 113. The maximum prediction error, performance in all PE groups, MAE, MedAE and standard deviation are worse for the BRDT model; insignificantly for MAE, MedAE, ±1.00 and ±0.50 PE groups, significantly for ±0.25 and ±0.75 PE groups at level 0.05.

PE [D]	CR	MPR	P value
ME	-0.37	-0.01	CR: < .0001, MPR: 0.79
MAE	0.46	0.58	< .001
MedAE	0.50	0.51	
Std	0.46	0.69	-
Min	-1.50	-1.58	-
Max	1.13	1.39	-
Eyes within PE [%]		666	
±0.25	40.74	19.8	< 0.05
±0.50	62.96	49.4	0.09
±0.75	85.19	71.6	< 0.05
±1.00	92.59	85.2	0.15

Table 113. Prediction errors in the SHORT axial length group - BRDT

MPR for the MEDIUM eyes group are presented in Table 114. The maximum prediction error and standard deviation are worse for the BRDT model. The ±1.00 PE group is insignificantly better for the BRDT model. The ±0.50 and ±0.75 PE groups are significantly better for the BRDT model at level 0.0001. The ±0.25 PE group is significantly better at level 0.05. ME is significantly different from zero for MPR.

PE [D]	CR	MPR	P value
ME	-0.47	0.06	CR: < .0001, MPR: <.05
MAE	0.52	0.40	< .0001
MedAE	0.50	0.33	
Std	0.42	0.51	-
Min	-1.88	-2.12	-
Max	0.88	1.78	-
Eyes within PE [%]			
±0.25	33.13	41.0	< .05
±0.50	56.88	69.4	< .0001
±0.75	79.79	86.9	< .0001
±1.00	92.92	93.8	0.68

Table 114. Prediction errors in the MEDIUM axial length group - BRDT

MPR for the LONG eyes group are presented in Table 115. The Minimum prediction error, maximum prediction error and standard deviation are worse for the BRDT model. Performance in all PE groups is insignificantly better for the BRDT model.

PE [D]	CR	MPR	P value
ME	-0.53	-0.07	CR: < .0001, MPR: 0.27
MAE	0.57	0.47	< .0001
MedAE	0.50	0.35	
Std	0.44	0.62	-
Min	-1.63	-1.92	-
Max	0.88	1.98	-
Eyes within PE [%]			
±0.25	28.72	33.0	0.60
±0.50	57.45	67.0	0.18
±0.75	72.34	79.8	0.23
±1.00	85.11	89.4	0.48

Table 115. Prediction errors in the LONG axial length group - BRDT

4.8. Gaussian Process Regression

Gaussian Process Regression (GPR) model parameters are presented in Table 116.

Kernel Function	SquaredExponential
Basis Function	Constant
Sigma	0. 0606
Beta	2.2608
Fit/Predict method	exact
Verification set MSE	0.0028
Verification set RMSE	0.0526

Table 116. GPR model parameters

MPR for the ALL eyes group are presented in Table 117. All tested parameters are significantly better than CR at level 0.0001. The maximum prediction error is worse for the GPR model.

PE [D]	CR	MPR	P value
ME	-0.46	0.01	CR: < .0001, MPR: 0.31
MAE	0.52	0.31	< .0001
MedAE	0.50	0.25	
Std	0.43	0.39	-
Min	-1.88	-1.49	-
Max	1.13	1.41	-
Eyes within PE [%]			
±0.25	33.44	48.1	< .0001
±0.50	57.71	82.7	< .0001
±0.75	79.39	93.7	< .0001
±1.00	91.76	97.6	< .0001

Table 117. Prediction errors in the ALL axial length group - GPR

MPR for the SHORT eyes group are presented in Table 118. The GPR model performs significantly better for MAE and MedAE at level 0.0001, and the ±0.50 and ±0.75 PE groups at level 0.05. The ±0.25 and ±1.00 PE groups are insignificantly better.

PE [D]	CR	MPR	P value
ME	-0.37	0.03	CR: < .0001, MPR: 0.42
MAE	0.46	0.32	< .0001
MedAE	0.50	0.26	
Std	0.46	0.40	-
Min	-1.50	-0.89	-
Max	1.13	1.07	-
Eyes within PE [%]			
±0.25	40.74	48.6	0.41
±0.50	62.96	77.8	< .05
±0.75	85.19	95.1	< .05
±1.00	92.59	98.8	0.13

Table 118. Prediction errors in the SHORT axial length group - GPR

MPR for the MEDIUM eyes group are presented in Table 119. All tested variables are significantly better for the GPR model at level 0.0001 except for the ±1.00 PE group, which is significantly better at level 0.001. The maximum prediction error is worse for the GRP model.

PE [D]	CR	MPR	P value
ME	-0.47	0.01	CR: < .0001, MPR: 0.45
MAE	0.52	0.31	< .0001
MedAE	0.50	0.25	
Std	0.42	0.39	-
Min	-1.88	-1.51	-
Max	0.88	1.40	-
Eyes within PE [%]			
±0.25	33.13	49.2	< .0001
±0.50	56.88	83.1	< .0001
±0.75	79.79	93.3	< .0001
±1.00	92.92	97.3	< .001

Table 119. Prediction errors in the MEDIUM axial length group - GPR

MPR for the LONG eyes group are presented in Table 120. Most of the parameters tested are significantly better than CR; MAE, MedAE, the ±0.50 and ±0.75 PE groups at level 0.0001 and the ±1.00 PE group at level 0.05. The ±0.25 PE group is insignificantly better. The maximum prediction error is worse for the GPR model.

PE [D]	CR	MPR	P value
ME	-0.53	-0.02	CR: < .0001, MPR: 0.73
MAE	0.57	0.31	< .0001
MedAE	0.50	0.27	
Std	0.44	0.39	-
Min	-1.63	-1.00	-
Max	0.88	1.24	-
Eyes within PE [%]			
±0.25	28.72	42.6	0.07
±0.50	57.45	85.1	< .0001
±0.75	72.34	94.7	< .0001
±1.00	85.11	97.9	< .05

Table 120. Prediction errors in the LONG axial length group - GPR

4.9. Boosted Regression Tree Ensembles

Boosted Regression Tree Ensemble (BRTE) model parameters are presented in Table 121.

Method	LSBoost
Training cycles	414
Learn rate	0.06928
Minimal observations per leaf	8
MaxNumSplits	6
Verification set MSE	0.0035
Verification set RMSE	0.0589

Table 121. BRTE model parameters

MPR for the ALL eyes group are presented in Table 122. MAE, MedAE, the ±0.50 PE group and the ±0.75 PE group are significantly better at level 0.0001. The ±0.25 PE group and the ±1.00 PE group are significantly better at level 0.05. The maximum prediction error and standard deviation are worse for the BRTE model.

PE [D]	**CR**	**MPR**	**P value**
ME	-0.46	0.01	CR: 4.67e-82, MPR: 0.87
MAE	0.52	0.39	< .0001
MedAE	0.50	0.34	
Std	0.43	0.51	-
Min	-1.88	-1.48	-
Max	1.13	1.99	-
Eyes within PE [%]			
±0.25	33.44	44.7	< .05
±0.50	57.71	77.1	< .0001
±0.75	79.39	90.2	< .0001
±1.00	91.76	96.2	< .05

Table 122. Prediction errors in the ALL axial length group - BRTE

MPR for the SHORT eyes group are presented in Table 123. Compared to the CR, the BRTE model produces worse results for most of the evaluated parameters. The maximum prediction error, performance in all prediction error groups and the standard deviation are worse for the BRTE model. ME is significantly different from zero at level 0.05.

PE [D]	CR	MPR	P value
ME	-0.37	0.19	CR: < .0001, MPR: < .05
MAE	0.46	0.55	< .0001
MedAE	0.50	0.49	
Std	0.46	0.67	-
Min	-1.50	-1.00	-
Max	1.13	1.99	-
Eyes within PE [%]			
±0.25	40.74	27.2	0.44
±0.50	62.96	55.6	0.26
±0.75	85.19	81.5	0.08
±1.00	92.59	88.9	0.30

Table 123. Prediction errors in the SHORT axial length group - BRTE

MPR for the MEDIUM eyes group are presented in Table 124. Compared to the CR, the BRTE model performs significantly better for all statistically tested parameters; for MAE, MedAE, ±0.50 PE group and ±0.75 PE group at level 0.0001, for ±1.00 PE group at level 0.001 and for ±0.25 PE group at level 0.05. The maximum prediction error and standard deviation are worse for the BRTE model.

PE [D]	CR	MPR	P value
ME	-0.47	0.02	CR: < .000, MPR: 0.34
MAE	0.52	0.36	< .0001
MedAE	0.50	0.31	
Std	0.42	0.45	-
Min	-1.88	-1.31	-
Max	0.88	1.64	-
Eyes within PE [%]			
±0.25	33.13	47.7	< .05
±0.50	56.88	80.8	< .0001
±0.75	79.79	91.5	< .0001
±1.00	92.92	93.8	< .001

Table 124. Prediction errors in the MEDIUM axial length group - BRTE

MPR for the LONG eyes group are presented in Table 125. Compared to the CR, the BRTE model performs insignificantly better for all tested PE groups. MAE and MedAE are significantly better for the BRTE model at level 0.0001. The maximum prediction error and standard deviation are worse for the BRTE model. ME is significantly different from zero for MPR.

PE [D]	**CR**	**MPR**	**P value**
ME	-0.53	-0.19	CR: < .0001, MPR: < .001
MAE	0.57	0.45	< .0001
MedAE	0.50	0.39	
Std	0.44	0.53	-
Min	-1.63	-1.48	-
Max	0.88	1.44	-
Eyes within PE [%]			
±0.25	28.72	44.7	0.51
±0.50	57.45	76.6	0.16
±0.75	72.34	91.5	0.07
±1.00	85.11	97.9	0.07

Table 125. Prediction errors in the LONG axial length group - BRTE

4.10. Stepwise Regression

Stepwise Regression (SR) model parameters are presented in Tables 126 and 127.

	Estimate	SE	tStat	P value
(Intercept)	-0.10622	0.0017521	-60.621	0
KM	-0.4617	0.007346	-62.85	0
ACD	0.062351	0.005817	10.719	6.7192e-26
AL	-1.025	0.012501	-81.995	0
Age	-0.00078272	0.0050178	-0.15599	0.87606
Rx-pre	0.052386	0.0076388	VI.79	1.0111e-11
KM:AL	-0.10609	0.013945	-7.6074	4.8571e-14
ACD:Age	-0.045833	0.011859	-3.8646	0.00011591
AL:Rx-pre	-0.10588	0.012255	-8.6402	1.388e-17

Table 126. SR design parameters

Regression model	$IOL_{Predicted} \sim 1 + KM * AL + ACD * Age + AL * Rx_{pre}$
Verification set MSE	0.0035
Verification set RMSE	0.0589

Table 127. Regression model notation and errors

MPR for the ALL eyes group are presented in Table 128. All tested parameters are significantly better than CR at level 0.0001. The maximum prediction error is worse for the SR model.

PE [D]	CR	MPR	P value
ME	-0.46	0.01	CR: < .0001, MRS: 0.50
MAE	0.52	0.31	< .0001
MedAE	0.50	0.27	
Std	0.43	0.40	-
Min	-1.88	-1.51	-
Max	1.13	1.40	-
Eyes within PE [%]			
±0.25	33.44	46.3	< .0001
±0.50	57.71	82.9	< .0001
±0.75	79.39	94.0	< .0001
±1.00	91.76	97.4	< .0001

Table 128. Prediction errors in the ALL axial length group - SR

MPR for the SHORT eyes group are presented in Table 129. The SR model performs better for all PE groups at level 0.05 except for the ±0.25 PE group, which is insignificantly better. MAE and MedAE are significantly better for the SR model at level 0.0001.

PE [D]	CR	MPR	P value
ME	-0.37	0.02	CR: < .0001, MPR: 0.59
MAE	0.46	0.32	< .0001
MedAE	0.50	0.29	
Std	0.46	0.40	-
Min	-1.50	-0.93	-
Max	1.13	1.00	-
Eyes within PE [%]			
±0.25	40.74	44.4	0.74
±0.50	62.96	79.0	< .05
±0.75	85.19	95.1	< .05
±1.00	92.59	100.00	< .05

Table 129. Prediction errors in the SHORT axial length group - SR

MPR for the MEDIUM eyes group are presented in Table 130. All tested variables are significantly better for the SE model at level 0.0001 except for the ±1.00 PE group, which is significantly better at level 0.05. The maximum prediction error is worse for the SR model.

PE [D]	CR	MPR	P value
ME	-0.47	0.01	CR: < .0001, MP: 0.50
MAE	0.52	0.31	< .0001
MedAE	0.50	0.26	
Std	0.42	0.40	-
Min	-1.88	-1.51	-
Max	0.88	1.40	-
Eyes within PE [%]			
±0.25	33.13	47.7	< .0001
±0.50	56.88	83.3	< .0001
±0.75	79.79	93.5	< .0001
±1.00	92.92	97.1	< .05

Table 130. Prediction errors in the MEDIUM axial length group - SR

MPR for the LONG eyes group are presented in Table 131. All tested parameters are significantly better than CR at level 0.0001 except for the ±0.25 PE group, which is insignificantly better. The maximum prediction error is worse for the SR model.

PE [D]	CR	MPR	P value
ME	-0.53	-0.02	CR: < .0001, MPR: 0.79
MAE	0.57	0.32	< .0001
MedAE	0.50	0.29	
Std	0.44	0.40	-
Min	-1.63	-1.11	-
Max	0.88	1.27	-
Eyes within PE [%]			
±0.25	28.72	40.4	0.13
±0.50	57.45	84.0	< .0001
±0.75	72.34	95.7	< .0001
±1.00	85.11	96.8	< .0001

Table 131. Prediction errors in the LONG axial length group - SR

4.11. Mutual Evaluation

4.11.1. ALL axial length subgroup

Mutual comparison (Table 132.) of the ALL axial length subgroup using all evaluated models proved that there is not the significantly same proportion of success between the models in ±0.25 D, ±0.50 D, ±0.75 D and ±1.00 D PE groups at the level of P<.0001.

The best model in the ±0.25 D PE group was CS2_radbas. Therefore, every model for each PE group was statistically compared to this model.

In the ±0.25 D PE group SVM, CS1_radbas, FF1_radbas, CS1_logsig, CS2_tansig, FF1_logsig, GPR, FF2_logsig, FF2_tansig, FF2_radbas, FF1_tansig and FF3_radbas models were insignificantly worse. CS1_tansig, CS2_logsig, SR, CS2_purelin, CS1_purelin, FF2_purelin, and BRTE models were significantly worse at the level of P<.05. The FF1_purelin model was significantly worse at P<.001 and the BRTE model was significantly worse at the level of P<.0001.

In the ±0.50 D PE group SVM, the CS2_tansig, SR, GPR, CS1_radbas, FF2_tansig, FF1_logsig, CS1_tansig, FF1_tansig, FF1_radbas, FF2_logsig and FF2_radbas models were insignificantly better and the CS1_logsig, CS2_logsig, FF3_radbas, FF2_purelin and FF1_purelin models were insignificantly worse. The CS2_purelin and CS1_purelin models were significantly worse at the level of P<.05, and the BRTE and BRDT models were significantly worse at the level of P<.0001.

In the ±0.75 D PE group SR, the FF2_tansig and CS1_logsig performed the same. The CS1_tansig, FF1_radbas, FF3_radbas, GPR, FF1_tansig, SVM, CS2_tansig, CS1_radbas, FF2_logsig, FF2_radbas, CS2_logsig, FF1_logsig, FF1_purelin, CS1_purelin, FF2_purelin and CS2_purelin models performed insignificantly worse. The BRTE and BRDT models performed significantly worse at the level of P<.0001.

In the ±1.00 D PE group, the FF3_radbas, FF2_tansig, FF1_logsig, FF1_purelin, CS1_purelin, FF2_purelin and CS2_purelin models performed insignificantly better. The CS1_tansig, FF2_radbas, CS1_logsig, FF1_radbas, GPR, FF1_tansig, CS2_tansig, CS1_radbas, FF2_logsig, SR, SVM and CS2_logsig models performed the same or insignificantly worse. The BRTE and BRDT models performed significantly worse at the level of P<.05 and P<.0001, respectively.

Model	PE							
	±0.25 D		±0.50 D		±0.75 D		±1.00 D	
	[%]	P value	[%]	P value	[%]	P value	[%]	P value
CS2_radbas	**49.9**	$n_1=n_2$	82.0	$n_1=n_2$	94.0	$n_1=n_2$	97.7	$n_1=n_2$
SVM	48.9	0.43	83.5	0.09	93.6	0.32	97.4	0.48
FF1_radbas	48.9	0.35	82.3	0.69	93.9	0.65	97.6	0.56
CS1_radbas	48.9	0.32	82.7	0.23	93.6	0.26	97.6	0.56
CS1_logsig	48.9	0.29	82.0	1.00	94.0	1.00	97.6	0.56
CS2_tansig	48.7	0.27	82.9	0.22	93.6	0.26	97.6	0.56
FF1_logsig	48.4	0.16	82.6	0.39	93.4	0.10	97.9	0.65
FF2_logsig	48.1	0.10	82.3	0.67	93.6	0.37	97.6	0.56
GPR	48.1	0.09	82.7	0.25	93.7	0.48	97.6	0.56
FF2_tansig	47.8	0.05	82.6	0.39	94.0	1.00	97.9	0.56
FF2_radbas	47.8	0.07	82.1	0.84	93.6	0.32	97.7	1.00
CS1_tansig	47.8	<.05	82.6	0.35	93.9	0.71	97.7	1.00
FF1_tansig	47.6	0.05	82.6	0.43	93.7	0.48	97.6	0.65
CS2_logsig	47.2	<.05	81.8	0.81	93.6	0.18	97.4	0.32
FF3_radbas	47.0	0.06	80.3	0.15	93.9	0.82	98.0	0.41
SR	46.3	<.05	82.9	0.16	94.0	1.00	97.4	0.32
CS2_purelin	45.8	<.05	79.8	<.05	92.8	0.07	97.9	0.71
CS1_purelin	45.8	<.05	79.7	<.05	93.1	0.16	97.9	0.71
FF2_purelin	45.5	<.05	80.3	0.11	92.8	0.07	97.9	0.71
FF1_purelin	45.3	<.001	79.8	0.05	93.4	0.35	97.9	0.71
BRTE	44.7	<.05	77.1	<.001	90.2	<.0001	96.2	<.05
BRDT	37.3	<.0001	66.6	<.0001	84.0	<.0001	92.1	<.0001
Mutual P	**< .0001**		**< .0001**		**< .0001**		**< .0001**	

Table 132. Mutual evaluation of the PE results in the ALL axial length group. Equation n1(i)=n2(i) means that the compared vectors of prediction results were equal for all data entries.

4.11.2. SHORT axial length subgroup

Mutual comparison (Table 133.) of the SHORT axial length subgroup using all evaluated models proved that there is not the significantly same proportion of success between the models in the ±0.25 D, ±0.50 D, ±0.75 D and ±1.00 D PE groups at the level of P<.0001.

The best model in the ±0.25 D PE group was FF1_radbas. Therefore, every model for each PE group was statistically compared to this model.

In the ±0.25 D PE group, the CS1_logsig, GPR, SVM, CS2_radbas, FF1_tansig, CS1_radbas, CS2_tansig, FF1_logsig, FF2_radbas and FF3_radbas models were insignificantly worse.

The CS2_logsig, CS1_tansig, FF2_tansig, FF2_logsig, SR, CS1_purelin, FF1_purelin, FF2_purelin, CS2_purelin and BRTE models were significantly worse at the level of P<.05. The BRTE model was significantly worse at the level of P<.0001.

In the ±0.50 D PE group, the SR model was insignificantly better and the CS1_logsig, GPR, SVM, CS2_radbas, FF1_tansig, CS1_radbas, CS2_tansig, FF1_logsig, FF2_radbas, CS2_logsig, CS1_tansig, FF2_tansig, FF2_logsig, FF3_radbas, CS1_purelin, FF1_purelin, FF2_purelin and CS2_purelin models performed insignificantly worse or the same. The BRTE and BRDT models were significantly worse at the level of P<.001.

In the ±0.75 D PE group, the CS2_tansig model performed insignificantly better, and the CS1_logsig, GPR, SVM, CS2_radbas, FF1_tansig, CS1_radbas, CS1_tansig, FF2_tansig and SR models performed the same. The FF1_logsig, FF2_radbas, CS2_logsig, FF2_logsig, FF3_radbas, CS1_purelin, FF1_purelin, FF2_purelin and CS2_purelin models performed insignificantly worse. The BRTE and BRDT models performed significantly worse at the level of P<.001 and P<.0001, respectively.

In the ±1.00 D PE group, the FF1_tansig, FF2_tansig and SR models performed insignificantly better. The CS2_tansig, CS1_logsig, GPR, SVM, CS2_radbas, CS1_radbas, CS1_tansig, FF1_logsig and FF2_radbas models performed the same. The CS2_logsig, FF2_logsig, FF3_radbas, CS1_purelin, FF1_purelin, FF2_purelin and CS2_purelin models performed insignificantly worse. The BRTE and BRDT models performed significantly worse at the level of P<.05.

Model	PE							
	±0.25 D		±0.50 D		±0.75 D		±1.00 D	
	[%]	P value	[%]	P value	[%]	P value	[%]	P value
FF1_radbas	**51.8**	$n_1(i)=n_2(i)$	77.8	$n_1(i)=n_2(i)$	95.1	$n_1(i)=n_2(i)$	98.8	$n_1(i)=n_2(i)$
CS1_logsig	49.3	0.32	75.3	0.32	95.1	$n_1(i)=n_2(i)$	98.8	$n_1(i)=n_2(i)$
GPR	48.1	0.08	77.8	1.00	95.1	$n_1(i)=n_2(i)$	98.8	$n_1(i)=n_2(i)$
SVM	48.1	0.32	77.8	1.00	95.1	1.00	98.8	1.00
CS2_radbas	48.1	0.18	77.8	1.00	95.1	$n_1(i)=n_2(i)$	98.8	$n_1(i)=n_2(i)$
FF1_tansig	48.1	0.18	77.8	1.00	95.1	1.00	100.0	0.32
CS1_radbas	48.1	0.08	75.3	0.41	95.1	$n_1(i)=n_2(i)$	98.8	$n_1(i)=n_2(i)$
CS2_tansig	46.9	0.05	77.8	1.00	96.3	0.32	98.8	$n_1(i)=n_2(i)$
FF1_logsig	46.9	0.10	76.5	0.65	93.8	0.32	98.8	1.00
FF2_radbas	46.9	0.05	74.1	0.08	93.8	0.56	98.8	$n_1(i)=n_2(i)$
CS2_logsig	45.6	<.05	77.8	1.00	93.8	0.32	97.5	0.32
CS1_tansig	45.6	<.05	76.5	0.56	95.1	$n_1(i)=n_2(i)$	98.8	$n_1(i)=n_2(i)$
FF2_tansig	45.6	<.05	76.5	0.56	95.1	1.00	100.0	0.32
FF2_logsig	45.6	<.05	72.8	0.10	93.8	0.56	97.5	0.32
SR	44.4	<.05	79.0	0.65	95.1	$n_1(i)=n_2(i)$	100.0	0.32
FF3_radbas	43.2	0.05	70.4	0.06	93.8	0.65	97.5	0.32
CS1_purelin	39.5	<.05	71.6	0.10	93.8	0.65	96.3	0.16
FF1_purelin	38.2	<.05	71.6	0.10	93.8	0.65	96.3	0.16
FF2_purelin	38.2	<.05	70.4	0.06	90.1	0.16	96.3	0.16
CS2_purelin	37.0	<.05	70.4	0.06	90.1	0.16	96.3	0.16
BRTE	27.1	<.05	55.6	<.001	81.5	<.001	88.9	<.05
BRDT	19.7	<.0001	49.4	<.001	71.6	<.0001	85.2	<.05
Mutual P	**< .0001**		**< .0001**		**< .0001**		**< .0001**	

Table 133. Mutual evaluation of the PE results in the SHORT axial length group. Equation n1(i)=n2(i) means that the compared vectors of prediction results were equal for all data entries.

4.11.3. MEDIUM axial length subgroup

Mutual comparison (Table 134.) of the MEDIUM axial length subgroup using all evaluated models proved that there is not the significantly same proportion of success between the models in the ±0.25 D, ±0.50 D, ±0.75 D and ±1.00 D PE groups at the level of P<.0001.

The best model in ±0.25 D PE group was CS2_radbas. Therefore, every model for each PE group was statistically compared to this model.

In the ±0.25 D PE group, the CS2_tansig, SVM, CS1_logsig, GPR, FF1_logsig, CS1_radbas, FF2_logsig, FF2_tansig, FF1_radbas, FF2_radbas, CS1_tansig, FF1_tansig, FF3_radbas, CS2_logsig, BRTE and SR models were insignificantly worse. The CS2_purelin, CS1_purelin, FF2_purelin, FF1_purelin and BRDT models were significantly worse at the level of P<.05.

In the ±0.50 D PE group, the SVM, CS1_radbas, CS2_tansig, FF2_logsig, FF1_logsig, FF2_tansig, CS1_tansig, SR, GPR, FF2_radbas and FF1_tansig models were insignificantly better and the CS1_logsig, FF3_radbas, FF1_radbas, CS2_logsig, CS2_purelin, CS1_purelin, FF1_purelin and BRTE models performed insignificantly worse or same. The BRDT model was significantly worse at the level of P<.0001.

In the ±0.75 D PE group, the FF3_radbas, FF2_tansig and CS1_logsig models performed insignificantly better, and the FF1_radbas model performed the same. The FF2_logsig, CS1_tansig, SR, FF2_radbas, FF1_tansig, CS2_logsig, FF1_purelin, SVM, CS1_radbas, FF1_logsig, GPR, FF2_purelin, CS2_purelin, CS2_tansig and CS1_purelin models performed insignificantly worse. The BRTE and BRDT models performed significantly worse at the level of P<.05 and P<.0001, respectively.

In the ±1.00 D PE group, the FF1_purelin, FF2_purelin, CS2_purelin, CS1_purelin, FF3_radbas and FF1_radbas models performed insignificantly better. The FF2_tansig, CS1_logsig, CS2_radbas, FF2_logsig, CS1_tansig, FF2_radbas, CS2_logsig, SVM, CS1_radbas, FF1_logsig and CS2_tansig models performed the same. The GPR, SR, FF1_tansig and BRTE models performed insignificantly worse. The BRDT model performed significantly worse at the level of P<.001.

Model	PE							
	±0.25 D		±0.50 D		±0.75 D		±1.00 D	
	[%]	P value	[%]	P value	[%]	P value	[%]	P value
CS2_radbas	**50.4**	$n_1(i)=n_2(i)$	82.9	$n_1(i)=n_2(i)$	93.8	$n_1(i)=n_2(i)$	97.5	$n_1(i)=n_2(i)$
CS2_tansig	50.0	0.74	83.5	0.44	93.1	0.18	97.5	1.00
SVM	49.6	0.57	84.2	0.16	93.3	0.41	97.5	1.00
CS1_logsig	49.4	0.37	82.9	1.00	94.0	0.56	97.5	1.00
GPR	49.2	0.30	83.1	0.78	93.3	0.41	97.3	0.32
FF1_logsig	49.2	0.33	83.3	0.62	93.3	0.32	97.5	1.00
CS1_radbas	49.0	0.22	84.0	0.13	93.3	0.41	97.5	1.00
FF2_logsig	49.0	0.27	83.5	0.44	93.5	0.71	97.5	1.00
FF2_tansig	48.8	0.17	83.3	0.59	94.0	0.71	97.5	1.00
FF1_radbas	48.5	0.17	82.7	0.80	93.8	1.00	97.7	0.32
FF2_radbas	48.5	0.14	83.1	0.78	93.5	0.65	97.5	1.00
CS1_tansig	48.3	0.08	83.3	0.53	93.5	0.65	97.5	1.00
FF1_tansig	48.3	0.13	83.1	0.81	93.5	0.65	97.1	0.16
FF3_radbas	48.3	0.21	82.9	1.00	94.4	0.37	97.9	0.32
CS2_logsig	48.1	0.05	82.5	0.53	93.5	0.56	97.5	1.00
BRTE	47.7	0.22	80.8	0.14	91.5	<.05	97.1	0.48
SR	47.7	0.05	83.3	0.59	93.5	0.65	97.1	0.16
CS2_purelin	46.9	<.05	82.5	0.71	93.3	0.41	98.1	0.08
CS1_purelin	46.5	<.05	82.5	0.72	93.1	0.26	98.1	0.08
FF2_purelin	46.5	<.05	83.1	0.85	93.3	0.41	98.1	0.08
FF1_purelin	46.3	<.05	82.5	0.72	93.5	0.71	98.1	0.08
BRDT	41.0	<.05	69.4	<.0001	86.9	<.0001	93.8	<.001
Mutual P	**< .0001**		**< .0001**		**< .0001**		**< .0001**	

Table 134. Mutual evaluation of the PE results in the MEDIUM axial length group. Equation n1(i)=n2(i) means that the compared vectors of prediction results were equal for all data entries.

4.11.4. LONG axial length subgroup

Mutual comparison (Table 135.) of the LONG axial length subgroup using all evaluated models proved that there is not the significantly same proportion of success between the models in ±0.25 D, ±0.50 D, ±0.75 D and ±1.00 D PE groups at the level of P<.0001.

The best models in the ±0.25 D PE group were CS2_radbas and CS1_radbas. Since CS2_radbas was better in two other PE groups (±0.75 D and ±1.00 D), we deemed this model to be the best. Therefore, every model for each PE group was statistically compared to this model.

In the ±0.25 D PE group, the CS1_radbas model performed the same. The CS1_purelin, CS2_purelin, FF1_radbas, FF2_purelin, FF1_purelin, CS1_tansig, SVM, FF1_logsig, FF2_logsig, CS1_logsig, BRTE, FF2_radbas, FF2_tansig, FF3_radbas, FF1_tansig, CS2_tansig, CS2_logsig and GPR models were insignificantly worse. The SR and BRDT models were significantly worse at the level of P<.05.

In the ±0.50 D PE group, the SVM, GPR, FF1_radbas, CS1_tansig, FF1_logsig, FF2_logsig, FF2_radbas, FF2_tansig, FF1_tansig, CS2_tansig, SR, CS1_radbas and CS1_logsig models were insignificantly better and BRTE and FF3_radbas performed insignificantly worse. The CS2_purelin, FF2_purelin, FF1_purelin, CS1_purelin and BRDT models performed significantly worse at the level of P<.05.

In the ±0.75 D PE group, the SR model performed insignificantly better, and the GPR, CS1_tansig models performed the same. The SVM, FF1_radbas, FF1_logsig, FF2_logsig, FF2_radbas, FF2_tansig, FF1_tansig, CS2_tansig, CS1_radbas, CS1_logsig, CS2_logsig, CS2_purelin, FF2_purelin, FF1_purelin, CS1_purelin, BRTE and FF3_radbas models performed insignificantly worse. The BRDT model performed significantly worse at the level of P<.001.

In the ±1.00 D PE group, the FF1_logsig and FF3_radbas models performed insignificantly better. The GPR, CS1_tansig, CS2_radbas, FF2_logsig, FF2_radbas, FF2_tansig, FF1_tansig, CS2_purelin, FF2_purelin, FF1_purelin, CS1_purelin and BRTE models performed the same. The SR, CS2_tansig, CS1_radbas, CS1_logsig, CS2_logsig, SVM and FF1_radbas models performed insignificantly worse. The BRDT model performed significantly worse at the level of P<.05.

Model	PE							
	±0.25 D		±0.50 D		±0.75 D		±1.00 D	
	[%]	P value	[%]	P value	[%]	P value	[%]	P value
CS2_radbas	**48.9**	$n_1(i)=n_2(i)$	80.9	$n_1(i)=n_2(i)$	94.7	$n_1(i)=n_2(i)$	97.9	$n_1(i)=n_2(i)$
CS1_radbas	48.9	1.00	83.0	0.16	93.6	0.32	96.8	0.32
CS1_purelin	47.9	0.83	72.3	<.05	92.6	0.41	97.9	1.00
CS2_purelin	47.9	0.82	74.5	<.05	92.6	0.41	97.9	1.00
FF1_radbas	47.9	0.74	84.0	0.18	93.6	0.32	95.7	0.16
FF2_purelin	46.8	0.65	74.5	<.05	92.6	0.41	97.9	1.00
FF1_purelin	46.8	0.65	73.4	<.05	92.6	0.41	97.9	1.00
CS1_tansig	46.8	0.53	84.0	0.08	94.7	1.00	97.9	1.00
SVM	45.7	0.47	85.1	0.10	93.6	0.32	95.7	0.16
FF1_logsig	45.7	0.26	84.0	0.08	93.6	0.32	98.9	0.32
FF2_logsig	45.7	0.26	84.0	0.08	93.6	0.32	97.9	$n_1(i)=n_2(i)$
CS1_logsig	45.7	0.26	83.0	0.16	93.6	0.32	96.8	0.32
BRTE	44.7	0.50	76.6	0.35	91.5	0.26	97.9	1.00
FF2_radbas	44.7	0.29	84.0	0.26	93.6	0.32	97.9	$n_1(i)=n_2(i)$
FF2_tansig	44.7	0.21	84.0	0.08	93.6	0.32	97.9	$n_1(i)=n_2(i)$
FF3_radbas	43.6	0.30	75.5	0.13	91.5	0.08	98.9	0.32
FF1_tansig	43.6	0.10	84.0	0.18	93.6	0.32	97.9	1.00
CS2_tansig	43.6	0.10	84.0	0.18	93.6	0.32	96.8	0.32
CS2_logsig	43.6	0.06	81.9	0.56	93.6	0.32	96.8	0.32
GPR	42.6	0.11	85.1	0.05	94.7	1.00	97.9	1.00
SR	40.4	<.05	84.0	0.08	95.7	0.56	96.8	0.32
BRDT	33.0	<.05	67.0	<.05	79.8	<.001	89.4	<.05
Mutual P	**< .0001**		**< .0001**		**< .0001**		**< .0001**	

Table 135. Mutual evaluation of the PE results in the LONG axial length group. Equation n1(i)=n2(i) means that the compared vectors of prediction results were equal for all data entries.

5. PROSPECTIVE EVALUATION

The prospective evaluation was designed with regard to safety as a single-surgeon and single-clinic and was performed on a set of 45 eyes (21 right eyes, 24 left eyes) of 27 patients (13 male, 14 female) between 01/2019 and 03/2019. Patients were included in the prospective evaluation group and met the same criteria as described in section 3.1 for retrospective evaluation, but a different calculation method was used, namely the CS2_radbas model.

The subjective spherical equivalent was evaluated 68.29 ± 12.69 (46 - 94) days (mean ± standard deviation (minimum - maximum)) after the surgery. The prospective dataset population characteristics are summarized in Table 136, and the results of the prospective evaluation are presented in Table 137.

	Mean	**Median**	**Std**	**Min**	**Max**	**P_{SW}**	**P_{DP}**
Age [years]	58.80	60	7.14	40.00	69.00	0.0232	0.0460
K [D]	43.95	44.24	1.43	40.86	46.69	0.2568	0.4172
ACD [mm]	3.14	3.18	0.34	2.33	3.86	0.9447	0.9779
AL [mm]	22.84	22.9	0.97	20.27	24.59	0.4620	0.3612
Rx_{pre} [D]	1.73	1.75	1.37	-1.63	5.88	0.0046	0.0379
$IOL_{Implanted}$ [D]	22.70	22.00	2.98	18.00	30.00	0.0011	0.0264

Table 136. Prospective set population characteristics

PE [D]	**Prospective results $Rx_{post-Sbj}$**
ME	0.01
MAE	0.18
MedAE	0.13
Std	0.29
Min	-1.00
Max	0.63
Eyes within PE [%]	
±0.25	77.8
±0.50	93.3
±0.75	97.8
±1.00	100.0

Table 137. Results of the prospective testing

Prospective results are discussed in the Discussion and Conclusions chapter.

6. DISCUSSION AND CONCLUSIONS

This paper deals with intraocular lens (IOL) calculations in cataract surgery or refractive lens exchange surgery. The optical power of the lens is undoubtedly very important for a patient's postoperative vision. Based on the background provided in this paper's introduction, and the results documented from state-of-the-art research, one could say that the accuracy of the formulas in the present literature achieved ±0.5 D from the intended target refraction in only 60-80% of eyes [34]. Their accuracy decreases even further for eyes with non-standard biometric features such as eyes with short or long axial lengths [59, 64]. In the second chapter of the work, the goals of the thesis are defined.

The third chapter deals with the methodology of selecting and optimizing a dataset for machine learning. Selecting the appropriate data is a key process whose correct integration ensures that reliable models from data can be obtained. Incorrect or noisy data used in machine learning can lead to an undesirable training process and reduced prediction accuracy [126]. Therefore, the focus was on the exclusion of all preoperative, surgery and postoperative data that could cause the aforementioned. One of the important points of this chapter is also feature selection. The reason for the significantly worse results of the CR group could be the incorrect adaptation of the calculation method to the clinical workflow and is its simplicity, where only AL and K are used for the IOL power calculation (the SRK/T formula is used). In order to increase calculation accuracy, modern calculation methods take into account more circumstances, which could affect the refractive predictability of the surgery [3, 26, 127]. Input parameters used in our models are standard parameters acquired using regular patient examination prior to the cataract surgery. Thus, it does not introduce any additional requirement for data acquisition. Table 138 describes the input parameters used by the contemporary formulas Hill-RBF, HofferQ, Holladay 1, Holladay 2, SRK/T, Haigis and Olsen [127]. Our model input parameters are K (Mean Keratometry), ACD (Anterior Chamber Depth), AL (Axial Length), Age and Rx_{pre} (Preoperative distance objective refraction), which are all the possible calculation variables which can be extracted from the electronic health record (EHR) during the data mining process.

	Hill-RBF	HofferQ	Holladay 1	Holladay 2	SRK/T	Haigis	Olsen
K	x	x	x	x	x	x	x
AL	x	x	x	x	x	x	x
ACD	x			x		x	x
LT				x			x
WTW	x			x			x
Age				x			
Rx_{pre}				x			

Table 138. Overview of the input parameters used by the contemporary formulas.

The IOL Master 500 used in the biometry examination to gather the anatomical data is not able to measure lens-thickness (LT). However, the influence on the precision could probably be neglected as it is said to be the second least important calculation

factor [128]. On the other hand, it can have a greater influence on the IOL calculation than K [129]. One of the other ways to improve the accuracy of calculations would be to find a way to extract information from incomplete white-to-white (WTW) measurements as this value is considered the third most important in predicting postoperative effective lens position (ELP) [130]. It is possible to find a way to handle missing values in datasets in order to maximize information gain [131].

Poor CR group results could also be because of the non-optimized constant of the implanted IOL. This is seen in the mean error of the CR group, which has a range between -0.37 to -0.53 D among all axial length subsets. Our method of IOL_{Ideal} calculation optimizes the mean error of prediction to zero. This mechanism of IOL_{Ideal} calculation can thus influence the mean error based on the desired refraction.

The proposed method's underlying concept is to train the models on the ideal results of surgeries. That is, training on measurement data in relation to IOL would not induce any residual post-operative refraction error in the patient. To achieve this goal, a method for calculating the optimal IOL for a given eye based on the measured results has been proposed. At the end of the third chapter, machine learning models, algorithms and methods used in their training, and methodology of evaluation and comparison of the results are described. Furthermore, the method of selecting the best model that is subjected to prospective testing is presented.

In order to avoid distortion of statistical analysis by correlated data, it is recommended that only one eye per patient be included in the analyses [132]. Our Verification set contained less than 10% of the data that came from both eyes of the patients. This means that the intra-class correlation factor will be less than 0.1 in the worst possible scenario (between eyes correlation equals to 1 – for every applicable patient in the Verification set) indicating extremely poor correlation [133, 134]. We have thus concluded that it is safe to use conventional methods of statistical analysis while including maximum number of eyes in our datasets.

In the fourth chapter of the thesis, the parameters of settings and the results of testing of all examined artificial neural networks (ANNs) and machine learning models, which are mutually compared at the end of this chapter, are reported. The accuracy of the models is evaluated based on the percentage of eyes with prediction errors between ±0.25 D, as it represents the most accurate PE group for evaluating refractive predictability. In the ideal case, we want to have 100% of all cases in this group, which would yield an extremely accurate prediction model and result in a small percentage of subsequent refractive corrections. This PE group also has the greatest variability of results across all axial length groups. In other PE groups, the degree of variability of the results decreases with increasing diopters, and it is no exception that, eg., in ±1.00 D PE group more than half of the models have exactly the same results (SHORT and LONG axial length subgroups). Furthermore, for the sake of simplicity through highlights, the results of the comparisons are presented.

For the ALL axial length subset:

- CS2_radbas (best model) was the model with the highest accuracy in the ±0.25 D PE group and was significantly better than CR
- SVM had the highest accuracy among non-ANN models and was insignificantly worse than CS2_radbas and significantly better than CR
- All ANN models with the linear transfer function had significantly worse accuracy compared to the best model in this category

For the SHORT axial length subset:

- FF1_radbas (best model) was the model with the highest accuracy in the ±0.25 D PE group, but this was not significant compared to CR
- SVM had the highest accuracy among non-ANN models and was insignificantly worse than FF1_radbas and insignificantly better than CR
- All ANN models with the linear transfer function had significantly worse accuracy compared to the best model in this category
- The BRTE model was significantly worse compared to CR
- The BRDT model was significantly worse than CR with more than half of the accuracy

For the MEDIUM axial length subset:

- CS2_radbas (best model) was the model with the highest accuracy in the ±0.25 D PE group and was significantly better compared to CR
- SVM had the highest accuracy among non-ANN models and was insignificantly worse than CS2_radbas and significantly better than CR
- All evaluated models were significantly better than CR
- All ANN models with the linear transfer function had significantly worse accuracy compared to the best model in this category

For the LONG axial length subset:

- CS2_radbas and CS1_radbas (best models) were the models with the highest accuracy in the ±0.25 D PE group
- SVM is the only non-ANN model with significantly better performance compared to CR; all other non-ANN machine learning algorithms were insignificantly better
- Cascade-Forward ANN seems to be more suitable than Feed-Forward

It follows from the above that Cascade-Forward MLNN in combination with the radial basis function in the hidden layer was best placed among the ANN based algorithms. To the contrary, the worst algorithm, among ANN based algorithms, was the ANN with a linear function, which is the effect we expected because the nonlinear space, which is

defined by the specifics of the patient's eye and the results of the operation, is inherently nonlinear and thus approximation by linear functions cannot provide sufficient precision. Among the non-ANN algorithms, SVMs were the best, and the BRDTs, which are known for their oversensitivity to irrelevant attributes and noise [135], were the worst.

An insignificant improvement occurred mostly for the SHORT and LONG axial length subsets. As such, and as previously mentioned, calculations for eyes with a short axial length are problematic due to the more complex ELP prediction and because of the higher probability of a steep cornea and a shallow ACD [136] and also in eyes with LONG axial length due to flatter corneas, thinner crystalline lenses and deeper ACD [137]. Compared to CR, most models in all AL subgroups had smaller standard deviations, which leads to higher certainty of the calculation method [65]. Compared to CR, all models predicted almost identically slightly larger maximum (Max) error. This appeared mostly for the MEDIUM and LONG axial length group. The most likely explanation for this result points to the residual errors in the input data since it occurred always in the same samples.

As the final goal of this work, a prospective evaluation was performed. Compared to the clinical results reached by the calculation method used in the clinical workflow, the CS2_radbas model rapidly improved clinical refractive results of cataract surgeries for the ±0.25 D, ±0.50 D, ±0.75 D and ±1.00 D PE groups by 28.5%, 18.2%, 10.0% and 4.6%, respectively. 100% of the eyes were within ±1.00 D of PE. Results of prospective testing are even better compared to CS2_radbas retrospective testing. This is most likely due to the fact that prospective testing was designed, for safety reasons, as single-clinic and single-surgeon. It is likely that less homogeneous measurement conditions, clinical workflow, patient selection and surgical techniques will cause a slight reduction in accuracy, but we do not expect them to exceed the accuracy achieved by retrospective testing.

Compared to the results of the contemporary formulas in eyes with all axial lengths which were gained from the literature (Table 139.), where the Barrett Universal II formula is often presented as the most accurate calculation formula [31, 32, 35, 65, 138], the accuracy achieved by the CS2_radbas model in our prospective testing is considerably better for the ±0.25 D, ±0.50 D and ±0.75 D PE groups by 16.7%, 13.3% and 3.3%, respectively. All eyes were within ±1.00 D of PE. In this case, subjective refraction is compared, which is more often presented in the literature. However, although this is a very promising result, in order to objectively compare the results, it would be necessary to evaluate all methods on the same datasets and not use the source of the outcomes in the literature.

PE [D]	Literature	CR_{Sbj}	Prospective results $Rx_{post\text{-}Sbj}$
ME	-0.19 – 0.05	-0.33	0.01
MAE	0.29 – 0.43	0.38	0.18
MedAE	0.20 – 0.35	0.38	0.13
Std	0.31 – 0.51	0.40	0.29
MaxAErr	1.30 – 2.96	1.50	1.00
Eyes within PE [%]			
±0.25	37.9 – 61.3	49.3	77.8
±0.50	66.6 – 80.0	75.1	93.3
±0.75	92.7 – 94.5	87.8	97.8
±1.00	92.0 – 99.9	95.4	100.0

Table 139. Prediction error comparison (MaxAErr – Maximal absolute error)

There is a discussion on the subject of correlation of the objective and subjective refraction in contemporary literature. There are opinions presenting which state that the rate of agreement between objective and subjective refraction depends on the type of multifocal IOL used, and in specific cases does not correlate [139] and that it does not statistically differ for other IOLs [140, 141].

For our purposes, it was considered more appropriate to use objective refraction measurements since they were always obtained using the same measurement method by the same measuring device. In the measurement of subjective refraction, we expected a larger factor of subjective error since the data was acquired by many different clinicians at numerous facilities. The correctness of this reasoning is confirmed by the fact that the prospective results of subjective refraction are even better than the objective results, and it can thus be said that, in our case, objective measurements of refraction are more appropriate for machine learning applications.

Our method does not use A constants like typical formulas; all models are designed as lens-specific, so the ELP prediction is coded directly into the model's internal structures. The machine learning model design for another IOL would require an entirely new Data Preparation, Model Design and Training and Evaluation process. However, due to the fact that there are many small dataset machine learning strategies, it would not be necessary to search for the same amount of training data [142, 143]. Another limitation could be the unknown training accuracy outside the input variables training range. The solution to this problem is to train the network on a larger data sample so that the estimation error for extreme eye cases is minimized as much as possible.

Our research indicated that ANN and other machine learning algorithms evaluated in this work have a strong potential for improving clinical IOL calculations. Greater accuracy of IOL calculations reduces the risk of subsequent reoperation or potential refractive laser corrections and the associated risk of complications and increases a patient's comfort.

The advantage in using ANN for IOL power determination is that they are able to learn and extract input-to-output data relations just from examples, which in our application, is from the patient examinations and surgery results. The training set can be created directly from the data selected in a clinical practice database, and the calculation system can be made to meet specific surgical techniques and conditions.

Most of the evaluated models showed they are able to effectively find input-to-output relations, accurately estimate the optical power of the IOL and thus provide a potentially new way of calculating optical power for the cataract and lens replacement ophthalmic surgeries.

The clinical implication of this work may mean greater refractive predictability for lens replacement surgery [34] and therefore, a smaller number of subsequent re-operations, which ultimately reduces the risk of potential complications.

AUTHOR PUBLICATIONS

Publications related to the topic of the dissertation

Publications in impacted journals

ŠRAMKA, Martin, Martin SLOVÁK, Jana TUČKOVÁ and Pavel STODŮLKA. Improving Clinical Intra-Ocular Lens Power Calculations by Support Vector Machine Regression Model and Multilayer Neural Network Ensemble Model. *PeerJ* — the Journal of Life and Environmental Sciences.

Author contribution: ŠRAMKA 70%, SLOVÁK 10%, TUČKOVÁ 10%, STODŮLKA 10%

ŠRAMKA, Martin, Martin SLOVÁK, Jana TUČKOVÁ and Pavel STODŮLKA. Evaluation of two transfer functions of the Multilayer Neural Network Ensemble model for calculating the optical power of intraocular lenses for long eyes**.** *Biocybernetics and Biomedical Engineering* [online]. 2016. ISSN 02085216. In review.

Author contribution: ŠRAMKA 70%, SLOVÁK 10%, TUČKOVÁ 10%, STODŮLKA 10%

Publications in peer-reviewed journals

SRAMKA, Martin and Alzbeta VLACHYNSKA. Artificial Neural Networks Application in Intraocular Lens Power Calculation. In: Linköping Electronic Conference Proceedings. Oulu: Linköping University Electronic Press, 2018, 2018-12-19, s. 25-30. DOI: 10.3384/ecp1714225. ISBN 978-91-7685-399-3. ISSN 1650-3740. Available at: http://www.ep.liu.se/ecp/article.asp?issue=142&article=

Author contribution: ŠRAMKA 70%, VLACHYNSKA 30%

Other publications

ŠRAMKA, Martin, Pavel STODŮLKA a Jana TUČKOVÁ. Nová kalkulace IOL umělou neuronovou sítí. In: XXVI. Výroční sjezd České oftalmologické společnosti ČLS JEP. Ústí nad Labem: BOS.org, 2018, s. 36. ISBN 978-80-87562-80-2.

Author contribution: ŠRAMKA 70%, STODULKA 15%, TUČKOVÁ 15%

ŠRAMKA, Martin a Pavel STODŮLKA. Nová kalkulace IOL umělou neuronovou sítí. In: XVI. Mezinárodní kongres České Společnosti Refrakční a Kataraktové Chirurgie ČLS JEP. Ústí nad Labem: BOS.org, 2018, s. 46. ISBN 978-80-906874-3-1.

Author contribution: ŠRAMKA 70%, STODULKA 15%, TUČKOVÁ 15%

ŠRAMKA, Martin and Alžběta VLACHYNSKÁ. Artificial Neural Networks Application in Intraocular Lens Power Calculation In: IEEE 2016 9th EUROSIM Congress on Modelling and Simulation. Santa Monica: IEEE, 2016. ISBN 978-1-5090-4119-0.

Author contribution: ŠRAMKA 70%, VLACHYNSKA 30%

TIHELKOVÁ, Eva, Andrea NOVÁKOVÁ, Martin ŠRAMKA a Pavel STODŮLKA. Refrakční prediktabilita u nitrooční čočky EnVista MX60. In: XXVI. Výroční sjezd České oftalmologické společnosti ČLS JEP. Ústí nad Labem: BOS.org, 2018, s. 43. ISBN 978-80-87562-80-2.

Equivalent contribution of all authors

TIHELKOVÁ, Eva, Andrea NOVÁKOVÁ, Martin ŠRAMKA a Pavel STODŮLKA. FineVision Micro F: Naše zkušenosti. In: XXVI. Výroční sjezd České oftalmologické společnosti ČLS JEP. Ústí nad Labem: BOS.org, 2018, s. 45. ISBN 978-80-87562-80-2.

Equivalent contribution of all authors

STODŮLKA, Pavel a Martin ŠRAMKA. První zkušenosti se sinusoidální trifokální čočkou bez ostrých struktur. In: XXVI. Výroční sjezd České oftalmologické společnosti ČLS JEP. Ústí nad Labem: BOS.org, 2018, s. 45. ISBN 978-80-87562-80-2.

Equivalent contribution of all authors

NOVÁKOVÁ, Andrea, Eva TIHELKOVÁ, Martin ŠRAMKA a Pavel STODŮLKA. Refrakční prediktabilita u nitrooční čočky enVista MX60. In: XVI. Mezinárodní kongres České Společnosti Refrakční a Kataraktové Chirurgie ČLS JEP. Ústí nad Labem: BOS.org, 2018, s. 48. ISBN 978-80-906874-3-1.

Equivalent contribution of all authors

TIHELKOVÁ, Eva, Andrea NOVÁKOVÁ, Martin ŠRAMKA a Pavel STODŮLKA. Kalkulace optické mohutnosti trifokální nitrooční čočky FineVision. In: XVI. Mezinárodní kongres České Společnosti Refrakční a Kataraktové Chirurgie ČLS JEP. Ústí nad Labem: BOS.org, 2018, s. 47. ISBN 978-80-906874-3-1.

Equivalent contribution of all authors

Publications not related to the topic of the dissertation

Publications in peer-reviewed journals

TUČKOVÁ, Jana and Martin ŠRAMKA. ANN application in emotional speech analysis. Int.J. of Data Analysis Techniques and Strategies. 2012, 4(3/2012), 256-276. ISSN 1755-8050.

Author contribution: TUČKOVÁ 60%, ŠRAMKA 40%

STODŮLKA, Pavel, Monika HORÁČKOVÁ, Martin ŠRAMKA and Martin SLOVÁK. Effective tissue layer separation of donor cornea for DMEK by fluid injection between Descemet membrane and corneal stroma: Results of the first series of operations. Czech and Slovak Ophthalmology. 2019, 1, 32-37. ISSN 1211-9059.

Equivalent contribution of all authors

Other publications

STODŮLKA, Pavel a Martin ŠRAMKA. Korekce presbyopie a myopie difrakční presbyopickou fakickou čočkou. In: 15. Mezinárodní kongres České společnosti refrakční a kataraktové chirurgie. Prague: ČLS JEP, 2017. p. 17. ISBN 978-80-906549-6-9.

Equivalent contribution of all authors

TUČKOVÁ, Jana and Martin ŠRAMKA. Emotional Speech Analysis using Artificial Neural Networks**.** In: Proceedings of the International Multiconference on Computer Science and Information Technology. Wroclaw: Polish Academy of Sciences, 2010. pp. 141-147. ISSN 1896-7094. ISBN 978-83-60810-27-9.

Equivalent contribution of all authors

VLACHYNSKA, Alzbeta, KOMINKOVA OPLATKOVA, Zuzana and Martin SRAMKA. The coordinate system of the eye in cataract surgery: Performance comparison of the circle Hough transform and Daugman's algorithm. In: Proceedings of International Conference on Numerical Analysis and Applied Mathematics 2016 (ICNAAM-2016). New York: AIP Conference Proceedings, 2017. AIP Conference Proceedings. vol. 1863. ISSN 0094-243X. ISBN 978-0-7354-1538-6.

Equivalent contribution of all authors

STODŮLKA, Pavel a Martin ŠRAMKA. Presbyopická fakická čočka pro korekci myopie: 2 roky sledování. In: *XXVI. Výroční sjezd České oftalmologické společnosti ČLS JEP*. Ústí nad Labem: BOS.org, 2018, s. 47. ISBN 978-80-87562-80-2.

Equivalent contribution of all authors

STODŮLKA, Pavel, Zuzana HALAŠOVÁ a Martin ŠRAMKA. Inovace v léčbě keratokonu. In: *XXVI. Výroční sjezd České oftalmologické společnosti ČLS JEP*. Ústí nad Labem: BOS.org, 2018, s. 85. ISBN 978-80-87562-80-2.

Equivalent contribution of all authors

STODŮLKA, Pavel, Monika HORÁČKOVÁ a Martin ŠRAMKA. DMEK - Nový operační postup In: Česká oftalmologická společnost 2016 Sborník abstraktů. Prague: ČLS JEP, 2016. p. 49-50. ISBN 978-80-87562-56-7.

Equivalent contribution of all authors

STODŮLKA, Pavel a Martin ŠRAMKA. Klinické výsledky implantace presbyopické fakické nitrooční čočky – 2 roky sledování. In: XVI. Mezinárodní kongres České Společnosti Refrakční a Kataraktové Chirurgie ČLS JEP. Ústí nad Labem: BOS.org, 2018, s. 32. ISBN 978-80-906874-3-1.

Equivalent contribution of all authors

STODŮLKA, Pavel a Martin ŠRAMKA. Presbyopická fakická čočka pro korekci myopie: 2 roky sledování. In: XXVI. Výroční sjezd České oftalmologické společnosti ČLS JEP. Ústí nad Labem: BOS.org, 2018, s. 47. ISBN 978-80-87562-80-2.

Equivalent contribution of all authors

STODŮLKA, Pavel, Zuzana HALAŠOVÁ a Martin ŠRAMKA. Inovace v léčbě keratokonu. In: XXVI. Výroční sjezd České oftalmologické společnosti ČLS JEP. Ústí nad Labem: BOS.org, 2018, s. 85. ISBN 978-80-87562-80-2.

Equivalent contribution of all authors

STODŮLKA, Pavel a Martin ŠRAMKA. Jak mu to říct?: Kasuistika nečekaného nálezu před refrakční operací. In: XXVI. Výroční sjezd České oftalmologické společnosti ČLS JEP. Ústí nad Labem: BOS.org, 2018, s. 103. ISBN 978-80-87562-80-2.

Equivalent contribution of all authors

STODŮLKA, Pavel a Martin ŠRAMKA. DMEK hydroseparací a zařízením pro sledování polohy hlavy. In: XXVI. Výroční sjezd České oftalmologické společnosti ČLS JEP. Ústí nad Labem: BOS.org, 2018, s. 109. ISBN 978-80-87562-80-2.

Equivalent contribution of all authors

STODŮLKA, Pavel a Martin ŠRAMKA. DMEK hydroseparací a zařízením pro sledování polohy hlavy. In: XXVI. Výroční sjezd České oftalmologické společnosti ČLS JEP. Ústí nad Labem: BOS.org, 2018, s. 109. ISBN 978-80-87562-80-2.

Equivalent contribution of all authors

ŠRAMKA, Martin. Diploma thesis: Classification of emotions. (in Czech: Klasifikace emocí.) Prague, CTU FEE 2010, unpublished.

List of Abbreviations

ACD Anterior chamber depth
AL Axial length
ANN Artifical neural network
BO Bayesian optimizer
BRDT Binary regression decision tree
BRTE Boosted regression tree ensemble
CDVA Corrected distance visual acuity
CNVA Corrected near distance visual acuity
CR Clinical results
D Diopters
EHR Electronic health record
EIP Expected improvement plus
ELP Effective lens position
GPR Gaussian process
IOL Intraocular lens
IOL_{Ideal} Optical power of an ideal intraocular lens
$IOL_{Implanted}$ Optical power of an implanted intraocular lens
$IOL_{Predicted}$ Optical power of predicted intraocular lens
IRB Institutional review board
K Mean keratometry
Logsig Log-Sigmoid transfer function
LT Lens thickness
MAE Mean absolute prediction error
Max Maximum, Maximum prediction error
MD Master dataset
ME Mean numerical prediction error
MedAE Median absolute prediction error
Min Minimum, Minimum prediction error
MLNN Multilayer neural network
MPR Model prediction results
MSE Mean squared normalized error
PE Prediction error
P_{DP} DAgostino & Pearson Test
P_{SW} Shapiro-Wilk Test
Purelin Linear transfer function
Radbas Radial Basis transfer function
Rx_{post} Postoperative distance objective refraction
Rx_{pre} Preoperative distance objective refraction
$Rx_{predicted}$ Predicted postoperative refraction
$Rx_{TheorPost}$ Refraction calculated for the eye with specific biometric parameters
SR Stepwise Regression

Std	Standard deviation
SVM	Support Vector Machine
Tansig	Hyperbolic Tangent Sigmoid transfer function
UDVA	Uncorrected distance visual acuity
UNVA	Uncorrected near visual acuity
V	Vertex distance
WTW	White to white measurement

List of Figures

List of Tables

REFERENCES

[1] WANG, Wei, William YAN, Kathy FOTIS, Noela M. PRASAD, Van Charles LANSINGH, Hugh R. TAYLOR, Robert P. FINGER, Damian FACCIOLO and Mingguang HE. Cataract Surgical Rate and Socioeconomics: A Global Study. *Investigative ophthalmology & visual science* [online]. 2016, **57**(14), 5872–5881. ISSN 1552-5783. Available at: doi:10.1167/iovs.16-19894

[2] ALLEN, David and Abhay VASAVADA. Cataract and surgery for cataract. *BMJ* [online]. 2006, **333**(7559), 128–132. ISSN 0959-8138. Available at: doi:10.1136/bmj.333.7559.128

[3] HAIGIS, Wolfgang. Challenges and approaches in modern biometry and IOL calculation. *Saudi Journal of Ophthalmology* [online]. 2012, **26**(1), 7–12. ISSN 13194534. Available at: doi:10.1016/j.sjopt.2011.11.007

[4] KHAIRALLAH, Moncef, Rim KAHLOUN, Rupert BOURNE, Hans LIMBURG, Seth R. FLAXMAN, Jost B. JONAS, Jill KEEFFE, Janet LEASHER, Kovin NAIDOO, Konrad PESUDOVS, Holly PRICE, Richard A. WHITE, Tien Y. WONG, Serge RESNIKOFF and Hugh R. TAYLOR. Number of People Blind or Visually Impaired by Cataract Worldwide and in World Regions, 1990 to 2010. *Investigative Opthalmology & Visual Science* [online]. 2015, **56**(11), 6762. ISSN 1552-5783. Available at: doi:10.1167/iovs.15-17201

[5] PASCOLINI, Donatella and Silvio Paolo MARIOTTI. Global estimates of visual impairment: 2010. *The British journal of ophthalmology* [online]. 2012, **96**(5), 614–8. ISSN 1468-2079. Available at: doi:10.1136/bjophthalmol-2011-300539

[6] BUSBEE, Brandon G., Melissa M BROWN, Gary C. BROWN and Sanjay SHARMA. Incremental cost-effectiveness of initial cataract surgery. *Ophthalmology* [online]. 2002, **109**(3), 606–12; discussion 612-3. ISSN 0161-6420. Available at: doi:10.1016/S0161-6420(01)00971-X

[7] FRAMPTON, Geoff, Petra HARRIS, Keith COOPER, Andrew LOTERY and Jonathan SHEPHERD. The clinical effectiveness and cost-effectiveness of second-eye cataract surgery: a systematic review and economic evaluation. *Health Technology Assessment* [online]. 2014, **18**(68), 1–206. ISSN 1366-5278. Available at: doi:10.3310/hta18680

[8] ABELL, Robin G. and Brendan J. VOTE. Cost-effectiveness of femtosecond laser-assisted cataract surgery versus phacoemulsification cataract surgery. *Ophthalmology* [online]. 2014, **121**(1), 10–16. ISSN 1549-4713. Available at: doi:10.1016/j.ophtha.2013.07.056

[9] CONGDON, Nathan. Self assessed benefit of cataract extraction. *The British journal of ophthalmology* [online]. 2005, **89**(8), 931. ISSN 0007-1161. Available at: doi:10.1136/bjo.2005.068114

[10] LUNDSTRÖM, Mats, Susanne ALBRECHT, Majvi NILSSON and Bengt ASTRÖM. Benefit to patients of bilateral same-day cataract extraction: Randomized clinical

study. *Journal of cataract and refractive surgery* [online]. 2006, **32**(5), 826–30. ISSN 0886-3350. Available at: doi:10.1016/j.jcrs.2006.01.075

[11] LINEBARGER, Eric J., David R. HARDTEN, Gaurav K. SHAH and Richard L. LINDSTROM. Phacoemulsification and Modern Cataract Surgery. *Survey of Ophthalmology* [online]. 1999, **44**(2), 123–147. ISSN 00396257. Available at: doi:10.1016/S0039-6257(99)00085-5

[12] LAMOUREUX, Ecosse L, Eva FENWICK, Konrad PESUDOVS and Donald TAN. The impact of cataract surgery on quality of life. *Current Opinion in Ophthalmology* [online]. 2011, **22**(1), 19–27. ISSN 1040-8738. Available at: doi:10.1097/ICU.0b013e3283414284

[13] AYAKI, Masahiko, Masahiro MURAMATSU, Kazuno NEGISHI and Kazuo TSUBOTA. Improvements in sleep quality and gait speed after cataract surgery. *Rejuvenation research* [online]. 2013, **16**(1), 35–42. ISSN 1557-8577. Available at: doi:10.1089/rej.2012.1369

[14] OWSLEY, Cynthia. Impact of Cataract Surgery on Motor Vehicle Crash Involvement by Older Adults. *JAMA* [online]. 2002, **288**(7), 841. ISSN 0098-7484. Available at: doi:10.1001/jama.288.7.841

[15] HARIPRIYA, Aravind, Hemant SONAWANE and R. D. THULASIRAJ. Changing techniques in cataract surgery: how have patients benefited? *Community eye health* [online]. 2018, **30**(100), 80–81. ISSN 0953-6833. Available at: http://www.ncbi.nlm.nih.gov/pubmed/29483751

[16] PALANKER, Daniel V., Mark S. BLUMENKRANZ, Dan ANDERSEN, Michael WILTBERGER, George MARCELLINO, Phillip GOODING, David ANGELEY, Georg SCHUELE, Bruce WOODLEY, Michael SIMONEAU, Neil J. FRIEDMAN, Barry SEIBEL, Juan BATLLE, Rafael FELIZ, Jonathan TALAMO and William CULBERTSON. Femtosecond Laser-Assisted Cataract Surgery with Integrated Optical Coherence Tomography. *Science Translational Medicine* [online]. 2010, **2**(58), 58ra85-58ra85. ISSN 1946-6234. Available at: doi:10.1126/scitranslmed.3001305

[17] MCMULLEN, Richard and Mary UTTER. Current developments in equine cataract surgery. *Equine Veterinary Journal* [online]. 2010, **42**(S37), 38–45. ISSN 04251644. Available at: doi:10.1111/j.2042-3306.2010.tb05633.x

[18] CHOI, Kup-Sze, Sophia SOO and Fu-Lai CHUNG. A virtual training simulator for learning cataract surgery with phacoemulsification. *Computers in biology and medicine* [online]. 2009, **39**(11), 1020–31. ISSN 1879-0534. Available at: doi:10.1016/j.compbiomed.2009.08.003

[19] NGUYEN, Pho and Vikas CHOPRA. Applications of optical coherence tomography in cataract surgery. *Current Opinion in Ophthalmology* [online]. 2013, **24**(1), 47–52. ISSN 1040-8738. Available at: doi:10.1097/ICU.0b013e32835aee7b

[20] AMENT, Christine S. and Bonnie A. HENDERSON. Optimizing resident education in cataract surgery. *Current Opinion in Ophthalmology* [online]. 2011, **22**(1), 64–67. ISSN 1040-8738. Available at: doi:10.1097/ICU.0b013e3283415040

[21] DEWEY, Steven, George BEIKO, Rosa BRAGA-MELE, Donald R. NIXON, Tal RAVIV and Kenneth ROSENTHAL. Microincisions in cataract surgery. *Journal of Cataract & Refractive Surgery* [online]. 2014, **40**(9), 1549–1557. ISSN 08863350. Available at: doi:10.1016/j.jcrs.2014.07.006

[22] ABELL, Robin G., Erica DARIAN-SMITH, Jeffrey B. KAN, Penelope L. ALLEN, Shaun Y.P. EWE and Brendan J. VOTE. Femtosecond laser–assisted cataract surgery versus standard phacoemulsification cataract surgery: Outcomes and safety in more than 4000 cases at a single center. *Journal of Cataract & Refractive Surgery* [online]. 2015, **41**(1), 47–52. ISSN 08863350. Available at: doi:10.1016/j.jcrs.2014.06.025

[23] ALKHARASHI, Majed, Walter J STARK and Yassine J DAOUD. Advances in cataract surgery. *Expert Review of Ophthalmology* [online]. 2013, **8**(5), 447–456. ISSN 1746-9899. Available at: doi:10.1586/17469899.2013.840238

[24] ATCHISON, David A. Optics of the Human Eye. In: *Encyclopedia of Modern Optics* [online]. B.m.: Elsevier, 2018, p. 43–63. ISBN 9780750637756. Available at: doi:10.1016/B978-0-12-803581-8.09773-3

[25] NORRBY, Sverker. Sources of error in intraocular lens power calculation. *Journal of Cataract & Refractive Surgery* [online]. 2008, **34**(3), 368–376. ISSN 08863350. Available at: doi:10.1016/j.jcrs.2007.10.031

[26] GÖKCE, Sabite Emine, Ildamaris MONTES DE OCA, David L. COOKE, Li WANG, Douglas D. KOCH and Zaina AL-MOHTASEB. Accuracy of 8 intraocular lens calculation formulas in relation to anterior chamber depth in patients with normal axial lengths. *Journal of Cataract & Refractive Surgery* [online]. 2018, **44**(3), 362–368. ISSN 08863350. Available at: doi:10.1016/j.jcrs.2018.01.015

[27] NGUYEN, Jason, Liliana WERNER, Jason LUDLOW, Joah ALIANCY, Larry HA, Bryan MASINO, Sean ENRIGHT, Ray K. ALLEY and Ruth SAHLER. Intraocular lens power adjustment by a femtosecond laser. *Journal of Cataract & Refractive Surgery* [online]. 2018, **44**(2), 226–230. ISSN 08863350. Available at: doi:10.1016/j.jcrs.2017.09.036

[28] FORD, Joshua, Liliana WERNER and Nick MAMALIS. Adjustable intraocular lens power technology. *Journal of Cataract & Refractive Surgery* [online]. 2014, **40**(7), 1205–1223. ISSN 08863350. Available at: doi:10.1016/j.jcrs.2014.05.005

[29] SAHLER, Ruth, Josef F. BILLE, Sean ENRIGHT, Somaly CHHOEUNG and Kevin CHAN. Creation of a refractive lens within an existing intraocular lens using a femtosecond laser. *Journal of Cataract & Refractive Surgery* [online]. 2016, **42**(8), 1207–1215. ISSN 08863350. Available at: doi:10.1016/j.jcrs.2016.05.005

[30] ARISTODEMOU, Petros, John M. SPARROW and Stephen KAYE. Evaluating Refractive Outcomes after Cataract Surgery. *Ophthalmology* [online]. 2019, **126**(1), 13–18. ISSN 01616420. Available at: doi:10.1016/j.ophtha.2018.07.009

[31] KANE, Jack X., Anton VAN HEERDEN, Alp ATIK and Constantinos PETSOGLOU. Accuracy of 3 new methods for intraocular lens power selection. *Journal of*

Cataract & Refractive Surgery [online]. 2017, **43**(3), 333–339. ISSN 08863350. Available at: doi:10.1016/j.jcrs.2016.12.021

[32] COOKE, David L. and Timothy L. COOKE. Comparison of 9 intraocular lens power calculation formulas. *Journal of Cataract & Refractive Surgery* [online]. 2016, **42**(8), 1157–1164. ISSN 08863350. Available at: doi:10.1016/j.jcrs.2016.06.029

[33] HUANG, Jinhai, Colm MCALINDEN, Yingying HUANG, Daizong WEN, Giacomo SAVINI, Ruixue TU and Qinmei WANG. Meta-analysis of optical low-coherence reflectometry versus partial coherence interferometry biometry. *Scientific Reports* [online]. 2017, **7**(1), 43414. ISSN 2045-2322. Available at: doi:10.1038/srep43414

[34] MELLES, Ronald B., Jack T. HOLLADAY and William J. CHANG. Accuracy of Intraocular Lens Calculation Formulas. *Ophthalmology* [online]. 2018, **125**(2), 169–178. ISSN 01616420. Available at: doi:10.1016/j.ophtha.2017.08.027

[35] KANE, Jack X., Anton VAN HEERDEN, Alp ATIK and Constantinos PETSOGLOU. Intraocular lens power formula accuracy: Comparison of 7 formulas. *Journal of Cataract & Refractive Surgery* [online]. 2016, **42**(10), 1490–1500. ISSN 08863350. Available at: doi:10.1016/j.jcrs.2016.07.021

[36] ARISTODEMOU, Petros, Nathaniel E. KNOX CARTWRIGHT, John M. SPARROW and Robert L. JOHNSTON. Formula choice: Hoffer Q, Holladay 1, or SRK/T and refractive outcomes in 8108 eyes after cataract surgery with biometry by partial coherence interferometry. *Journal of Cataract & Refractive Surgery* [online]. 2011, **37**(1), 63–71. ISSN 08863350. Available at: doi:10.1016/j.jcrs.2010.07.032

[37] LADAS, John G., Aazim A. SIDDIQUI, Uday DEVGAN and Albert S. JUN. A 3-D "Super Surface" Combining Modern Intraocular Lens Formulas to Generate a "Super Formula" and Maximize Accuracy. *JAMA Ophthalmology* [online]. 2015, **133**(12), 1431. ISSN 2168-6165. Available at: doi:10.1001/jamaophthalmol.2015.3832

[38] FARAMARZI, Amir, Ali AGHAJANI and Leila GHIASIAN. Accuracy of various intraocular lens power calculation formulas in steep corneas. *Journal of Ophthalmic and Vision Research* [online]. 2017, **12**(4), 385. ISSN 2008-322X. Available at: doi:10.4103/jovr.jovr_20_17

[39] JEONG, Jinho, Han SONG, Jimmy K. LEE, Roy S. CHUCK and Ji-Won KWON. The effect of ocular biometric factors on the accuracy of various IOL power calculation formulas. *BMC Ophthalmology* [online]. 2017, **17**(1), 62. ISSN 1471-2415. Available at: doi:10.1186/s12886-017-0454-y

[40] REINSTEIN, Dan Z., Timothy E. YAP, Glenn I. CARP, Timothy J. ARCHER and Marine GOBBE. Reproducibility of manifest refraction between surgeons and optometrists in a clinical refractive surgery practice. *Journal of Cataract & Refractive Surgery* [online]. 2014, **40**(3), 450–459. ISSN 08863350. Available at: doi:10.1016/j.jcrs.2013.08.053

[41] SHAMMAS, H. John and Maya C. SHAMMAS. Measuring the cataractous lens.

Journal of Cataract & Refractive Surgery [online]. 2015, **41**(9), 1875–1879. ISSN 08863350. Available at: doi:10.1016/j.jcrs.2015.10.036

[42] KOCH, Douglas D., Shazia F. ALI, Mitchell P. WEIKERT, Mariko SHIRAYAMA, Richard JENKINS and Li WANG. Contribution of posterior corneal astigmatism to total corneal astigmatism. *Journal of Cataract & Refractive Surgery* [online]. 2012, **38**(12), 2080–2087. ISSN 08863350. Available at: doi:10.1016/j.jcrs.2012.08.036

[43] ZHANG, Lijun, Mary Ellen SY, Harry MAI, Fei YU and D. Rex HAMILTON. Effect of posterior corneal astigmatism on refractive outcomes after toric intraocular lens implantation. *Journal of Cataract & Refractive Surgery* [online]. 2015, **41**(1), 84–89. ISSN 08863350. Available at: doi:10.1016/j.jcrs.2014.04.033

[44] LEE, Tae Hee, Mi Sun SUNG, Lian CUI, Ying LI and Kyung Chul YOON. Factors Affecting the Accuracy of Intraocular Lens Power Calculation with Lenstar. *Chonnam Medical Journal* [online]. 2015, **51**(2), 91. ISSN 2233-7385. Available at: doi:10.4068/cmj.2015.51.2.91

[45] KALOGEROPOULOS, Chris, Miltiadis ASPIOTIS, Maria STEFANIOTOU and Konstantinos PSILAS. Factors influencing the accuracy of the SRK formula in the intraocular lens power calculation. *Documenta Ophthalmologica* [online]. 1994, **85**(3), 223–242. ISSN 0012-4486. Available at: doi:10.1007/BF01664930

[46] YAMAGUCHI, Takefumi, Kazuno NEGISHI and Kazuo TSUBOTA. Functional visual acuity measurement in cataract and intraocular lens implantation. *Current Opinion in Ophthalmology* [online]. 2011, **22**(1), 31–36. ISSN 1040-8738. Available at: doi:10.1097/ICU.0b013e3283414f36

[47] ASTBURY, Nick and Balasubramanya RAMAMURTHY. How to avoid mistakes in biometry. *Community eye health* [online]. 2006, **19**(60), 70–1. ISSN 0953-6833. Available at: http://www.ncbi.nlm.nih.gov/pubmed/17515971

[48] THULASI, Praneetha, Sumitra S. KHANDELWAL and J. Bradley RANDLEMAN. Intraocular lens alignment methods. *Current Opinion in Ophthalmology* [online]. 2016, **27**(1), 65–75. ISSN 1040-8738. Available at: doi:10.1097/ICU.0000000000000225

[49] WASFI, Ehab, P PAI and Alaa ABD-ELSAYED. Patient satisfaction with cataract surgery. *International Archives of Medicine* [online]. 2008, **1**(1), 22. ISSN 1755-7682. Available at: doi:10.1186/1755-7682-1-22

[50] KOCH, Douglas D., Warren HILL, Adi ABULAFIA and Li WANG. Pursuing perfection in intraocular lens calculations: I. Logical approach for classifying IOL calculation formulas. *Journal of Cataract & Refractive Surgery* [online]. 2017, **43**(6), 717–718. ISSN 08863350. Available at: doi:10.1016/j.jcrs.2017.06.006

[51] HOLLADAY, Jack T, Kathryn H MUSGROVE, Thomas C PRAGER, John W LEWIS, Thomas Y CHANDLER and Richard S RUIZ. A three-part system for refining intraocular lens power calculations. *Journal of Cataract & Refractive Surgery* [online]. 1988, **14**(1), 17–24. ISSN 08863350. Available at: doi:10.1016/S0886-

3350(88)80059-2

[52] RETZLAFF, John A., Donald R. SANDERS and Manus C. KRAFF. Development of the SRK/T intraocular lens implant power calculation formula. *Journal of Cataract & Refractive Surgery* [online]. 1990, **16**(3), 333–340. ISSN 08863350. Available at: doi:10.1016/S0886-3350(13)80705-5

[53] HOFFER, Kenneth J. The Hoffer Q formula: A comparison of theoretic and regression formulas. *Journal of Cataract & Refractive Surgery* [online]. 1993, **19**(6), 700–712. ISSN 08863350. Available at: doi:10.1016/S0886-3350(13)80338-0

[54] OLSEN, Thomas and Peter HOFFMANN. C constant: New concept for ray tracing–assisted intraocular lens power calculation. *Journal of Cataract & Refractive Surgery* [online]. 2014, **40**(5), 764–773. ISSN 08863350. Available at: doi:10.1016/j.jcrs.2013.10.037

[55] HILL, Warren. Hill-RBF Method - White Paper. *Summary of clinical papers* [online]. 2016 [accessed. 2019-01-12]. Available at: https://www.haag-streit.com/fileadmin/Haag-Streit_Diagnostics/biometry/EyeSuite_IOL/Brochures_Flyers/White_Paper_Hill-RBF_Method_20160819_2_0.pdf

[56] BARRETT, Graham D. An improved universal theoretical formula for intraocular lens power prediction. *Journal of Cataract & Refractive Surgery* [online]. 1993, **19**(6), 713–720. ISSN 08863350. Available at: doi:10.1016/S0886-3350(13)80339-2

[57] SCHRÖDER, Simon, Christina LEYDOLT, Rupert MENAPACE, Timo EPPIG and Achim LANGENBUCHER. Determination of Personalized IOL-Constants for the Haigis Formula under Consideration of Measurement Precision. *PLOS ONE* [online]. 2016, **11**(7), e0158988. ISSN 1932-6203. Available at: doi:10.1371/journal.pone.0158988

[58] ROBERTS, Timothy V., Chris HODGE, Gerard SUTTON and Michael LAWLESS. Comparison of Hill-radial basis function, Barrett Universal and current third generation formulas for the calculation of intraocular lens power during cataract surgery. *Clinical & Experimental Ophthalmology* [online]. 2018, **46**(3), 240–246. ISSN 14426404. Available at: doi:10.1111/ceo.13034

[59] ABULAFIA, Adi, Graham D. BARRETT, Michael ROTENBERG, Guy KLEINMANN, Adi LEVY, Olga REITBLAT, Douglas D. KOCH, Li WANG and Ehud I. ASSIA. Intraocular lens power calculation for eyes with an axial length greater than 26.0 mm: Comparison of formulas and methods. *Journal of Cataract & Refractive Surgery* [online]. 2015, **41**(3), 548–556. ISSN 08863350. Available at: doi:10.1016/j.jcrs.2014.06.033

[60] BANG, Stacy, Erica EDELL, Qilu YU, Kim PRATZER and Walter STARK. Accuracy of Intraocular Lens Calculations Using the IOLMaster in Eyes with Long Axial Length and a Comparison of Various Formulas. *Ophthalmology* [online]. 2011, **118**(3), 503–506. ISSN 01616420. Available at: doi:10.1016/j.ophtha.2010.07.008

[61] CARIFI, Gianluca, Francesco AIELLO, Vasiliki ZYGOURA, Nikolaos KOPSACHILIS and Vincenzo MAURINO. Accuracy of the Refractive Prediction Determined by Multiple Currently Available Intraocular Lens Power Calculation Formulas in Small Eyes. *American Journal of Ophthalmology* [online]. 2015, **159**(3), 577–583. ISSN 00029394. Available at: doi:10.1016/j.ajo.2014.11.036

[62] CLARKE, Gerald P. and Jeanne BURMEISTER. Comparison of intraocular lens computations using a neural network versus the Holladay formula. *Journal of Cataract & Refractive Surgery* [online]. 1997, **23**(10), 1585–1589. ISSN 08863350. Available at: doi:10.1016/S0886-3350(97)80034-X

[63] EOM, Youngsub, Su-Yeon KANG, Jong Suk SONG, Yong Yeon KIM and Hyo Myung KIM. Comparison of Hoffer Q and Haigis Formulae for Intraocular Lens Power Calculation According to the Anterior Chamber Depth in Short Eyes. *American Journal of Ophthalmology* [online]. 2014, **157**(4), 818-824.e2. ISSN 00029394. Available at: doi:10.1016/j.ajo.2013.12.017

[64] SHRIVASTAVA, Ankur K., Pranayee BEHERA, Binod KUMAR and Siddhartha NANDA. Precision of intraocular lens power prediction in eyes shorter than 22 mm: An analysis of 6 formulas. *Journal of Cataract & Refractive Surgery* [online]. 2018, **44**(11), 1317–1320. ISSN 08863350. Available at: doi:10.1016/j.jcrs.2018.07.023

[65] SHAJARI, Mehdi, Carolin M. KOLB, Kerstin PETERMANN, Myriam BÖHM, Michael HERZOG, Nina DE'LORENZO, Sabrina SCHÖNBRUNN and Thomas KOHNEN. Comparison of 9 modern intraocular lens power calculation formulas for a quadrifocal intraocular lens. *Journal of Cataract & Refractive Surgery* [online]. 2018, **44**(8), 942–948. ISSN 08863350. Available at: doi:10.1016/j.jcrs.2018.05.021

[66] REITBLAT, Olga, Adi LEVY, Guy KLEINMANN, Tsahi T. LERMAN and Ehud I. ASSIA. Intraocular lens power calculation for eyes with high and low average keratometry readings: Comparison between various formulas. *Journal of Cataract & Refractive Surgery* [online]. 2017, **43**(9), 1149–1156. ISSN 08863350. Available at: doi:10.1016/j.jcrs.2017.06.036

[67] HAAG-STREIT AG KOENIZ, Switzerland. *Hill-RBF Method - White Paper*. 2017.

[68] SNYDER, E., Michael. Hill-RBF Calculator in Clinical Practice. *New frontiers in iol prediction for improved refractive outcomes* [online]. 2017 [accessed. 2019-01-22]. Available at: https://crstodayeurope.com/articles/new-frontiers-in-iol-prediction-for-improved-refractive-outcomes/hill-rbf-calculator-in-clinical-practice/

[69] HILL, Warren. ASCRS Announces Hill-RBF Calculator for Cataract Surgery IOL Power Calculations. *The American Society of Cataract and Refractive Surgery - News room* [online]. 2016 [accessed. 2018-12-05]. Available at: http://ascrs.org/about-ascrs/news-about/ascrs-announces-hill-rbf-calculator-cataract-surgery-iol-power-calculations

[70] HILL, Warren. *Hill-RBF Calculator* [online]. 2016 [accessed. 2018-12-09]. Available

at: www.rbfcalculator.com

[71] CHEN, Yen-An, Nino HIRNSCHALL and Oliver FINDL. Evaluation of 2 new optical biometry devices and comparison with the current gold standard biometer. *Journal of Cataract & Refractive Surgery* [online]. 2011, **37**(3), 513–517. ISSN 08863350. Available at: doi:10.1016/j.jcrs.2010.10.041

[72] CONRAD-HENGERER, Ina, Mayss AL SHEIKH, Fritz H. HENGERER, Tim SCHULTZ and H. Burkhard DICK. Comparison of visual recovery and refractive stability between femtosecond laser–assisted cataract surgery and standard phacoemulsification: Six-month follow-up. *Journal of Cataract & Refractive Surgery* [online]. 2015, **41**(7), 1356–1364. ISSN 08863350. Available at: doi:10.1016/j.jcrs.2014.10.044

[73] KONONENKO, Igor and Matjaž KUKAR. Chapter 7 - Data Preprocessing. In: Igor KONONENKO and Matjaž KUKAR, eds. *Machine Learning and Data Mining* [online]. B.m.: Woodhead Publishing, 2007, p. 181–211. ISBN 978-1-904275-21-3. Available at: doi:https://doi.org/10.1533/9780857099440.181

[74] LEYS, Christophe, Christophe LEY, Olivier KLEIN, Philippe BERNARD and Laurent LICATA. Detecting outliers: Do not use standard deviation around the mean, use absolute deviation around the median. *Journal of Experimental Social Psychology* [online]. 2013, **49**(4), 764–766. ISSN 00221031. Available at: doi:10.1016/j.jesp.2013.03.013

[75] OLSEN, Thomas. Calculation of intraocular lens power: a review. *Acta Ophthalmologica Scandinavica* [online]. 2007, **85**(5), 472–485. ISSN 1395-3907. Available at: doi:10.1111/j.1755-3768.2007.00879.x

[76] GATINEL, Damien. Calculation of implant - theoretical formula. *Biométrie oculaire, calcul d'implant* [online]. 2018 [accessed. 2019-02-13]. Available at: https://www.gatinel.com/en/recherche-formation/biometrie-oculaire-calcul-dimplant/calcul-dimplant-formule-theorique/

[77] MATHWORKS INC. *Matlab R2017a (9.2.0.556344) documentation* [online]. 2017 [accessed. 2019-03-15]. Available at: https://www.mathworks.com/help/releases/R2017a/index.html

[78] MONGILLO, Michael. Choosing Basis Functions and Shape Parameters for Radial Basis Function Methods. *SIAM Undergraduate Research Online* [online]. 2011, **4**, 190–209. ISSN 23277807. Available at: doi:10.1137/11S010840

[79] WU, Yue, Hui WANG, Biaobiao ZHANG and K.-L. DU. Using Radial Basis Function Networks for Function Approximation and Classification. *ISRN Applied Mathematics* [online]. 2012, **2012**, 1–34. ISSN 2090-5572. Available at: doi:10.5402/2012/324194

[80] FERRARI, Silvia and Robert STENGEL. Smooth Function Approximation Using Neural Networks. *IEEE Transactions on Neural Networks* [online]. 2005, **16**(1), 24–38. ISSN 1045-9227. Available at: doi:10.1109/TNN.2004.836233

[81] PARK, Jooyoung and Irwin SANDBERG. Universal Approximation Using Radial-Basis-Function Networks. *Neural Computation* [online]. 1991, **3**(2), 246–257.

ISSN 0899-7667. Available at: doi:10.1162/neco.1991.3.2.246

[82] GIROSI, Federico, Tomaso POGGIO and Bruno CAPRILE. Extensions of a Theory of Networks for Approximation and Learning. In: *NIPS'90 Proceedings of the 3rd International Conference on Neural Information Processing Systems*. Denver, Colorado: Morgan Kaufmann Publishers Inc., 1990, p. 750–756. ISBN 1-55860-184-8.

[83] LAMPARIELLO, Francesco and Marco SCIANDRONE. Efficient training of RBF neural networks for pattern recognition. *IEEE Transactions on Neural Networks* [online]. 2001, **12**(5), 1235–1242. ISSN 10459227. Available at: doi:10.1109/72.950152

[84] KURBAN, Tuba and Erkan BEŞDOK. A Comparison of RBF Neural Network Training Algorithms for Inertial Sensor Based Terrain Classification. *Sensors* [online]. 2009, **9**(8), 6312–6329. ISSN 1424-8220. Available at: doi:10.3390/s90806312

[85] TUCKOVA, Jana. *Selected applications of the artificial neural networks at the signal processing*. Prague: Nakladatelství ČVUT. 2009. ISBN 978-80-01-04229-8 (in Czech)

[86] HAYKIN, Simon. *Neural Networks: A Comprehensive Foundation*. 2nd ed. Upper Saddle River, NJ, USA: Prentice Hall PTR. 1998. ISBN 0132733501

[87] NOVÁK, Mirko a kol. *Umělé neuronové sítě: teorie a aplikace.* Praha: C.H.Beck. 1998. ISBN 80-7179-132-6 (in Czech)

[88] RANGANATHAN, Ananth. The Levenberg-Marquardt Algorithm. *Tutoral on LM algorithm* [online]. 2004 [accessed. 2019-01-21]. Available at: doi:http://dx.doi.org/10.1.1.10.2258

[89] KOURENTZES, Nikolaos, Devon K. BARROW and Sven F. CRONE. Neural network ensemble operators for time series forecasting. *Expert Systems with Applications* [online]. 2014, **41**(9), 4235–4244. ISSN 09574174. Available at: doi:10.1016/j.eswa.2013.12.011

[90] NGUYEN, Derrick and Bernard WIDROW. Improving the learning speed of 2-layer neural networks by choosing initial values of the adaptive weights. In: *1990 IJCNN International Joint Conference on Neural Networks* [online]. San Diego, CA, USA: IEEE, 1990, p. 21–26 vol.3. ISBN 0263774X (ISSN). Available at: doi:10.1109/IJCNN.1990.137819

[91] REFAEILZADEH, Payam, Lei TANG and Huan LIU. Cross-Validation. In: *Encyclopedia of Database Systems* [online]. Boston, MA: Springer US, 2009, p. 532–538. ISBN 9783805596992. Available at: doi:10.1007/978-0-387-39940-9_565

[92] MONTEGRANARIO, Hebert and Jairo ESPINOSA. Radial Basis Functions. In: *SpringerBriefs in Computer Science* [online]. 2014, p. 69–81. ISBN 9780511543241. Available at: doi:10.1007/978-1-4939-0533-1_8

[93] SELMIC, Rastko and Frank LEWIS. Neural-network approximation of piecewise

continuous functions: application to friction compensation. *IEEE Transactions on Neural Networks* [online]. 2002, **13**(3), 745–751. ISSN 1045-9227. Available at: doi:10.1109/TNN.2002.1000141

[94] ANASTASSIOU, George A. Multivariate hyperbolic tangent neural network approximation. *Computers & Mathematics with Applications* [online]. 2011, **61**(4), 809–821. ISSN 08981221. Available at: doi:10.1016/j.camwa.2010.12.029

[95] ROMERO REYES, Ilyakay V., Irina V. FEDYUSHKINA, Vladlen S. SKVORTSOV and Dmitry A. FILIMONOV. Prediction of progesterone receptor inhibition by high-performance neural network algorithm. *International Journal of Mathematical Models and Methods in Applied Sciences* [online]. 2013, **7**(3), 303–310. ISSN 19980140. Available at: http://www.naun.org/main/NAUN/ijmmas/2001-108.pdf

[96] JAP, Dirmanto, Marc STÖTTINGER and Shivam BHASIN. Support vector regression. In: *Proceedings of the Fourth Workshop on Hardware and Architectural Support for Security and Privacy - HASP '15* [online]. New York, New York, USA: ACM Press, 2015, p. 1–8. ISBN 9781450334839. Available at: doi:10.1145/2768566.2768568

[97] HERBRICH, Ralf. Support vector learning for ordinal regression. In: *9th International Conference on Artificial Neural Networks: ICANN '99* [online]. Edinburgh, United Kingdom: IEE, 1999, p. 97–102. ISBN 0 85296 721 7. Available at: doi:10.1049/cp:19991091

[98] TRAFALIS, Theodore and Huseyin INCE. Support vector machine for regression and applications to financial forecasting. In: *Proceedings of the IEEE-INNS-ENNS International Joint Conference on Neural Networks. IJCNN 2000. Neural Computing: New Challenges and Perspectives for the New Millennium* [online]. B.m.: IEEE, 2000, p. 348–353 vol.6. ISBN 0-7695-0619-4. Available at: doi:10.1109/IJCNN.2000.859420

[99] CHUN-HSIN, Wu, Wei CHIA-CHEN, Su DA-CHUN, Chang MING-HUA and Ho JAN-MING. Travel time prediction with support vector regression. In: *Proceedings of the 2003 IEEE International Conference on Intelligent Transportation Systems* [online]. B.m.: IEEE, 2003, p. 1438–1442. ISBN 0-7803-8125-4. Available at: doi:10.1109/ITSC.2003.1252721

[100] YU, Pao-Shan, Shien-Tsung CHEN and I-Fan CHANG. Support vector regression for real-time flood stage forecasting. *Journal of Hydrology* [online]. 2006, **328**(3–4), 704–716. ISSN 00221694. Available at: doi:10.1016/j.jhydrol.2006.01.021

[101] WANG, Binghui and Neil Zhenqiang GONG. Stealing Hyperparameters in Machine Learning. In: *2018 IEEE Symposium on Security and Privacy (SP)* [online]. B.m.: IEEE, 2018, p. 36–52. ISBN 978-1-5386-4353-2. Available at: doi:10.1109/SP.2018.00038

[102] ZHI-QIANG, Zeng, Yu HONG-BIN, Xu HUA-RONG, Xie YAN-QI and Gao JI. Fast training Support Vector Machines using parallel sequential minimal optimization. In: *2008 3rd International Conference on Intelligent System and Knowledge*

Engineering [online]. B.m.: IEEE, 2008, p. 997–1001. ISBN 978-1-4244-2196-1. Available at: doi:10.1109/ISKE.2008.4731075

[103] SNOEK, Jasper, Hugo LAROCHELLE and Ryan P ADAMS. Practical Bayesian Optimization of Machine Learning Algorithms. In: *NIPS'12 Proceedings of the 25th International Conference on Neural Information Processing Systems - Volume 2* [online]. 2012, p. 2951–2959. Available at: http://arxiv.org/abs/1206.2944

[104] BERGSTRA, James S., Rémi BARDENET, Yoshua BENGIO and Balázs KÉGL. Algorithms for Hyper-Parameter Optimization. In: *NIPS'11 Proceedings of the 24th International Conference on Neural Information Processing Systems* [online]. 2011, p. 2546–2554. Available at: https://papers.nips.cc/paper/4443-algorithms-for-hyper-parameter-optimization.pdf

[105] KRZYWINSKI, Martin and Naomi ALTMAN. Classification and regression trees. *Nature Methods* [online]. 2017, **14**(8), 757–758. ISSN 1548-7091. Available at: doi:10.1038/nmeth.4370

[106] MENG, Xue-Hui, Yi-Xiang HUANG, Dong-Ping RAO, Qiu ZHANG and Qing LIU. Comparison of three data mining models for predicting diabetes or prediabetes by risk factors. *The Kaohsiung Journal of Medical Sciences* [online]. 2013, **29**(2), 93–99. ISSN 1607551X. Available at: doi:10.1016/j.kjms.2012.08.016

[107] XU, Min, Pakorn WATANACHATURAPORN, P VARSHNEY and Manoj ARORA. Decision tree regression for soft classification of remote sensing data. *Remote Sensing of Environment* [online]. 2005, **97**(3), 322–336. ISSN 00344257. Available at: doi:10.1016/j.rse.2005.05.008

[108] BITTENCOURT, Helio Radke and Robin CLARKE. Feature Selection by Using Classification and Regression Trees (CART). In: *International Archives of Photogrammetry remote sensing and spatial information sciences*. 2004, p. 66–70. ISSN 16821750.

[109] MENDES-MOREIRA, João, Carlos SOARES, Alípio Mário JORGE and Jorge Freire De SOUSA. Ensemble approaches for regression. *ACM Computing Surveys* [online]. 2012, **45**(1), 1–40. ISSN 03600300. Available at: doi:10.1145/2379776.2379786

[110] REN, Ye, Le ZHANG and P.N. SUGANTHAN. Ensemble Classification and Regression-Recent Developments, Applications and Future Directions [Review Article]. *IEEE Computational Intelligence Magazine* [online]. 2016, **11**(1), 41–53. ISSN 1556-603X. Available at: doi:10.1109/MCI.2015.2471235

[111] AVNIMELECH, Ran and Nathan INTRATOR. Boosting Regression Estimators. *Neural Computation* [online]. 1999, **11**(2), 499–520. ISSN 0899-7667. Available at: doi:10.1162/089976699300016746

[112] CALANDRA, Roberto, Jan PETERS, Carl Edward RASMUSSEN and Marc Peter DEISENROTH. Manifold Gaussian Processes for regression. In: *2016 International Joint Conference on Neural Networks (IJCNN)* [online]. B.m.: IEEE, 2016, p. 3338–3345. ISBN 978-1-5090-0620-5. Available at: doi:10.1109/IJCNN.2016.7727626

[113] CHU, Wei and Zoubin GHAHRAMANI. Preference learning with Gaussian processes. In: *Proceedings of the 22nd international conference on Machine learning - ICML '05* [online]. New York, New York, USA: ACM Press, 2005, p. 137–144. ISBN 1595931805. Available at: doi:10.1145/1102351.1102369

[114] BANERJEE, Sudipto, Alan E. GELFAND, Andrew O. FINLEY and Huiyan SANG. Gaussian predictive process models for large spatial data sets. *Journal of the Royal Statistical Society: Series B (Statistical Methodology)* [online]. 2008, **70**(4), 825–848. ISSN 13697412. Available at: doi:10.1111/j.1467-9868.2008.00663.x

[115] FOSTER, Dean P. and Robert A. STINE. Variable Selection in Data Mining. *Journal of the American Statistical Association* [online]. 2004, **99**(466), 303–313. ISSN 0162-1459. Available at: doi:10.1198/016214504000000287

[116] TSO, Geoffrey K.F. and Kelvin K.W. YAU. Predicting electricity energy consumption: A comparison of regression analysis, decision tree and neural networks. *Energy* [online]. 2007, **32**(9), 1761–1768. ISSN 03605442. Available at: doi:10.1016/j.energy.2006.11.010

[117] LIU, Zhan-yu, Jing-feng HUANG, Jing-jing SHI, Rong-xiang TAO, Wan ZHOU and Li-li ZHANG. Characterizing and estimating rice brown spot disease severity using stepwise regression, principal component regression and partial least-square regression. *Journal of Zhejiang University SCIENCE B* [online]. 2007, **8**(10), 738–744. ISSN 1673-1581. Available at: doi:10.1631/jzus.2007.B0738

[118] WILKINSON, Grahan and C. E. ROGERS. Symbolic Description of Factorial Models for Analysis of Variance. *Applied Statistics* [online]. 1973, **22**(3), 392. ISSN 00359254. Available at: doi:10.2307/2346786

[119] WANG, Li, Douglas D. KOCH, Warren HILL and Adi ABULAFIA. Pursuing perfection in intraocular lens calculations: III. Criteria for analyzing outcomes. *Journal of Cataract & Refractive Surgery* [online]. 2017, **43**(8), 999–1002. ISSN 08863350. Available at: doi:10.1016/j.jcrs.2017.08.003

[120] MAHDAVI, Shareef and Jack HOLLADAY. IOLMaster® 500 and Integration of the Holladay 2 Formula for Intraocular Lens Calculations. *European Ophthalmic Review* [online]. 2011, **05**(02), 134. ISSN 1756-1795. Available at: doi:10.17925/EOR.2011.05.02.134

[121] MERCIER, Émeric, Armelle EVEN, Elodie MIRISOLA, Delphine WOLFERSBERGER and Marc SCIAMANNA. Numerical study of extreme events in a laser diode with phase-conjugate optical feedback. *Physical Review E* [online]. 2015, **91**(4), 042914. ISSN 1539-3755. Available at: doi:10.1103/PhysRevE.91.042914

[122] WESTFALL, Peter H., James F. TROENDLE and Gene PENNELLO. Multiple McNemar Tests. *Biometrics* [online]. 2010, **66**(4), 1185–1191. ISSN 0006341X. Available at: doi:10.1111/j.1541-0420.2010.01408.x

[123] TATE, Merle W. and Sara M. BROWN. Note on the Cochran Q Test. *Journal of the American Statistical Association* [online]. 1970, **65**(329), 155–160. ISSN 0162-1459. Available at: doi:10.1080/01621459.1970.10481069

[124] ROTHMAN, Kenneth J. No Adjustments Are Needed for Multiple Comparisons. *Epidemiology* [online]. 1990, **1**(1), 43–46. ISSN 1044-3983. Available at: doi:10.1097/00001648-199001000-00010

[125] SAVILLE, David J. Multiple Comparison Procedures: The Practical Solution. *The American Statistician* [online]. 1990, **44**(2), 174–180. ISSN 0003-1305. Available at: doi:10.1080/00031305.1990.10475712

[126] NETTLETON, David F., Albert ORRIOLS-PUIG and Albert FORNELLS. A study of the effect of different types of noise on the precision of supervised learning techniques. *Artificial Intelligence Review* [online]. 2010, **33**(4), 275–306. ISSN 0269-2821. Available at: doi:10.1007/s10462-010-9156-z

[127] OLSEN, Thomas. *Calculation of intraocular lens power: A review* [online]. 2007. ISBN 1395-3907 (Print)r1395-3907 (Linking). Available at: doi:10.1111/j.1755-3768.2007.00879.x

[128] GALE, Robert Peter, Manuel SALDANA, Roy JOHNSTON, Bruno ZUBERBUHLER and Martin MCKIBBIN. Benchmark standards for refractive outcomes after NHS cataract surgery. *Eye* [online]. 2009, **23**(1), 149–152. ISSN 0950-222X. Available at: doi:10.1038/sj.eye.6702954

[129] OLSEN, Thomas. Prediction of the effective postoperative (intraocular lens) anterior chamber depth. *Journal of Cataract & Refractive Surgery* [online]. 2006, **32**(3), 419–424. ISSN 08863350. Available at: doi:10.1016/j.jcrs.2005.12.139

[130] MAHDAVI, Shareef and Jack HOLLADAY. IOLMaster® 500 and Integration of the Holladay 2 Formula for Intraocular Lens Calculations. *European Ophthalmic Review* [online]. 2011, **05**, 134. Available at: doi:10.17925/EOR.2011.05.02.134

[131] KAISER, Jiri. Dealing with Missing Values in Data. *Journal of Systems Integration* [online]. 2014, **5**(1), 42–51. ISSN 18042724. Available at: doi:10.20470/jsi.v5i1.178

[132] ARMSTRONG, Richard A. Statistical guidelines for the analysis of data obtained from one or both eyes. *Ophthalmic and Physiological Optics* [online]. 2013, **33**(1), 7–14. ISSN 02755408. Available at: doi:10.1111/opo.12009

[133] CICCHETTI, Domenic V. Guidelines, criteria, and rules of thumb for evaluating normed and standardized assessment instruments in psychology. *Psychological Assessment* [online]. 1994, **6**(4), 284–290. ISSN 1939-134X. Available at: doi:10.1037/1040-3590.6.4.284

[134] KOO, Terry K and Mae Y LI. A Guideline of Selecting and Reporting Intraclass Correlation Coefficients for Reliability Research. *Journal of Chiropractic Medicine* [online]. 2016, **15**(2), 155–163. ISSN 15563707. Available at: doi:10.1016/j.jcm.2016.02.012

[135] MAIMON, Oded and Lior ROKACH. Data Cleansing: A Prelude to Knowledge Discovery. In: Oded MAIMON and Lior ROKACH, eds. *The Data Mining and Knowledge Discovery Handbook* [online]. New York: Springer-Verlag, 2005. ISBN 0-387-24435-2. Available at: doi:10.1007/b107408

[136] HOFFER, Kenneth J. Biometry of 7,500 Cataractous Eyes. *American Journal of Ophthalmology* [online]. 1980, **90**(3), 360–368. ISSN 00029394. Available at: doi:10.1016/S0002-9394(14)74917-7

[137] HOFFER, Kenneth J. and Giacomo SAVINI. IOL Power Calculation in Short and Long Eyes. *Asia-Pacific Journal of Ophthalmology* [online]. 2017, **6**(4). ISSN 21620989. Available at: doi:10.22608/APO.2017338

[138] MELLES, Ronald B., Jack T. HOLLADAY and William J. CHANG. Accuracy of Intraocular Lens Calculation Formulas. *Ophthalmology* [online]. 2018. ISSN 15494713. Available at: doi:10.1016/j.ophtha.2017.08.027

[139] VAN DER LINDEN, Jan Willem, Violette VRIJMAN, Rana EL-SAADY, Ivanka J. VAN DER MEULEN, Maarten P. MOURITS and Ruth LAPID-GORTZAK. Autorefraction versus subjective refraction in a radially asymmetric multifocal intraocular lens. *Acta Ophthalmologica* [online]. 2014, **92**(8), 764–768. ISSN 1755375X. Available at: doi:10.1111/aos.12410

[140] MUÑOZ, Gonzalo, César ALBARRÁN-DIEGO and Hani F. SAKLA. Autorefraction after Multifocal IOLs. *Ophthalmology* [online]. 2007, **114**(11), 2100-2100.e1. ISSN 01616420. Available at: doi:10.1016/j.ophtha.2007.05.049

[141] BISSEN-MIYAJIMA, Hiroko, Keiichiro MINAMI, Mami YOSHINO, Mariko NISHIMURA and Shinchi OKI. Autorefraction after implantation of diffractive multifocal intraocular lenses. *Journal of Cataract & Refractive Surgery* [online]. 2010, **36**(4), 553–556. ISSN 08863350. Available at: doi:10.1016/j.jcrs.2009.10.047

[142] JIANG, Yuan, Ming LI and Zhi-Hua ZHOU. Mining extremely small data sets with application to software reuse. *Software: Practice and Experience* [online]. 2009, **39**(4), 423–440. ISSN 00380644. Available at: doi:10.1002/spe.905

[143] OLSON, Matthew, Abraham WYNER and Richard BERK. Modern Neural Networks Generalize on Small Data Sets. In: *NIPS'18 Proceedings of the 32nd International Conference on Neural Information Processing Systems*. 2018, p. 3623–3632.